Physiological, biochemical and root proteome responses of maize seedlings to drought stress

Lerato Moloi

2013075318

Dissertation submitted in fulfilment of the requirements for the degree Magister Scientiae in the Faculty of Natural and Agricultural Sciences, Department of Plant Sciences, University of the Free State -QwaQwa Campus

Supervisor: Dr Rudo Ngara

Co-supervisor: Dr Arun Gokul

December 2022

Declaration

I, Lerato Moloi, declare that the Master's Degree research dissertation that I herewith submit for the Master's Degree qualification in Botany at the University of the Free State is my independent work and that I have not previously submitted it for a qualification at another institution of higher education.

I, Lerato Moloi, hereby declare that I am aware that the copyright is vested in the University of the Free State.

I, Lerato Moloi, hereby declare that all royalties as regards intellectual property that was developed during the course of and/ or in connection with the study at the University of the Free State will accrue to the University.

Lerato Moloi (Miss)

Dedication

I dedicate this to Mrs Tiisetso Alice Moloi, my special mother. My family thank you for your patience and support as I conducted my research. Your prayers and words of encouragement gave me the motivation to carry on with my studies. There would be no me without any of you.

Acknowledgements

My deepest gratitude is beyond words to my supervisor, Dr. Rudo Ngara; you have taught me much more than laboratory and research work and for your encouragements and believing in me throughout the research journey. To Dr. Arun Gokul, I thank you for your patience, guidance, and leadership.

To my mentor Ms Sellwane Jeanette Moloi, who became more like a sister to me, thank you for your assistance with laboratory work, your never-ending support, encouragement, and guidance when things became hard for me. Special thanks to the Plant Biotechnology Research group and UFS postgraduate team, your warm welcome, teamwork, and friendliness have made my research journey here a lot easier. You people have given me a home away from home.

To Dr. Stephen Chivasa and his team at Durham University, UK, I thank you for dedicating your time to assist with iTRAQ analysis.

I wish to also thank the National Research Foundation (NRF) for financial assistance.

I am thankful to my Father, the Lord Almighty, who gave me this opportunity and guided me all the way through.

Table of contents

List of figures

List of Tables

List of abbreviations

1D	One-dimensional
1D-SDS-PAGE	One-dimensional sodium dodecyl sulfate polyacrylamide gel electrophoresis
APS	Ammonium persulfate
APX	Ascorbate peroxidase
BSA	Bovine serum albumin
CHAPS	3-[(3-Cholamidopropyl) dimethylammonio]-1propanesulfonate
HILIC SPE	Hydrophilic interaction liquid chromatography – mass spectrometry
iTRAQ	Isobaric tags for relative and absolute quantitation
kDa	kilo Dalton
LC/MS	Liquid chromatography mass spectrometry
MDA	Malondialdehyde
MW	Molecular weight
NBT	Nitroblue tetrazolium
PAGE	Polyacrylamide gel electrophoresis
ROS	Reactive oxygen species
SDS	Sodium dodecyl sulfate
SOD	Superoxide dismutase

TBA	Thiobarbituric acid
TCA	Trichloroacetic acid
v/v	volume to volume
w/v	weight to v

Abstract

A primary limiting factor for maize during its growing period is drought stress. With the decrease in yield and biomass triggered by drought stress in maize, drought has become a critical issue that must be considered due to the changing climate conditions. This study aimed to comparatively analyse the morpho-physiological, biochemical and root proteome changes of two maize varieties in response to drought stress. In this study, two maize varieties CN07/8-224 and CN07/8-292 with unknown drought phenotypes were used. The plant growth experiments were conducted in a growth chamber for mild stress with ~ 54% and ~48% of soil moisture content and a greenhouse for severe stress with ~51% and ~43% soil moisture content. In both growth experiments, 7-day-old maize seedlings were exposed to a 14-day drought stress treatment, while continuing to water the controls every other day. Thereafter, a range of morpho-physiological parameters such as shoot and root length/weight, leaf relative water content, chlorophyll and carotenoid content were measured. In addition, biochemical parameters such as the level of lipid peroxidation and hydrogen peroxide, as well as the activities of superoxide dismutase (SOD), and ascorbate peroxide (APX) were measured. The root proteome was analysed using the isobaric tags for absolute and relative quantitation (iTRAQ) method coupled with liquid chromatography- tandem mass spectrometry to identify differentially expressed proteins in response to drought stress. To annotate the proteins, bioinformatics studies were carried out by using the UniProt and InterPro databases. The Gene Ontology (GO) annotation and protein families were allocated to each protein that showed differential expression in response to the drought stress. Then, the proteins were functionally categorized using a modified version of the Bevan classification scheme. The results of the study showed some significant differences between the drought treated plants and control plants of CN07/8-224 and CN07/8-292, as well as between the maize varieties. Results indicated that both maize varieties experienced reductions in chlorophyll a, b, and carotenoids

during drought stress. In addition, there were differences in the amounts of chlorophyll that accumulated in the various varieties. These reductions may be attributed to a reduced water supply observed in soil moisture content, which reduced the synthesis of photosynthetic pigments in maize plants. However, only the drought-stressed CN07/8-224 maize variety lengthened its roots to adapt to limited water supply. Higher lipid peroxidation and hydrogen peroxide levels correlated with increased antioxidant activities of CN07/8-292 drought-stressed roots as compared to control plants. This could be because there was more significant ROS detoxification under drought stress, which led to higher activities of SOD and APX in comparison to control plants. The root samples of CN07/8-224 and CN07/8-292 maize varieties were used to conduct iTRAQ analysis. A total of 1 232 and 1 558 proteins were positively identified in CN07/8-224 and CN07/8-292 varieties, respectively in response to mild drought stress conditions. A total of 116 and 146 of these proteins were responsive to the mild stress. The CN07/8-224 and CN07/8-292 varieties shared seven drought-responsive proteins, while the rest were unique to each variety. Collectively, the drought responsive proteins of both maize varieties were involved in primary/secondary metabolism, disease defence, and protein synthesis, all of which are involved in the response of maize varieties to drought. However, the expression of drought responsive proteins varied across the maize varieties. Overall, physiological and biochemical results have shown how the CN07/8-224 and CN07/8-292 maize varieties responded to drought stress using a range of mechanisms. In addition, strong root system architecture, as shown by higher root length and fresh root weight in CN07/8-224 variety under drought stress, could be responsible for the improved growth and greater stress tolerance. On the other hand, CN07/8-292 variety might happen to be sensitive to drought stress relative to CN07/8-224 based on the observed results. The obtained results would help researchers to find solutions on the impact of gene expression under drought.

Chapter 1

Literature review

1.1. Drought stress and its effects on plant growth and physiology

Plant growth and productivity are greatly affected by drought stress (Farooq *et al.*, 2009; Shao *et al.*, 2009; Kaur *et al.*, 2019). Drought is defined as a prolonged period of limited rainfall, resulting in insufficient water in the soil (Shao *et al.*, 2009; Tumová *et al.*, 2018). Like many other stresses, drought alters physiological and metabolic processes in plants (Mittler, 2006; Farooq *et al.*, 2009; Anjum *et al.*, 2011), such as growth, productivity, reproductive capacity, or survival (Rhodes, 2001). For example, reduced soil moisture content affects a plant's water relations such as relative water content (RWC), osmotic potential, and turgor pressure, as well as chlorophyll content and photosynthetic capacity (Blum, 2005; Wei *et al.*, 2009; Mohammadi *et al.*, 2022). Water stress also inhibits photosynthetic activities in plants due to stomatal closure (Andrés *et al.*, 2014; Agurla *et al.*, 2018; Carminati and Javaux, 2020).

Due to the reduction in turgor pressure, cell development is one of the physiological processes in plants that is most vulnerable to drought (Anjum *et al.*, 2011). As such, drought stress inhibits plant development and growth in various ways (Figure 1.1). Extensive loss of water in plants can also disrupt metabolic processes, cell structure, and possibly lead to the death of a plant (Shao *et al.*, 2009; Araújo *et al.*, 2012).

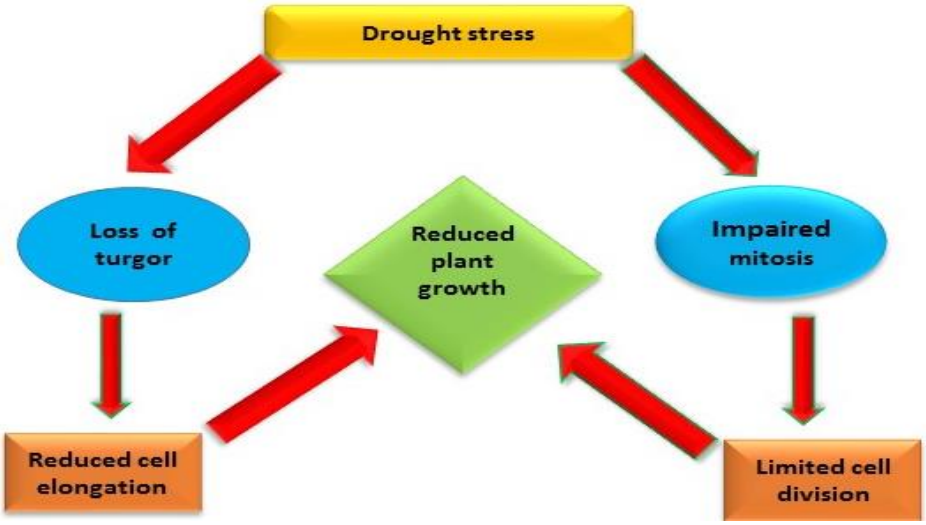

Figure1.1: Causes of growth reduction in plants under drought conditions. Adapted from Farooq *et al*., (2009).

Drought stress disrupts nutrient uptake due to reduced transpiration, and impairs active transport processes, and membrane permeability (Bagheri *et al.*, 2018; Li *et al.*, 2021). A reduction in leaf water potential lowers the uptake of macronutrients such as nitrogen, phosphorus, potassium, calcium and magnesium in plants under drought conditions (Hu *et al.*, 2008; Asgharipour, 2011; Sassine *et al.*, 2021).

The production of reactive oxygen species (ROS) tends to be greatest in plants when abiotic factors such as drought stress are prevailing (Jakubczyk *et al.*, 2020; Mittler *et al.*, 2022). The ROS consists of superoxide radicals, hydroxyl radicals, and hydrogen peroxide (Smirnoff and Arnaud, 2019; Jakubczyk *et al.*, 2020). The over accumulation of ROS in plants may initiate oxidative damage to proteins, lipids and DNA, thus impairing the normal functioning of cells (Kaur and Asthir, 2017; Song *et al.*, 2019). The subcellular production sites of ROS include chloroplasts, mitochondria, cytosols, vacuoles, peroxisomes, plasma membrane, apoplast, and

cell walls (Kohli *et al.*, 2019). Regardless of how harmful these species are, at low concentrations, hydrogen peroxide frequently serve as a signalling molecule that controls the expression of several genes and other stress-responsive pathways (Nadarajah, 2020). However, plants have developed defence mechanisms to counteract the negative effects of drought stress to survive and complete their life cycles (Shahzad *et al.*, 2016).

1.2. Plant responses to drought stress

Plants sense and adapt to drought by regulating their metabolism, growth patterns, and mobilizing various defence mechanisms at subcellular, cellular, and organ levels (Kaur and Asthir, 2017). Some of these strategies include drought escape, avoidance, and tolerance (Badr *et al*, 2020; Islam *et al*, 2022) and are briefly described below.

1.2.1. Drought escape

In the drought escape strategy, plants complete their life cycle quickly, thereby allowing rapid plant development, and growth before the environment becomes dry (Riboni *et al.*, 2016; Shavrukov *et al.*, 2017). Drought escape is widely used by ephemeral plants (Shavrukov *et al.*, 2017). This life strategy has also been adopted by some type of wheat (*Triticum aestivum*) to reduce exposure to dehydration during flowering and post-anthesis grain filling stages and to promote rapid development (Hasanuzzaman *et al.*, 2019).

1.2.2. Drought avoidance

Drought avoidance can be defined as a plant's ability to maintain high tissue water potential under drought conditions (Kaur *et al*, 2019). This strategy is achieved in plants either by absorbing more water from the soil or by reducing water loss via transpiration (Tarrisse *et al*,

2022). For example, water uptake by plants may be enhanced through extensive root systems (Asseng *et al.*, 1998; Andrés *et al*, 2014; Barrios-Masias *et al.*, 2015; Bagheri *et al.*, 2018). Moreover, in desert environments, plants like the Saguaro cactus (*Carnegiea gigantea*) have long root systems that spread out wide below the ground to absorb more water (Dev *et al.*, 2018; Naorem *et al.*, 2022). Drought avoiding plants also have a range of other adaptations such as modified leaves and stems, thick cuticles, and waxy surfaces to reduce water loss (Shahzad *et al.*, 2016; Fàbregas and Fernie, 2019; Rad *et al.*, 2021).

1.2.3. Drought tolerance

When a plant is under drought stress, its capacity to maintain regular functions at low water potential involves changes in the expression of specific genes, proteins, and metabolites (Kaur *et al.*, 2019; Zeng *et al.*, 2019). Below is a brief discussion of some of the drought tolerance mechanisms in plants.

1.2.3.1. Role of abscisic acid (ABA) in response to drought

In roots and shoots, seeds, leaf veins, and guard cells, drought stress causes the production and accumulation of ABA (Nayyar and Walia, 2003; Xiong *et al.*, 2006; Brandt *et al.*, 2012). Abscisic acid controls how plants respond to environmental stress by acting as a signalling mediator (Cai *et al.*, 2011; Kaur *et al.*, 2019). During drought stress conditions, ABA production increases in roots resulting in the closure of stomata, which eventually limits the loss of water through transpiration (Shao *et al.*, 2009). Additionally, ABA modifies numerous aspects of plant growth, including leaf area and the ratio of dry root to shoot weight (Anjum *et al.*, 2011). This phytohormone serves as a stress-response hormone, and it stimulates the production of several genes whose gene products are essential for stress tolerance. Examples include osmoprotectants, late embryogenesis abundant (LEA) proteins, chaperones, and

transcriptional factors (TFs) (Osakabe *et al.*, 2014). Figure 1.2 summarizes some of the signal functions of ABA under drought stress.

Yan *et al*, (2020) investigated the interaction between hydrogen-rich water (HRW) and ABA on tomato seedlings under drought stress. Both HRW and ABA were found to increase plant height, stem diameter, and root activity, as well as improve drought tolerance through increased photosynthesis, antioxidant enzyme activity, and gene expression of antioxidant enzymes (Yan *et al.*, 2020). Overall, the study demonstrates that H_2 can regulate plant response to abiotic stress through ABA regulation.

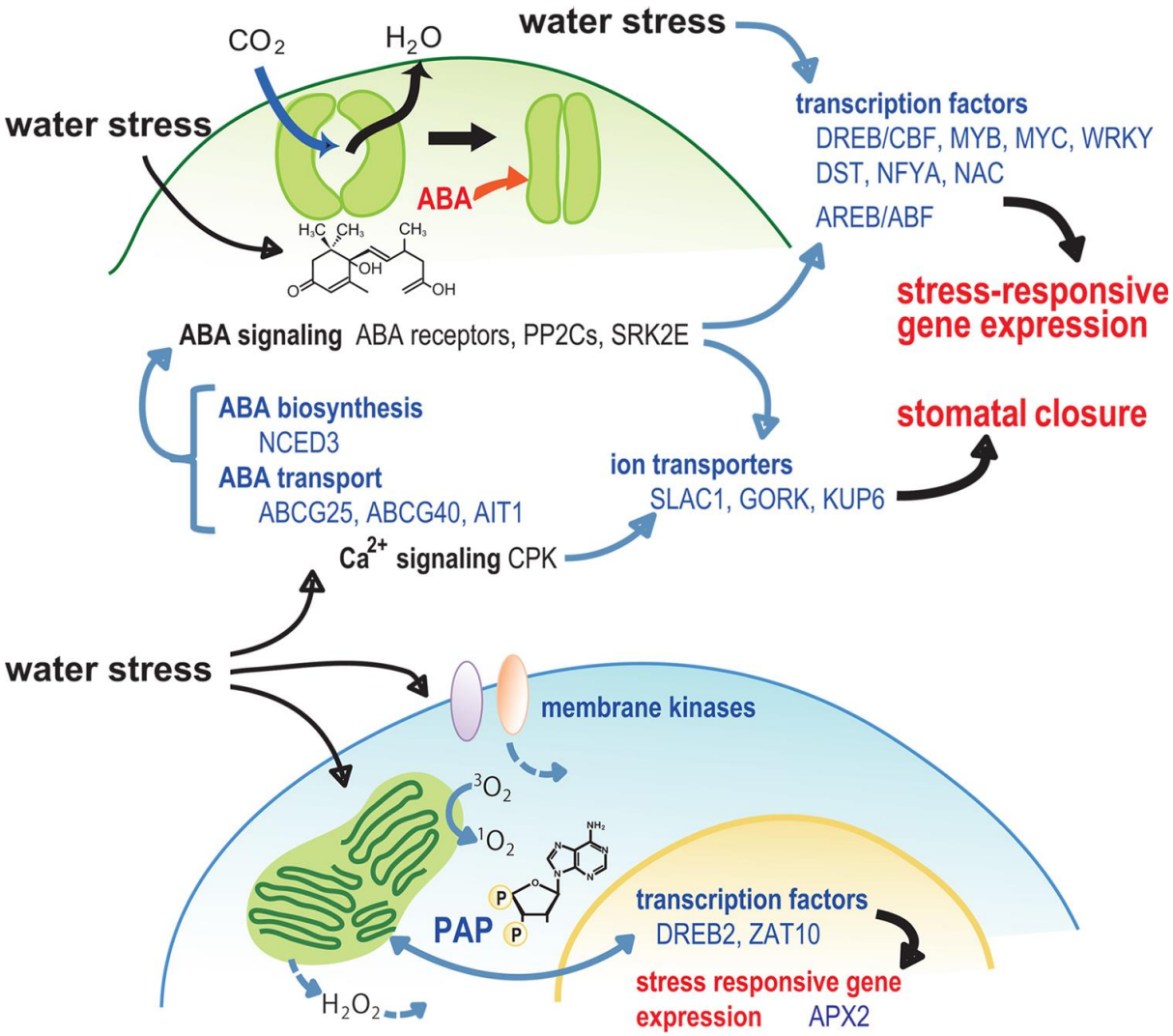

Figure 1.2: Role of ABA in stomatal closure and stress responsive gene expression under drought stress. Adapted from Osakabe *et al.* (2014).

1.2.3.2. Osmolyte accumulation

During drought stress, plants synthesize a variety of organic solutes such as polyhydric alcohols, ammonium compounds, proline, and glycine betaines for use in a process called osmotic adjustment (Blum, 2017). Osmotic adjustment is the lowering of the osmotic potential because of the net accumulation of solutes in response to water deficits (Blum, 2017). Accumulated osmolytes protect enzymes and cellular macromolecules from the damaging effects of ROS (Farooq *et al.*, 2009). They further stimulate the ability of root systems to absorb more water from the soil's dry conditions when there is water scarcity (Szabados and Savoure, 2010).

Chimenti *et al,* (2006) assessed osmotic adjustment of maize plants during the early growth and flowering stages under conditions of limited water supply. The findings demonstrated that osmotic adjustment enhanced the ability of maize plants to withstand drought both before and throughout the flowering stage (Chimenti *et al.*, 2006). Proline is an essential amino acid that accumulates primarily in leaves during drought stress and is utilized to stabilize macromolecules like enzymes and proteins and maintain membrane integrity (Anjum *et al.*, 2011; Kaur and Asthir, 2017). Additionally, proline helps to stabilize cellular redox potential by quenching free radicals (Ashraf and Foolad, 2007). According to Szabados and Savouré, (2010), proline may also serves as a source of energy, carbon, and nitrogen during the post-drought recovery process. Similarly, Nayyar *et al*, (2003), observed an increase in proline accumulation in wheat genotypes under drought conditions. The study also reported that a wheat genotype that was drought-tolerant had a higher proline concentration than the susceptible one (Nayyar *et al.*, 2003).

Glycine betaine is a quaternary ammonium compound that is commonly studied in a range of crops under stressful environments (Farooq *et al.*, 2009; Kaur and Asthir, 2017). This osmolyte functions in protecting enzymes, membranes, and lipids of the photosynthetic apparatus from dehydration-induced damage (Rhodes and Nadolska, 2001; and Anjum *et al.*, 2017). Another study assessed whether foliar application of glycine betaine alters growth, gas exchange and mineral nutrition of maize plants under drought stress (Shafiq *et al.*, 2021). The study found that wheat genotypes' growth, yield, gas exchange characteristics, and mineral nutrients were all negatively impacted by drought stress (Shafiq *et al.*, 2021), while glycine betaine applied directly under conditions of water stress significantly increased shoot fresh and dry biomass of all cultivars (Shafiq *et al.*, 2021).

1.2.3.3. The antioxidant defence system

Reactive oxygen species interfere with normal plant metabolism through membrane lipid peroxidation and protein denaturation (Farooq *et al.*, 2009). However, plants have developed defense systems that protect cell structures against stress damage through ROS scavenging processes (Nadarajah, 2020). Components of enzymatic and non-enzymatic antioxidant systems accumulate largely in stressed plants to counteract the negative effects of ROS (Anjum *et al.*, 2011). Among the enzyme-based antioxidants are catalase (CAT), superoxide dismutase (SOD), glutathione reductase (GR), and ascorbate peroxidase (APX). These enzymes regulate ROS homeostasis in plants and are involved in the reduction of superoxide radicals and hydrogen peroxide under drought stress (Kohli *et al.*, 2019; Nadarajah, 2020). Tocopherols, carotenoids, and ascorbic acid are non-enzymatic antioxidants that reduce ROS activity and prevent oxidative damage (Nadarajah, 2020).

In the chloroplast, tocopherol and carotenoid antioxidants are bound to the lipid matrix of thylakoid and chloroplast membranes for their protection against oxidative damage (Farooq *et al.*, 2009). Carotenoids scavenge the superoxide radicals and singlet oxygen, while tocopherols scavenge singlet oxygen and lipid peroxy radicals, which destroy membranes (Reddy *et al.*, 2004). In the ascorbate-glutathione cycle, enzymes such as APX, GR, and monodehydro-ascorbate reductase allow the scavenging of superoxide radicals (Farooq *et al.*, 2009). All the above-mentioned enzymatic and non-enzymatic antioxidants contribute to a key role of quenching ROS under environmental stresses (Farooq *et al.*, 2019).

Three maize hybrids were the subject of a study by Anjum *et al*, (2017) to evaluate the drought-induced oxidative damage in terms of ROS generation and activation of enzymatic and non-enzymatic antioxidants. The findings indicated that the three maize hybrids accumulated more enzymatic and non-enzymatic antioxidants under drought stress (Anjum *et al.*, 2017), possibly to lessen the negative impact of oxidative stress. The study by Gholamin and Khayatnezhad (2020), examined the effects of drought-induced stress on physiological parameters and antioxidant enzyme activities of bread wheat genotypes. The study found that drought stress increased catalase activity while decreasing peroxidase and superoxide dismutase levels (Gholamin and Khayatnezhad, 2020). The study also observed decreased chlorophyll concentration and relative water content in the flag leaves under the harsh environmental conditions (Gholamin and Khayatnezhad, 2020). The above-mentioned studies highlight the importance of the antioxidant defence systems in protecting plant against oxidative stress caused by drought stresses.

1.2.3.4 Maize responses to drought stress

Maize (*Zea mays*) is a cereal crop mainly used as a staple food around the world (Sandhya *et al.*, 2010). It is a monocot from the *Poaceae* family and normally grows in summer seasons (Bizana *et al*, 2014). With the climate changing, maize crop production has decreased and thus posing a threat to global food security (Bizana *et al.*, 2014). Under drought conditions, the metabolic activity and photosynthetic rate of maize is adversely affected resulting in reduced biomass and food production (Cattivelli *et al.*, 2008). Since maize is important for world food security, it is vital to work towards developing more drought tolerant maize varieties, which can produce good yields under drought conditions (Ahmad *et al.*, 2016).

Zhang *et al*, (2018) used the RNA sequencing technique to analyse the transcriptome responses of maize seedlings to drought. Using a maize reference line B73, the researchers examined the physiological reactions and overall gene expression patterns brought on by treatments for 3- and 6-day droughts and 1-day water recovery. Genes exhibiting functions including oxygen-evolving complex, stimulus responses, and oxidoreductase activities were among the 6107 genes that were found to be drought-responsive (Zhang *et al.*, 2018). Measurements of plant morphology and physiology revealed that drought stress reduced photosynthetic efficiency and prevented plant cell division, resulting in relatively small seedling leaves (Zhang *et al.*, 2018).

Saad-Allah *et al*, (2021) investigated the effects of drought on maize production and identified five maize genotypes with varying drought tolerance capacities. The experiment included mild and severe water stress treatments for two successive seasons, reducing plant growth and yield for all maize genotypes. However, the length of the watering interval was found to increase the concentration of several metabolic compounds and enzymes. Saad-Allah *et al*, (2021) also identified drought-responsive genes expressed in maize plants. The genotypes G10 and G123

were found to be relatively water stress tolerant due to their improved osmoregulatory, antioxidant, and metabolic activities, as well as their possession of stress-responsive genes (Saad-Allah *et al.*, 2021).

Yang *et al*, (2015) used two different maize genotypes, one with high drought tolerance and the other with low drought tolerance, and exposed them to drought stress. The study found that the genotype with low drought tolerance had higher levels of reactive oxygen and nitrogen species, which can cause damage to plant cells, compared to the drought-tolerant genotype (Yang *et al.*, 2015). Dong *et al*, (2020) conducted a comparative proteomics analysis of two maize hybrids to understand the mechanisms that make them tolerant to drought stress. The study identified several differentially expressed proteins involved in various metabolic pathways, including photosynthesis, energy metabolism, and stress response (Dong *et al.*, 2020). They found that proteins related to photosynthesis, carbon metabolism, and stress response were upregulated in the tolerant hybrid, while some proteins related to protein synthesis and energy metabolism were downregulated (Dong *et al.*, 2020). The results suggest that the two hybrids have distinct mechanisms for coping with drought stress, with one relying on energy conservation and the other on stress signal transduction (Dong *et al.*, 2020). The findings provide insights into the complex molecular mechanisms underlying drought tolerance in maize and can guide future efforts to breed crops that are more resilient to environmental stress (Dong *et al.*, 2020).

Zeng *et al*, (2019) used proteomics to identify proteins that were differentially expressed in the drought-tolerant Chang 7-2 and drought-sensitive TS141 maize varieties under drought stress. The study found that the drought-tolerant variety had higher levels of proteins involved in stress response, energy metabolism, and antioxidant defence, while the drought-sensitive variety had

higher levels of proteins involved in cell wall metabolism and protein degradation (Zeng *et al.*, 2019). The study revealed mechanisms underlying drought tolerance in maize and could inform efforts to develop more drought-tolerant crops. Table 1 shows a summary of studies on maize under drought stress including the duration of water limiting conditions.

Table 1: List of maize varieties under different time points of drought stress treatment.

Maize type	Age of a plant	Temperature day/night	Duration of stress treatment	Sample tissue	Techniques	Growth medium	References
ND476 (Drought tolerant), ZX978 (Drought sensitive)	V12, VT, R1 and R4 stages		12 days drought stress	Leaf	RNA Sequencing and transcriptome profiling	Soil	Dong *et al*.,2020
(Chang 7-2) drought-tolerant and TS141(drought-sensitive)	2 days after sowing	25/20˚C	20% PEG 6000 Until V3 stage	Root	iTRAQ Quantitative analysis	Soil	Zeng *et al*.,2019
vp16 (Drought-tolerant mutant) and Vp16 (drought-sensitive wild-type)	3 days after sowing		7 days 20% polyethylene glycol (PEG)-6000 treatment.	Seed	qRT-PCR and RNA Extraction, cDNA	Whatman germination paper	Liu *et al*.,2019
B73	25 days after sowing	28 /22 ˚C	7 days	leaf	RNA-sequencing and bioinformatics analysis	Soil	Guo *et al*., 2021
FR697	15 days after sowing	26/18 ˚C	12 days	Leaf (xylem sap)	Proteome analysis	Soil	Alvarez *et al*., 2008
B73	3 leaf stage	28/22 ˚C	5 days	Leaf	qRT-PCR and iTRAQ quantitative analysis	Soil	Jiang *et al.*, 2019
KS140	25 days		10 days	Leaf	2-DE and qRT-PCR analysis	Sandy loam soil	Kim *et al*.,2015
GraceE5,Va353 and, Lo964 , A638, Lo1016, and B73	30 DAP (V3/4 growth stage)	35 to 42 ℃	9 days	Leaf	Principal component analysis (PCA)	Soil	Yang *et al*.,2015
Zheng Dan 958	8 leaf stage	22 to 28 ℃	8 hours PEG(−0.7 MPa) solution	Leaf	iTRAQ-based quantitative and LC-MS/MS	Hoagland's nutrient solution	Zhao *et al*.,2016

1.4. Aim and objectives of the study

The **aim** of this study was to perform a comparative morphological, physiological, biochemical and root proteome analyses of maize seedlings in response to drought stress.

The **objectives** of the study were to:

i. Evaluate the morphological, physiological, and biochemical changes in maize varieties in response to drought,
ii. Identify root proteome changes of the maize varieties using proteomic tools, and
iii. Functionally group the drought responsive proteins using bioinformatics tools.

Maize is an important food crop and is widely used as staple food in many developing countries. With the changing climate, it is important to work towards the development of more drought tolerant crops which can produce good yields under hot and dry conditions. Understanding these drought responses will assist in identifying genes that could be used in plant breeding programs for the development of drought tolerant maize varieties. Therefore, the acquired knowledge will improve future crop production and the growth of the agricultural sector and the economy.

Chapter 2

Material and methods

2.1 Plant materials

Dr. Kingstone Mashingaidze from the Agricultural Research Council Grain Crops Institute in Potchefstroom, South Africa, provided the maize (*Zea mays*) seeds. After preliminary tests, the maize varieties CN07/8-224 and CN07/8-292 were chosen for the study, although their drought phenotypes are not yet known.

2.2 Methods

2.2.1 Seed germination and seedling growth

Forty maize seeds of CNO7/8-224 and CN07/8-292 varieties were germinated at 28/18 °C (day/night) in a growth chamber for five days. Twenty seeds were placed in each Petri-dish with two layers of moist filter paper per variety. After 5 days, two seedlings were sown in each 10 cm polystyrene pot containing 150 g of loam soil (Culterra, Harrismith, South Africa). In order for plants to grow well, this soil was saturated with nutrient solution (Nitrosol, Braamfontein, South Africa) and left to drain for 2 hr. Each variety had 20 biological replicates. The seedlings were incubated in a growth chamber (Model: GC-539DH, Already Enterprises Inc, Taipei, Taiwan) in a controlled environment with a day/night temperature of 28/18 °C, with a photoperiod of 16 hr. Seedlings were also grown in a greenhouse at the University of the Free State QwaQwa Campus in a controlled environment with a temperature of 28 °C for 24 hr. The plants were irrigated with 40 ml of distilled water every second day. At the two-leaf stage (7 days after sowing), drought stress was imposed on maize plants by withholding water for 14 days, while continuing to water the control plants every second day.

2.2.2. Plant growth parameters

To detect changes in plant growth, shoot and root length and fresh weight were measured using a ruler and weighing balance, and recorded. Ten biological replicates were used for each treatment.

2.2.3. Soil moisture content (SMC)

A protocol by Vineeth *et al*, (2016) was used with some slight modifications to determine the soil moisture content. Following a 14-day treatment for drought stress, the soil moisture content was measured using the gravimetric method. The moist weight of the soil that was used to grow maize seedlings was weighed and recorded. The soil was then oven - dried at 105 °C for 72 hr after which the dry weight of the soil was measured and recorded. The soil moisture content (SMC) was calculated as

$SMC = [(WW – DW)/DW] \times 100$

Where WW = wet weight, and DW = dry weight.

2.2.4. Relative water content (RWC)

The leaf relative water content was measured using the third and fourth oldest leaves as previously described by Barrs and Weatherly, (1962). The third oldest leaf was harvested and weighed immediately for fresh weight measurements. The turgid weight was determined by weighing the leaf sample after 24 hr immersion in distilled water in a sealed 50 ml Falcon tube which was placed in the dark at 4 °C. The dry weight was obtained by measuring the leaf sample after oven drying for 48 hr at 60 °C. The same protocol was repeated for the fourth leaf. Five biological replicates were analysed per treatments for each variety.

The RWC was calculated using the formula,

$$\text{RWC} = \frac{FW-DW}{TW-DW} \times 100$$

Where RWC = relative water content, FW = fresh weight, DW = dry weight, TW= turgid weight as previously described by Barrs and Weatherly, (1962).

2.2.5. Chlorophyll content and carotenoids

Chlorophyll and carotenoid content were determined using the method followed by Wellburn, (1994) with slight modifications. A mass of 50 mg of frozen third leaf tissue was weighed and mixed with 20 ml of DMSO in a 50 ml Falcon tube. The mixture was then incubated in a water bath at 65 °C for 4 hr. Following the incubation, the mixture was vortexed for ten seconds to mix, and then it was allowed to settle before the absorbance was measured. One millilitre of the extract was transferred into a cuvette to measure the absorbance. Using 1 ml of DMSO as a blank, the absorbance was measured at 480, 649, and 665 nm wavelengths using a JENWAY 7300 spectrophotometer. The chlorophyll a, b and carotenoid content was calculated according to Wellburn, (1994) as follows:

Chlorophyll a (µg/ml) = $12.19(A_{665nm}) - 3.45(A_{649nm})$

Chlorophyll b (µg/ml) = $21.99(A_{649nm}) - 5.32(A_{665nm})$

Carotenoid: $[1000A_{480} = 2.14C_a\text{-}70.16C_b]/220$

2.2.6. Biochemical activity assays

2.2.6.1. Lipid peroxidation

The measurement of membrane damage was determined by measuring malondialdehyde (MDA) concentration using the protocol by Gokul *et al,* (2021) with slight modifications. Ground frozen third leaf and root material were used for the analysis. A 100 mg of the

powdered material was homogenized with 500 µl of cold 6 % (w/v) trichloroacetic acid (TCA) using a vortex mixer. The sample was then centrifuged at 15000 ×g for 15 min to pellet the material. The supernatant was removed from the tube and mixed with 450 µl of 0.5 % (w/v) thiobarbituric acid (TBA) made in 20% TCA. The mixture was incubated on a heating block at 90°C for 20 min. The sample was then allowed to cool in an ice bath for 5 min. The sample was centrifuged at 10000 ×g for 5 min. The absorbance of the supernatant was recorded at 532 and 600 nm using a JENWAY 7300 spectrophotometer.

2.2.6.2. Hydrogen peroxide

Following a method previously described by Gokul *et al* (2021), the hydrogen peroxide (H_2O_2) concentration was determined for the different treatments. The H_2O_2 standard curve was produced with the concentrations 0, 250, 500, 750, 1000, and 1250 mM. The H_2O_2 standards were done in triplicates. The TCA extraction that was done for root and leaf as described in Section 2.2.7.1. was used to perform this assay. A volume of 94 µl of TCA extracts was mixed with 656 µl reaction buffer containing [1.25 mM K_2HPO_4 at (pH 5.0) and 250 mM KI]. Reactions were incubated for 25 min at room temperature. The absorbance of the standards and samples were measured at 390 nm on a JENWAY 7300 spectrophotometer.

2.2.6.3. Superoxide

The superoxide content was determined using a method described by Gokul *et al*, (2021) with slight modifications. Two centimetres of freshly harvested third leaf tissues were incubated in a 2 ml Eppendorf tube with a solution containing [10 mM potassium cyanide (for inhibiting Cu / Zn SODs), 10 mM H_2O_2 (inhibiting Mn and Cu/Zn SODs), and 80 µM nitrotetrazolium Blue chloride]. The tubes were then filled with distilled water to a final volume of 800 µl and incubated for 20 min at room temperature. After the incubation period, the plant material was

crushed with a miniature pestle to release the superoxide present in the sample. The tubes were then centrifuged at 15000 ×g for 5 min. The supernatant was transferred to a clean 1.5 ml tube, and 750 µl was loaded into the cuvettes. The absorbance was read at a wavelength of 600 nm on a JENWAY 7300 spectrophotometer. An extinction coefficient of 12.8 mM^{-1} cm^{-1} for was used to calculate superoxide content. The blackish-purple colour that formed during the experiment was an indication of superoxide levels.

2.2.6.4 Protein extraction for biochemical activity assays

Root material was harvested and ground into a fine powder using a cold mortar and pestle. The 50 mg of root sample was homogenized in 800 µl of 0.004 M phosphate buffer, 1mM ethylenediaminetetraacetic acid (EDTA), and 5 % (w/v) PVP in distilled water. The sample was vortexed and centrifuged at 9000 ×g for five min. The supernatant was transferred into a new 1.5 ml Eppendorf tube. Followed by protein concentrations quantification using Bradford assay.

2.2.6.5. Superoxide dismutase activity

Nitroblue tetrazolium (NBT) photo-reduction was used to estimate superoxide dismutase activity (SOD) using the method reported by Gokul *et al*, (2021) with some minor modification. The reaction mixture contained 20 mM phosphate buffer (pH 7.8), 0.0005 mM riboflavin, 0.1 mM NBT, 0.1 mM ethylenediaminetetraacetic acid (EDTA), and 10 mM methionine. The enzyme extract (20 µl) was added to the reaction mixture and was made up to 750 µl with distilled water. The reaction mixture was placed on the light box and allowed to incubate for 20 min. Following the incubation, the absorbance of the mixture was read at 560 nm using a JENWAY 7300 spectrophotometer. One unit of SOD activity was defined as the amount of enzyme that inhibited 50% of NBT photo reduction.

2.2.6.6. Ascorbate peroxidase activity

Ascorbate peroxidase activity was assessed using the protocol of Gokul *et al*, (2021). The protein sample was extracted from frozen ground material as described in Section 2.2.7.4. After being aliquoted into 0.5 ml Eppendorf tubes, the protein extracts were treated with 2 mM ascorbate for 5 min. The protein samples were applied to a 96-well microtiter plate in triplicate. Each well containing a reaction mixture of a total volume of 200 ml had 71.43 mM K_2HPO_4 phosphate buffer (pH 7.0), 0.36 mM ascorbic acid, and 20 µM H_2O_2. To each well, 10 µl protein sample was added. The hydrogen peroxide substrate was added as the last component to start the reaction. The decrease in absorbance was recorded at 290 nm using a spectrophotometer (Fluostar, BMG). The extinction coefficient of 2.8 $mM^{-1}cm^{-1}$ was used to calculate the ascorbate activity.

2.2.7. Protein extraction for proteomics

The total soluble proteins were extracted from the maize roots using the method followed by Ngara, (2009). A 100 milligrams of frozen root samples were ground finely into powder using sterilized cold mortar and pestle and transferred into new 2 ml Eppendorf tubes. The samples were mixed with one millilitre of 10% (w/v) trichloroacetic acid (TCA) and centrifuged at 9300×g for ten min at room temperature. The supernatant was discarded after centrifuging the pellet three times with 1.5 ml of cold 80% (v/v) acetone at 9300×g for 10 min each wash. The pellets were air-dried for five minutes. The proteins were extracted for around 8 hr with vigorous vortexing at room temperature after adding the extraction buffer (9 M urea, 2 M thiourea, and 4% (w/v) 3-(3-Cholamidopropyl) dimethylammonio]-1-propane sulfonate (CHAPS)] to the pellet. The homogenate was subsequently centrifuged at 21000 ×g for 10 minutes and the supernatant containing total soluble proteins (TSP) was collected.

2.2.8. Protein quantification

The protein concentration of extracts was determined using a Bradford assay (Bradford, 1976) with slight modifications previously described (Ngara, 2009). The one milligram of Bovine serum albumin (BSA) was weighed and mixed with extraction buffer [9 M urea, 2 M thiourea and 4% 3-(3-Cholamidopropyl) dimethylammonio]-1-propanesulfonate (CHAPS)] to prepare the BSA stock solution. The BSA stock solution was prepared in duplicates for the standard curve by mixing 10 µl of 0.1 M HCl and 80 µl distilled water in 1.5 ml of plastic cuvettes. Protein extracts were also prepared in duplicate by mixing 10 µl of each protein extract with 10 µl of 0.1 M HCl and 80 µl distilled water in 1.5 ml plastic cuvettes. All the BSA standards and the protein samples were mixed with 900 µl of the diluted Bradford reagent and incubated for five minutes at room temperature, and the absorbance was read at 595 nm. The 0 mg/mL BSA standard solution was used as a blank. To calculate the unknown protein sample concentrations, the BSA standards were used to plot a standard curve.

2.2.9. One dimensional gel electrophoresis

The quantified protein samples, together with an unstained protein ladder (New England Biolabs Inc, Massachusetts, USA) with known sizes, were electrophoresed on a 12% (v/v) 1D sodium dodecyl sulfate (SDS) polyacrylamide gel as previously described (Laemmli, 1970). Following the manufacturer's instructions, the gels were cast using the Mini PROTEAN Tetra Cell gel casting equipment (Bio-Rad) on 1 mm thick plates. Protein samples were combined in a 1:1 ratio with 2X sample buffer (100 mM Tris-HCL pH 6.8, 200 mM (w/v) DTT, 4% (w/v) SDS, 20% glycerol, and a trace amount of bromophenol blue). The samples were pulse vortexed and centrifuged before being heated for three minutes at 100°C on a heat block. The gel wells were loaded with all of the denatured protein samples. An electrode running buffer

[25 mM Tris, 192 mM glycine, 0.1% (w/v) SDS] was used in gel electrophoresis on a Mini PROTEAN Tetra Cell (Bio-Rad) using a Basic PowerPac (Bio-Rad).

After gel electrophoresis, the gels were incubated in a Sypro Ruby fixing solution (40% (v/v) methanol, 10 % (v/v) acetic acid) for at least 30 min in Pyrex glass dishes. After the fixing step, the gels were immersed in Sypro Ruby Protein gel stain overnight in the dark with gentle shaking. After overnight staining, the gel was rinsed once with distilled water. Lastly, the gel was immersed in a destaining solution (10% (v/v) methanol and 6% (v/v) acetic acid) for 30 min per was for two washes with gentle shaking. The gel was scanned using the correct gel platform and filters on a Gel Doc^{TM} XR+ Molecular imager with Image Lab^{TM} software version 5.2.1 (Bio-Rad).

2.2.10. Protein precipitation

The protein extracts were precipitated in 80 % (v/v) acetone overnight at -20°C and the samples were centrifuged at 3000 rpm for 10 min. The pellets were washed three times with ice-cold 80% (v/v) acetone by centrifuging the protein precipitates at 21000 ×g for 10 min. Following that, protein pellets were covered with an appropriate volume of 80% (v/v) acetone before being were sent to Durham University in the UK for isobaric tags for absolute and relative quantitation (iTRAQ) analysis. However, all the data analyses were performed at the University of the Free State's QwaQwa Campus.

2.2.11. iTRAQ analysis

2.2.11.1. Sample labelling

Following the manufacturer's instructions, the samples were air-dried and re-solubilized using an iTRAQ Reagent-Multiplex Buffer Kit (AB Sciex). Root samples of both maize varieties

CN07/8-224 and CN07/8-292 were separately digested with trypsin and prepared for iTRAQ analysis. For each maize variety, the four biological replicates of the control were labelled with tags of molecular weight 113, 114, 115, and 116, while the drought stressed samples were labelled with tags of molecular weight 117, 118, 119, and 121. This gave rise to two separate iTRAQ experiments, each consisting of the control and drought samples for each maize variety.

2.2.11.2. Sample clean up

To remove unincorporated labels and buffer salts, samples were cleaned using Hydrophilic interaction liquid chromatography – mass spectrometry (HILIC SPE) cartridges (Poly-LC Inc.) containing 300 mg of 12 m poly Hydroxyethyl-A. After adding 4.3 ml of the binding solution (85% acetonitrile, 30 mM ammonium formate pH 3.0), 4.3 ml of the releasing solution (5% acetonitrile, 30 mM ammonium formate pH 3.0) was used to equilibrate the cartridges. The dry iTRAQ-labelled peptide residue was dissolved in 75 µl of 3% acetonitrile, 0.1% formic acid, and 150 µl of 0.3 M ammonium formate, pH 3. Trifluoroacetic acid was used, if necessary, to bring the mixture's pH to 3.0. The samples were combined with 1275 µl of acetonitrile after being clarified by centrifugation (9300 ×g, 10 min). The 1.5 ml sample from this process was transferred to the SPE cartridge, and the flow-through was retained and passed through again. Then, two washes of 2 ml binding solution were applied to the column. The peptides were then extracted using a 2 x 1 ml releasing solution. The eluate was freeze-dried and re-suspended in 3% acetonitrile and 0.1% formic acid for liquid chromatography-mass spectrometry.

2.2.11.3. Liquid chromatography-mass spectrometry analysis

A Triple TOF 6600 mass spectrometer and Eksigent 425 LC system with Sciex Nanospray III source were used to perform gel liquid chromatography-mass spectrometry (LC-MS/MS). Five µg protein peptides were used for each run, and peptides were separated using a trap and elute

method. Samples were cleaned using a Triart C18 guard column acting as a trap and then separated online using a Triart C18 column over 87 min at a 5 µl/minute flow rate. The separation process used a mixture of 0.1% formic acid in water (Buffer A) and 0.1% formic acid in acetonitrile (Buffer B). Sequential linear gradients of 3 to 5% B over 2 min, 5 to 30% B over 66 min, 30 to 35 % B over 5 min, and 35 to 80% B over 2 min were followed by a three 28-min column wash in 80% B. Return to 3% B was over 1 minute before column re-equilibration for 8 min. Up to 30 ions were selected for fragmentation during the 85 min using collision energy adjusted for iTRAQ-labelled peptides. Precursor-ion scans were conducted at 400 to 1600 m/z and lasted 250 ms, followed by CID fragmentation and MS/MS spectrometry at a range of m/z 100-1500 for 50 ms. A cycle time of 1.8 secs was used, and a 15-sec exclusion was enforced to prevent multiple instances of the same peptide's fragmentation. The Analyst TF 1.7.1 software from AB Sciex was used to control and process the data.

2.2.11.4. Mass spectra data

With a few minor adjustments, data analyses for mass spectrometry were carried out as previously described by Smith *et al*, 2015. A minimum protein score threshold of 2.0 at a 99% confidence interval was specified for protein identification, whereas a minimum threshold of 1.3 at a 95% confidence interval was set for each discovered peptide. The dataset was purged of any proteins determined by a single peptide. The amount of each protein in each sample was calculated as a ratio to the 113-tagged sample for quantitative analysis. The average ratios for each protein in the control and drought-stressed samples were computed across the four biological replicates. The ratio of the sample average under drought stress to the control sample average served as a measure of the fold change in protein expression. The drought stress sample averages served as the numerators, with the controls serving as the denominators, and a negative sign indicated downregulation for the drought stress-responsive proteins. The

probability values for comparing the control averages with the sample averages under drought stress were computed using the Student's *t*-test.

2.2.12. Bioinformatics analysis

The UniProt database (http://www.uniprot.org) and Gene Ontology (GO) analysis were used to functionally annotate the discovered proteins. Gene Ontology annotation (http://geneontology.org/) categorized proteins into three groups based on their biological processes, molecular functions, and cellular components.

2.2.13 Statistical analysis

The means of the physiological and biochemical outcomes were compared using the One-way ANOVA test, Tukey HSD test using SPSS, with a 5% level of significance.

Chapter 3

Physiological and biochemical responses of CN07/8-224 and CN07/8-292 maize varieties to drought stress

3.1. Introduction

Plants require sufficient water supply for their growth, development, and reproductive processes (Fang and Xiong, 2015). Therefore, prolonged drought stress can severely disrupt plant physiology and biochemistry (Osakabe *et al.*, 2014). Water deficit also triggers stomatal closure to limit water loss. In turn, the rate of carbon dioxide uptake is restricted, eventually reducing the plant's photosynthetic capacity (Fang and Xiong, 2015). As a result, factors that determine morphology and growth, such as plant height and fresh and dry shoot biomass, are adversely impacted (Qi *et al.*, 2018).

However, plants modulate their morphology, physiology, and biochemistry in various ways to survive (Farooq *et al.*, 2009). For example, during drought stress, plants develop extensive root systems to maintain high water uptake for improved growth and development (Islam *et al.*, 2011). Yang *et al*, (2015) conducted a study investigating the sensitivity of morpho-physiological traits of wheat (*Triticum aestivum)* to different levels of soil water deficits. According to the findings, a limited water supply had a negative impact on plant height, shoot relative water content, net photosynthetic rate, stomatal conductance, transpiration rate, and nutritional levels (Yang *et al.*, 2015). Furthermore, the results showed differing levels of sensitivity of each wheat trait to different levels of soil water availability (Yang *et al.*, 2015).

Reactive oxygen species (ROS) are produced in abundance and accumulated under drought stress, which can contribute to oxidative stress (Parveen *et al.*, 2019). ROS are essential

elements of signal transduction pathways that initiate stress responses (Laxa *et al.*, 2019), while their over accumulation can cause damage to lipids, cellular membranes, proteins, and DNA (Parveen *et al.*, 2019). Under conditions of oxidative stress, lipid peroxidation occurs (Osakabe *et al.*, 2014), leading to increases in the levels of malondialdehyde (MDA), a lipid peroxidation product (Anjum *et al.*, 2011). Some plants are able to detoxify excess ROS in cells using a range of enzymatic and non-enzymatic antioxidants, thus counteracting the negative effects of oxidative stress (Qi *et al.*, 2018).

In another study, three Mexican maize landraces were investigated for changes in physiological properties and gene expression patterns under drought stress and recovery, including one drought-susceptible (85-2) genotype and two drought-tolerant (Cajete criollo and Michoaca'n 21) genotypes (Hayano-Kanashiro *et al.*, 2009). The drought stress was imposed on 30-day-old maize seedlings by withholding water for 17 days, followed by 10 hr of re-watering for the recovery phase. The results showed gene expression changes associated with several physiological mechanisms of drought adaptation (Hayano-Kanashiro *et al.*, 2009). For example, genes encoding PSI, PSII, and photosynthesis-related enzymes were significantly up-regulated after recovery, primarily in the tolerant genotypes. Furthermore, both drought-tolerant genotypes exhibited a rapid increase in photosynthesis during recovery compared to the drought-sensitive genotype. Meanwhile, the gene expression results indicated that the drought-tolerant genotypes were best able to rapidly regulate more stress-genes during drought and recovery in comparison to the susceptible genotype (Hayano-Kanashiro *et al.*, 2009). Overall, the study showed that genotypes with different drought phenotypes exhibit varying degrees of responses to water deficit stress, with the tolerant genotypes being better equipped to manage the stressful conditions.

The above-mentioned studies highlight some of the physiological and biochemical mechanisms that are utilised by plants in response to drought. Therefore, this chapter aimed to evaluate the morphological, physiological and biochemical changes of two different maize varieties in response to water limitation. During the course of the experiments mild stress was imposed in a growth chamber plants while the severe stress was imposed in greenhouse plants to compare the tolerance mechanisms of both CN07/8-224 and CN07/8-292 maize varieties. The following experiments were conducted from the growth chamber-grown plants: soil moisture content, phenotype, relative water content (RWC), malondialdehyde (MDA), hydrogen peroxide, superoxide radical anion content, and antioxidant enzymes, while from the greenhouse grown plants, assays conducted included, soil moisture content, RWC, and superoxide radical anion content

3.2 Results

3.2.1. Mild drought stress experiments with maize seedlings grown in a growth chamber

3.2.1.1. The effects of drought stress on soil moisture content

Seven-days old seedlings of CN07/8-224 and CN07/80-292 maize varieties were drought-stressed for 14 days, while the controls were watered every second day until the day of harvest when the experiment was terminated. This experiment evaluated the difference in moisture content present in the soil of control plants as well as the drought stressed maize plants. When compared to their respective controls that were able to maintain a 100% field capacity, the drought-stressed treatment pots had significantly lower amounts of soil moisture (Figure 3.1). The soil moisture content of the water limited pots of CN07/8-224 and CN07/8-292 varieties, significantly decreased by ~ 53.8 % and 47.9 %, respectively (Figure 3.1).

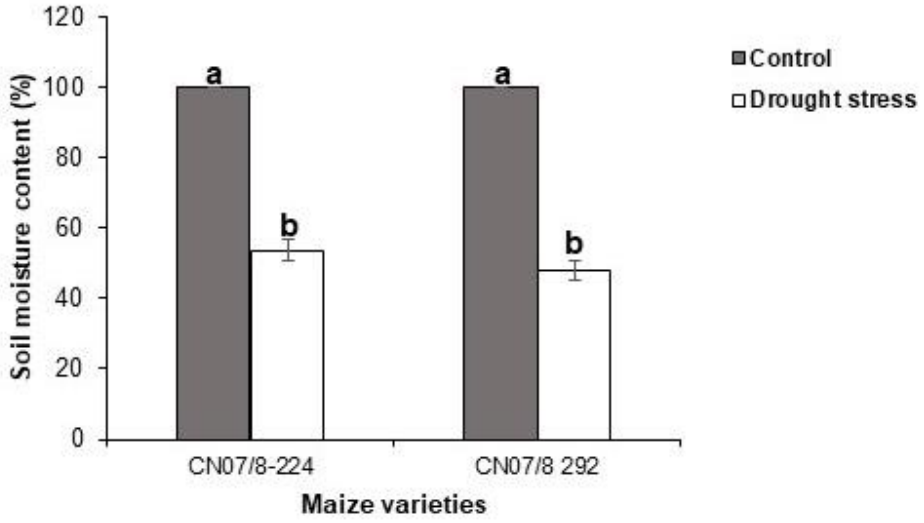

Figure 3.1: Soil moisture content as influenced by the mild drought stress. Data is presented as the mean ± standard error (n = 6). Significant difference is symbolized by different letters (ANOVA, Turkey HSD, $p \leq 0.05$).

3.2.1.2 Changes of morphological parameters in response to water deprivation

Following the 14-days of water limitation, the maize plants of both varieties showed slight changes in morphological appearance relative to their controls (Figure 3.2). It was obsereved that the first and second oldest leaves were drying out in both maize varieties. For CN07/8-224, the entire plant's leaves were wilting, while for cultivar CN07/8-292 the drought-treated maize leaves were rolling towards the end.

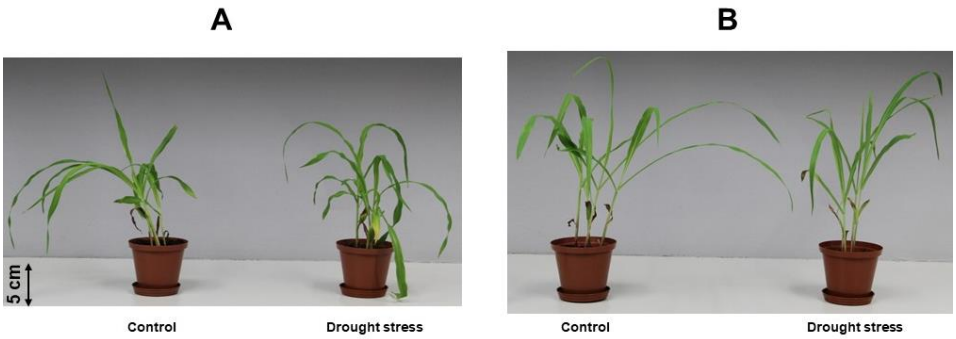

Figure 3.2: The different phenotypic responses of two maize varieties under mild drought stress. The phenotypic characteristics above are for seedlings in the fourth leaf stage after experiencing a 14-day water deficiency treatment in a growth chamber. Five biological replicates for control and drought treated plants were generated for (A) CN07/8-224 and (B) CN07/8-292 varieties.

3.2.1.2.1 Measuring the shoot and root length of maize plants

The root and shoot length readings were recorded on day 14 of the water stress treatment. The results observed are shown in Figure 3.3 below. No significant difference was observed in the fresh shoot length of the drought treated plants of both maize varieties when compared to their respective controls (Figure 3.3. A). A similar trend was observed for the fresh root length of CN07/8-292 following the drought stress treatment (Figure 3.3 B). In contrast the fresh root length of CN07/8-224 increased by about 36% following the drought treatment in comparison to the control plants (Figure 3.3 B). No significant difference was observed when comparing the CN07/8-224 drought treated plants to CN07/8-292 (Figure 3.3A & B).

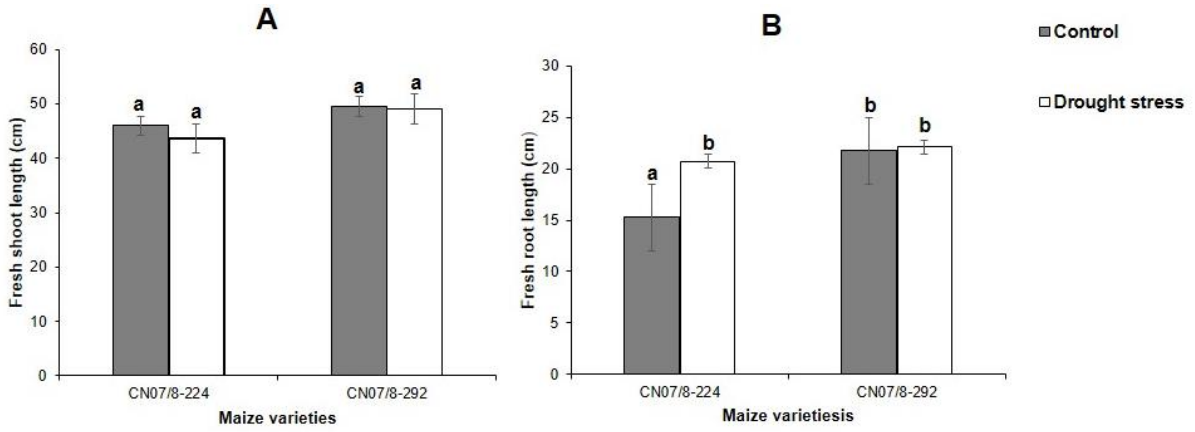

Figure 3.3: Effect of drought stress on fresh shoot (A) and root (B) length of the two maize varieties. Measurements were taken on day 14 of drought stress treatment. Data are presented as the mean ± standard error (n = 4). Significant difference is symbolized by different letters (ANOVA, Turkey HSD, $p \leq 0.05$).

3.2.1.2.2 Measuring the shoot and root weight of maize plant

The fresh shoot and root weight results are shown in Figure 3.4 below. There was no significant difference in the fresh shoot weight of the drought treated CN07/8-224 plants when compared to their controls. However, there was an ~18.2 % decrease in the fresh shoot weight of CN07/8-292 drought treated plants when compared to the CN07/8-292 controls. A significant decrease in fresh shoot weight of ~ 29.5% was also observed when comparing the CN07/8-292 drought treated plants with CN07/8-224 drought treated plants (Figure 3.4 A). When assessing the fresh root weight, a significant increase of ~ 33% was observed in the drought treated CN07/8-224 plants relative to their controls. However, no significant difference was observed between the fresh root weights of drought treated CN07/8-292 plants and their controls. No significant difference was observed between the drought treated CN07/8-224 and CN07/8-292 variety (Figure 3.4 B). The dry shoot (Figure 3.5 A) and dry root (Figure 3.5 B) weight readings showed no significant difference between the control and drought treated plants for both maize varieties.

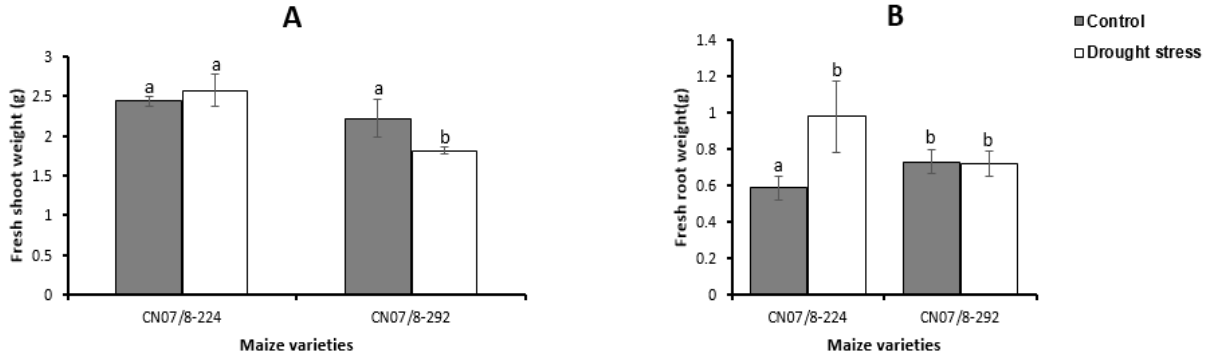

Figure 3.4: Effect of mild drought stress on fresh (A) shoot (B) root weight of the two maize varieties. Measurements were taken on 14 day of drought stress treatment. Data are presented as the mean ± standard error (n = 4). Significant difference is symbolized by different letters (ANOVA, Turkey HSD, $p \leq 0.05$).

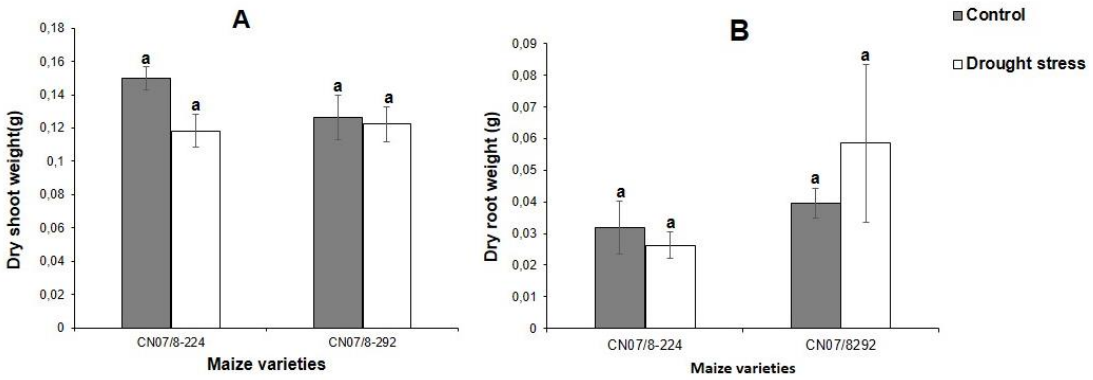

Figure 3.5: Effect of mild drought stress on dry (A) shoot weight and (B) root weight of maize varieties measurements on 14th day of drought stress treatment. Data is presented as the mean ± standard error (n = 4). Significant difference is symbolized by different letters (ANOVA, Turkey HSD, $p \leq 0.05$).

3.2.1.3. Physiological and biochemical changes in response to water deprivation

3.2.1.3.1. Leaf relative water content (RWC)

The relative water content of the 4th oldest leaf was estimated on day 14 of the water deficit treatment (Figure 3.6). The results showed no significant difference between the RWC of the watered control and drought stressed leaf samples of both varieties.

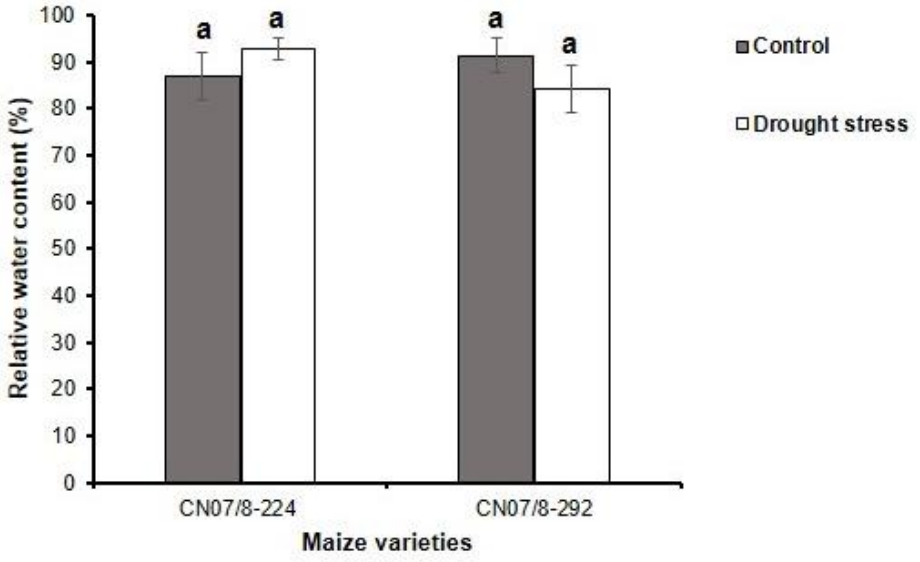

Figure 3.6: Effect of mild drought stress on the RWC of the fourth leaf of two maize varieties. Data is presented as the mean ± standard error (n = 4). Significant difference is symbolized by different letters (ANOVA Turkey HSD, $p \leq 0.05$).

3.2.1.3.2 Chlorophyll and carotenoid content

In this study, the 14-day drought stress treatment resulted in the reduction of both chlorophyll a and b, as well as carotenoid contents in the leaves of both maize varieties (Figures 3.7 A & B and Figure 3.8). There was a significant decrease in chlorophyll a of ~52.6% in the drought treated CN07/8-224 plants when compared to their control plants. However, no significant difference was observed between the chlorophyll a content of CN07/8-292 control and drought stressed plants. When comparing the CN07/8-224 drought-treated plants with the CN07/8-292 drought-treated plants it was observed that a significant reduction of ~56% in chlorophyll a was noted. (Figure 3.7A).

With regards to the chlorophyll b content, a significant decrease of ~53% and ~46% was observed for the drought treated CN07/8-224 and CN07/8-292 plants, respectively, when compared to their controls (Figure 3.7 B). Overall, the CN07/8-292 plants had a greater amounts of chlorophyll b before and after the drought stress treatment when compared to CN07/8-224 plants (Figure 3.7 B).

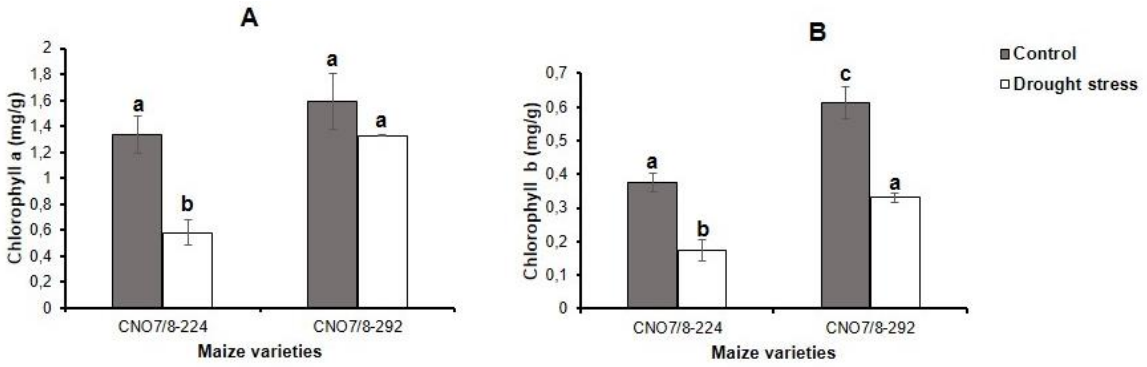

Figure 3.7: Effect of mild drought stress treatment on the chlorophyll content of third leaf material in two maize varieties. Data is presented as the mean ± standard error (n = 3). Significant difference is symbolized by different letters (ANOVA Turkey HSD, $p \leq 0.05$).

The amount of total carotenoids in the leaves of the drought-treated CN07/8-224 were significantly lower than in the leaves of the control plant by ~30%. The total carotenoids content in leaves of drought treated CN07/8-292 showed a decrease of ~42% when compared to CN07/8-292 control plants (Figure 3.8). However, there was a significant increase of ~42% in CN07/8-292 drought treated plants compared to CN07/8-224 drought treated plants (Figure 3.8).

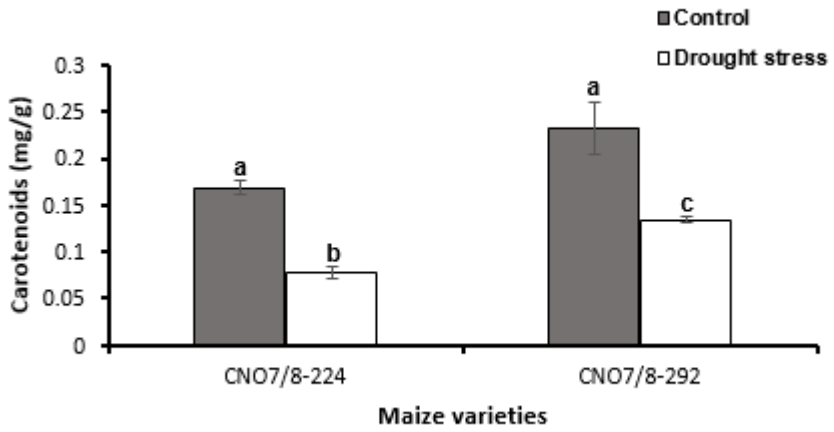

Figure 3.8: Effect of mild drought stress treatment on the carotenoids content of third leaf material in two maize varieties. Data is presented as the mean ± standard error (n = 3). Significant difference is symbolized by different letters (ANOVA Turkey HSD, $p \leq 0.05$).

3.2.1.3.3 The effects of drought stress on the MDA content in leaves and roots of two maize varieties

In this study, the level of lipid peroxidation was measured as the amount of MDA content in the leaves and roots of maize varieties. The results indicated that there was significant difference of ~18% between the MDA content of the drought-treated leaves and the control leaves of CN07/8-224 maize variety (Figure 3.9 A). There was no significant difference when comparing CN07/8-292 drought-treated leaves and the control leaves (Figure 3.9 A). A significant reduction in MDA concentration of ~32% was observed in the CN07/8-224 drought-treated leaves when compared to CN07/8-292 drought-treated leaves (Figure 3.9 A). No significant difference was observed for the root tissues of both varieties (Figure 3.9 B). The MDA concentration of the roots in CN07/8-224 and CN07/8-292, which had been exposed to drought stress did not however, show a significant difference (Figure 3.9 B).

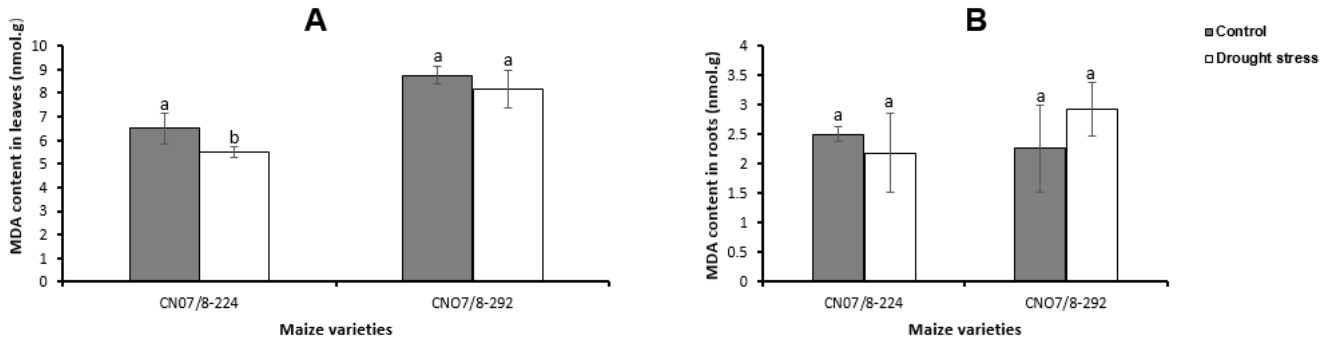

Figure 3.9: Effect of mild drought stress treatment on MDA content of leaves (A) and roots (B) in two maize varieties. Data is presented as the mean ± standard error (n = 4). Significant difference is symbolized by different letters (ANOVA Turkey HSD, $p \leq 0.05$).

3.2.1.3.4 Assessing the impact of drought stress on antioxidant levels

The levels of hydrogen peroxide concentration of leaves and roots were estimated, as shown by the results in Figure 3.10. There was no significant change in the hydrogen peroxide content of drought stressed CNO7/8-224 maize leaves (Figure 3.10 A) and roots (Figure 3.10 B) when compared to their respective controls. The CN07/8-292 drought treated maize leaves showed an ~15% increase in hydrogen peroxide concentration when compared to the CN07/8-292 control plants (Figure 3.10 A). A similar trend was observed in the CN07/8-292 roots, in which a significant increase of ~ 35% in hydrogen peroxide concentration was recorded in the drought treated roots when compared to their respective control plants. Comparing the roots of the drought-treated plants of CN07/8-292 to those of CN07/8-224 revealed a significant increase of ~ 75% in the amount of hydrogen peroxide produced (Figure 3.10 B).

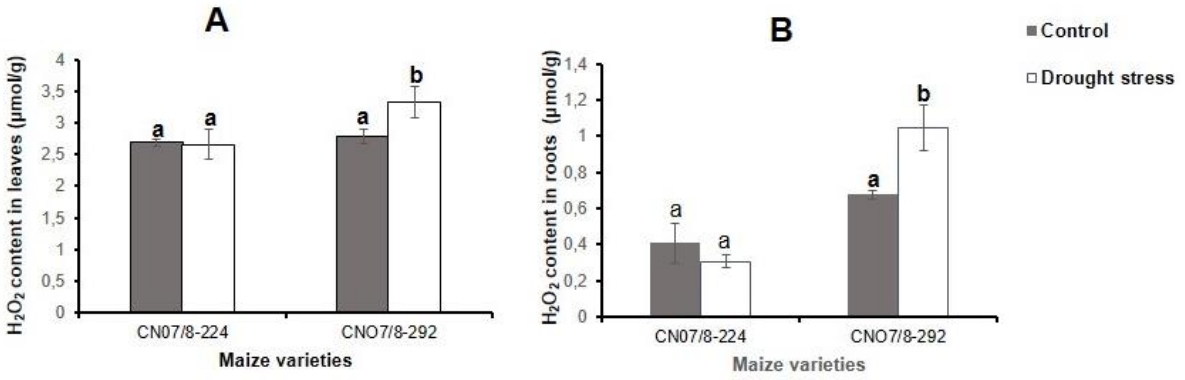

Figure 3.10: Effect of drought stress treatment on H_2O_2 content of leaves (A) and roots (B) material in two maize varieties. Data is presented as the mean ± standard error (n = 4). Significant difference is symbolized by different letters (ANOVA Turkey HSD, $p \leq 0.05$).

3.2.1.3.5 Superoxide dismutase and ascorbate peroxidase enzymes activities

The enzyme activity of superoxide dismutase was estimated in root tissues of both maize varieties following the water deficit stress (Figure 3.11 A). The results showed no significant difference in superoxide dismutase activity of drought treated CN07/8-224 root tissues as compared to the CN07/8-224 controls. However, a significant increase of ~73.5% in superoxide dismutase activity of CN07/8-292 drought treated roots compared to its CN07/8-292 control variety was observed. When comparing the CN07/8-292 drought-treated variety against the CN07/8-224 drought-treated variety lower superoxide dismutase activity of about 73.5% was observed. (Figure 3.11 A).

Estimations of ascorbate peroxidase activity in root tissues showed a general increase in enzyme activity in the drought stressed samples of both maize varieties (Figure 3.11 B). There was no significant increase of ~42% and ~56% in the drought treated roots of CN07/8-224 and CN07/8-292 varieties, respectively, when compared to their controls. However, no significant difference in the ascorbate peroxidase enzymes activity was observed when comparing the CN07/8-224 and CN07/8-292 drought treated plants activity (Figure 3.11 B).

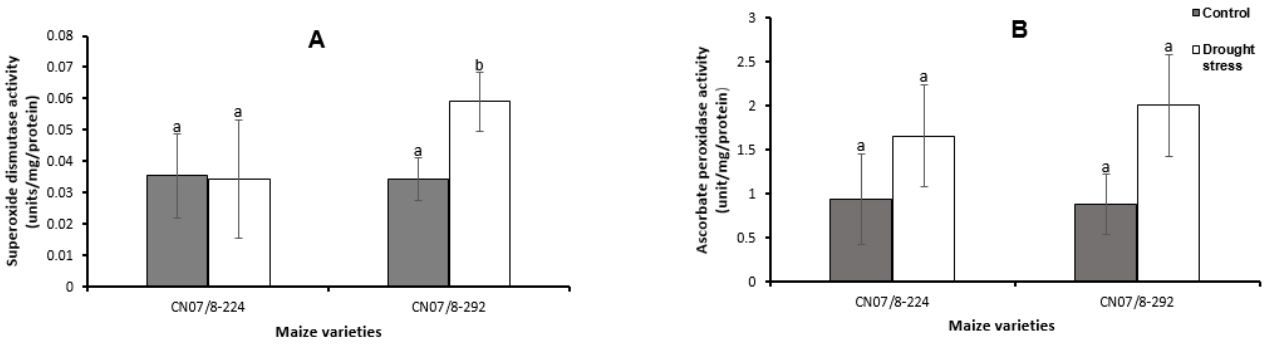

Figure 3.11: Superoxide dismutase (A) and ascorbate peroxidase (B) activities in controlled and the drought stress roots of CN07/8-224 and CN07/8-292. Data is presented as the mean ± standard error (n = 4). Significant difference is symbolized by different letters (ANOVA Turkey HSD, $p \leq 0.05$).

3.2.2. Experiments on maize seedlings grown in a greenhouse under severe drought stress

The growth experiments conducted using a growth chamber were replicated in a greenhouse at 28 ºC. The greenhouse became operational in April 2022. After collecting data from the growth chamber experiments, greenhouse experiments were conducted to evaluate the physiology and biochemical responses under drought stress.

3.2.2.1. Soil moisture content

CN07/8-224 drought treated pots showed a significant decrease of ~56% soil moisture content when compared to the control pots. CN07/8-292 drought-treated plants showed a significant decrease in soil moisture of 42% when compared to the CN07/8-292 control pots. However, there was no significant difference observed between drought treated CN07/8-224 and CN07/8292 varieties.

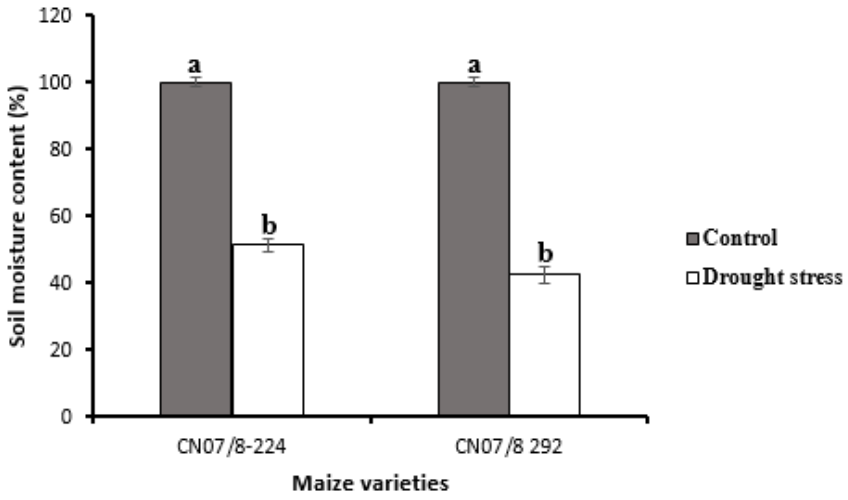

Figure 3.12: Soil moisture content as influenced by drought stress in the greenhouse experiment. Data is presented as the mean ± standard error (n = 5). Significant difference is symbolized by different letters (ANOVA Turkey HSD, $p \leq 0.05$).

3.2.2.2. Phenotypic responses to drought stress in maize seedlings

After 14 days of drought stress, plants exhibited symptoms of water limitation stress. The CN07/8-224 leaves showed wilt symptoms, while the CN07/8-292 leaves had a leaf rolling phenotype throughout the experiment.

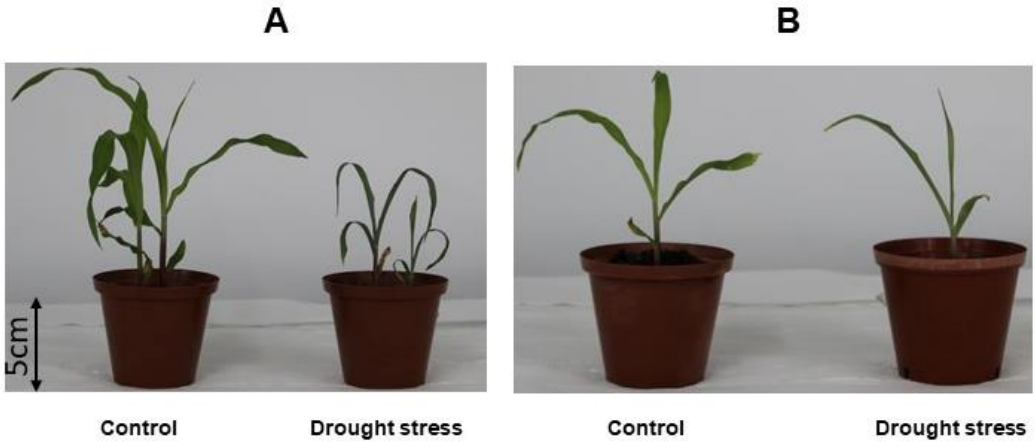

Figure 3.13: The two maize varieties show different phenotypic responses to drought stress in the greenhouse experiment. The phenotypic displays above are for seedlings in the fourth leaf stage after experiencing a 14-day water deficiency treatment in a greenhouse. (A) CN07/8-224 variety (B) CN07/8-292 variety.

3.2.2.3. Relative water content of the two maize plants under severe drought stress

Under severe drought stress, there was an ~67% decrease in the leaf relative water content for CN07/8-224 drought treated plants when compared to the CN07/8-224 control plants. In contrast, there was an ~49% decrease in leaf relative water content observed in the CN07/8-292 drought treated plants when compared to the CN07/8-292 control plants. When comparing the CN07/8-224 drought treated with plants CN07/8-292 drought treated plants a decrease of ~35% in relative water content was observed. (Figure 3.14).

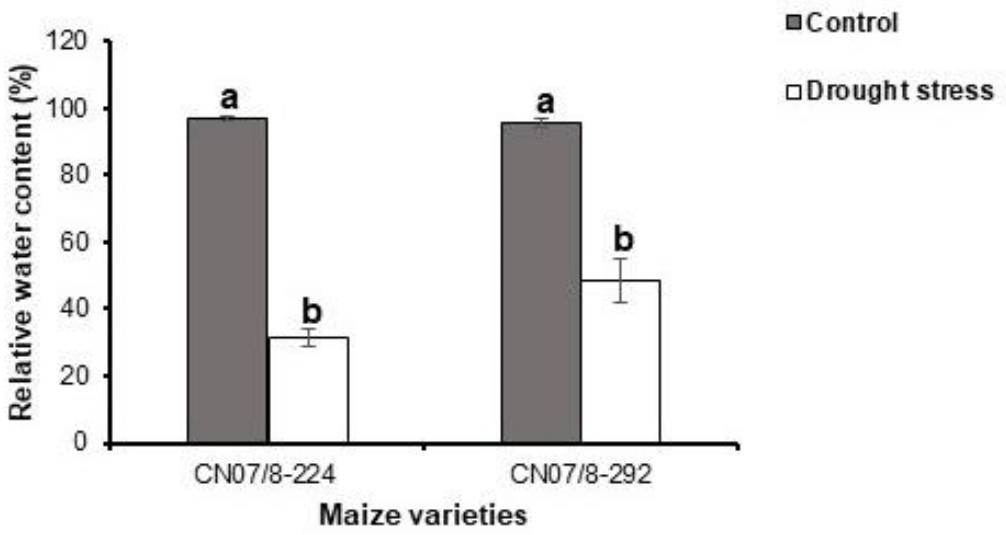

Figure 3.14: The effect of drought stress on RWC of the third leaf of the two maize varieties in the greenhouse experiment. Data is presented as the mean ± standard error (n = 4). Significant difference is symbolized by different letters (ANOVA Turkey HSD, $p \leq 0.05$).

3.2.2.4. Superoxide content

The superoxide content analysis of maize leaves and roots was done on fresh material. There was ~72% decrease in the superoxide content of the CN07/8-224 drought treated leaves relative to the CN07/8-224 control leaves. There was significant difference of ~ 63% observed in the superoxide content of the CN07/8-292 drought treated leaves when compared to the CN07/8-292 control leaves. The CN07/8-229 variety displayed no significant difference when comparing the drought treated roots to their respective controls (Figure 3.15 B). There was a significance difference observed in the superoxide content of the CN07/8-224 drought stressed roots compared to their respective controls (Figure 3.15 B).

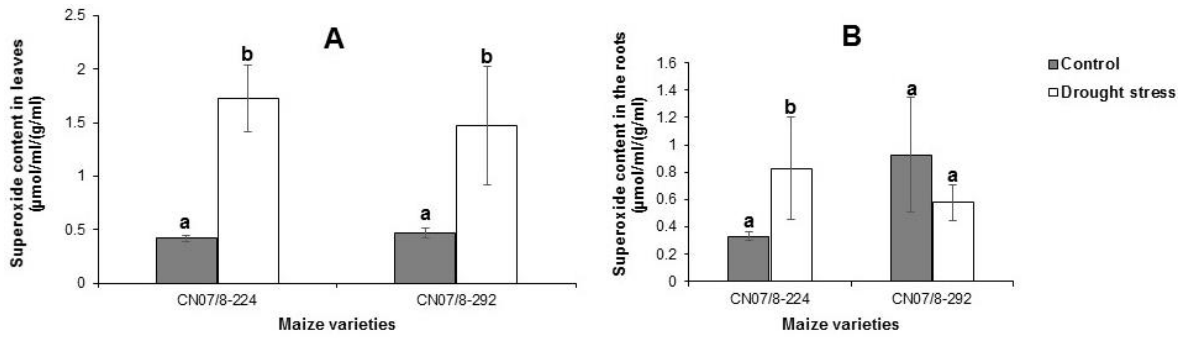

Figure 3.15: Effect of drought stress on superoxide content activity on the (A) third leaf and (B) roots two maize varieties. Data is presented as the mean ± standard error (n = 4). Significant difference is symbolized by different letters (ANOVA Turkey HSD, $p \leq 0.05$).

3.3. Discussion

Lack of water causes physiological, biochemical, and molecular changes in plants, which affect all growth phases of a plant's life cycle, including the final yield (Ali *et al.*, 2013; Khan *et al.*, 2019). The 14 days of drought stress on maize plants aimed to evaluate each variety's ability to withstand drought. This study used a gravimetric method to measure the soil moisture content of stressed and well- watered pots of each maize type. Drought stress significantly

decreased the soil moisture content of both maize varieties (Figure 3.1). Similarly, Praba *et al*, (2009) observed a significant decline in the soil moisture content of rice and wheat in response to drought stress.

During the harvesting process at the end of the experiment pictures were taken for physical observations. When looking at the CN07/8-224 plants, the leaves showed a yellow discoloration. It should be noted that CN07/8-224 had darker green color under control conditions compared to CN07/8-292 (Figure 3.2), possibly due to the difference in its chlorophyll a and b composition. Drought stress slows plant growth and negatively influences several physiological and biochemical functions, including respiration, and photosynthesis. No significant difference was observed in fresh shoot length of drought treated CN07/8-224 and CN07/8-292 (Figure 3.3 A). In the CN07/8-224 variety, there was an increase in root length of the drought-treated CNO7/8-224 variety compared to CN07/8-224 control plants (Figure 3.3 B). Hameed *et al*, (2010) reported an increase in the root length of tolerant wheat genotypes under drought stress. It could be that the roots elongated in order to search for water. There was no change in the leaf relative water content for both varieties CN07/8-224 under growth chamber conditions. This observation could mean that these varieties could conserve water during the drought.

In this study, CN07/8-224 drought-treated plants significantly increased fresh shoot weight compared to the drought-treated plants of CN07/8-292. As stated before, there was no significant difference in shoot weight for the CN07/8-224 variety. The results could mean that the CN07/8-224 variety adapted to drought stress by shortening their plants to conserve energy and water while elongating their root to access water and minerals to survive.

Dry weight analysis was done for both cultivars under control and drought conditions. For the dry shoot weigh no significant difference was observed for variety CN07/8-224 and CN07/8-292 drought-treated plants compared to their respective controls. A study on maize plants found that a severe drought conditions greatly affected the shoot and dry root weight of maize plant (Talaat *et al.*, 2015). In addition, Hameed *et al*, (2013) observed a decrease in the dry weight of wheat seedling's which were sensitive to drought.

No significant difference was observed in the leaf relative water content of drought-treated plants for CN07/8-224 and CN07/8-292 varieties when compared to their respective controls. In contrast, Bayoumi *et al*, (2008) reported a reduction in the relative water content of wheat genotypes under drought stress. Chlorophyll pigments play an essential role in energy dissipation and light absorption during plant growth (Hossain *et al.*, 2020). It is well known that water deficit stress inhibits the rate of photosynthesis by reducing the chlorophyll content in plant leaves. There were significant reductions in chlorophyll a, b, and carotenoid content of the drought-treated CN07/8-224 leaves relative to CN07/8-224 control plants. A significant decrease in chlorophyll b, and carotenoid content was also observed in the drought-treated CN07/8-292 variety. The results showed that chlorophyll a decreased significantly in CN07/8-224. Decreased chlorophyll a level can be used as a diagnostic tool to assess the severity and impact of drought stress on maize plants. This reduction in chlorophyll levels can hinder the plants' ability to capture light energy effectively and impair photosynthesis.

Under abiotic stress, such as water deprivation, malondialdehyde is considered as a marker of free radical damage to the cell membranes (Anjum *et al.*, 2011). There was a significant decrease in the MDA content in the leaves of drought treated CN07/8-224 leaves when compared to CN07/8-224 control leaves. This could mean that CN07/8-224 drought treated

plants were able to maintain high membrane stability, which therefore lowered the lipid peroxidation under drought stress (Figure 3.9 A). The drought-treated CN07/8-292 type had higher MDA naturally compared to the drought-treated CN07/8-224 type (Figure 3.9). Moharramnejad *et al*, (2019) supports our findings where MDA content was mainly higher in drought sensitive maize cultivar. This could mean that CN07/8-292 is more susceptible to water deficit compared to CN07/8-224.

The MDA content of the roots for both cultivars subjected to drought did not change (Figure 3.9 B). In contrast, Aslam *et al*, (2013) observed a high accumulation of the MDA content in soya bean roots under drought stress conditions. Similarly, Cruz de Carvalho, (2008) reported that the imposed drought stress induced MDA content in the maize leaves and roots. The aforementioned studies could have shown contrasting results due to the drought stress regimes used being different from that of the current study.

Hydrogen peroxide, in particular, may play a role in a range of processes such as signalling pathways required for plant growth and development as well as stress responses (Cruz de Carvalho, 2008). The cellular protective factors that are accumulated because of the H_2O_2 stress response signalling pathways may influence cellular redox status directly or indirectly (Cruz de Carvalho, 2008). This could mean that although there was no significant change happening in the hydrogen peroxide content of the leaves (Figure 3.10 A), it could be that hydrogen peroxide acted as signal transduction pathway to protect the cellular membranes of the CN07/8-224 plants. There was an increase of hydrogen peroxide content in CN07/8-292 drought treated leaves relative to the CN07/8-292 control leaves. This could mean that the drought stress

imposed to CN07/8-292 leaves increased the production of ROS that further caused a higher accumulation of hydrogen peroxide in the CN07/8-292 leaves.

There was no significant difference between the hydrogen peroxide concentration of the drought-treated roots and the control roots for variety CN07/8-224 (Figure 3.10 B). This could suggest that their root was able to use water and nutrients efficiently, as previously observed in other parameters that CN07/8-224 elongated their roots in response to drought stress. In contrast, hydrogen peroxide activity was higher in the CN07/8-292 drought-treated plants, indicating that the CN07/8-292 variety experienced water stress (Figure 3.10). According to Ashraf *et al*, (2010), during drought stress, MDA and H_2O_2 levels were higher in the leaves of a maize sensitive genotype than in the tolerant maize genotypes. In addition to having different reported antioxidant accumulations in CN07/8-224 and CN07/8-292, the two maize types also have different stress tolerance levels.

In spite of the ROS accumulation, plants activate a variety of adaptive systems in response to environmental signals to regulate their growth, development, and stress reactions. It is well known that enzymatic antioxidants play a significant role in scavenging ROS in plants under stress, including drought stress (Qi *et al.*, 2018). The superoxide dismutase is an antioxidant that acts as an early line of defence against oxygen-free radicals (Yang *et al.*, 2015). Superoxide dismutase can remove superoxide radicals, reduce membrane lipid peroxidation, and protect cell membrane stability (Aslam *et al.*, 2013). In the variety CN07/8-292 drought treated plants, there was a significant increase in SOD activity (Figure 3.11 A). This could mean that the imposed drought stress led to the increased in superoxide dismutase activity. Furthermore, Marcinska *et al*, (2013) stated that decreased MDA levels indicate higher antioxidant activity and increased drought resistance in a plant.

Ascorbate peroxidase is one of the essential antioxidant enzymes that play a role in drought stress tolerance in plants, by detoxifying hydrogen peroxide and scavenging free radicals (Yang *et al.*, 2015). A significant increase in ascorbate peroxidase activity was observed in both drought-treated CN07/8-224 and CN07/8-292 varieties compared with the CN07/8-224 and CN07/8-292 control plants. However, a higher activity of APX in CN07/8-292 drought-treated plants when compared to the CN07/8-224 drought treated plants. As observed in previous results (Figure 3.9 and 3.10), MDA and hydrogen peroxide contents were very high in the drought-treated plants of CN07/8-292 compared to CN07/8-224. The findings of Aslam *et al*, (2013) correlate with this study, which found that maize plants under drought stress had an increase in antioxidant activities. The increase of antioxidant enzymes in the drought stressed plants could mean that CN07/8-224 and CN07/8-292 plants were affected by stress, although they responded differently to mild drought stress.

Studies on the impact of drought stress on the vegetative and root growth of maize in a greenhouse revealed that drought stress decreased shoots and root growth (Ramadan *et al.*, 1986). After observing the plants and their physiological parameters in a greenhouse, relative water content is the key indicator that shows plant survival capability and leaf water status. CN07/8292 variety compared to the CN07/8-224 variety displayed a significantly improved relative water content which could be due to it being better in extracting water from the soil. In addition, Choi *et al*, (2015) also found that cultivation in the growth chamber had an advantage over greenhouses in the formation of photosynthetic pigments in the leaves of strawberries.

We first discussed the RWC content in mild drought stress separately, however in more severe stress, we saw that there was a great decrease in the RWC of the drought-treated plants. Water stress had a significant inhibitory effect on the plant water status. As observed in Figure 3.12, the phenotypic characteristics of the two drought-treated maize varieties showed a great decrease in plant growth in the greenhouse compared to the growth chamber plants. These results correlate with the obtained leaf relative water content results. Based on our data, using the greenhouse might take shorter time for screening drought tolerant maize than using a growth chamber.

Chapter 4

Comparative proteomic analysis of CN07/8-224 and CN07/8-292 maize root proteins in response to mild drought stress

4.1 Introduction

When plants are exposed to conditions of inadequate water supply, they modify their cellular processes in response to the changing environment (Dong *et al.,* 2020). For example, plants activate signalling pathways and transcription factors, which in turn modulate the expression of genes and proteins under drought conditions (Zeng *et al.,* 2019). These drought-responsive proteins function as direct effectors of stress response (Kosová *et al*., 2011), and examples include protein kinases, dehydrins, late embryonic abundant (LEA) proteins, heat shock proteins (HSPs), and antioxidant enzymes (Liu *et al.*, 2020). Collectively, stress proteins play important functions in regulating further gene and protein expression patterns under limited water supply and or directly protecting cell components from dehydration-induced damage (Kosová *et al.*, 2011). For example, protein kinases are involved in gene regulatory functions. Heat shock proteins are molecular chaperones responsible for re-folding of damaged proteins, while antioxidant enzymes scavenge reactive oxygen species (ROS) and thus protect cells from oxidative damage (Kosová *et al.*, 2011; Nadarajah, 2020).

A range of proteomics methods have been used to study molecular mechanisms of drought response in maize leaf (Zenda *et al.,* 2018; Liu *et al.*, 2020; Li *et al.*, 2021) and root (Wang *et al.*, 2019; Zeng *et al.,* 2019) tissues. For instance, Li *et al*, (2021) conducted a comparative tandem mass tag (TMT) -based proteomic study in maize leaves of the hybrid Shaanke 9 under mild and severe drought stress conditions. Plants were watered up to 60–70% of soil water content for mild drought stress, and up to 35–45% for the severe stress treatment. The results

showed that this maize hybrid responded to mild drought conditions by activating the antioxidant system, which resulted in an up-regulation of superoxide dismutase, peroxidase, glutathione S-transferase, ascorbate peroxidase, and catalase. These enzymes are known to scavenge ROS and decrease oxidative damage in plant tissues under water stress (Li *et al.*, 2021). On the other hand, most of the identified ribosomal proteins were down-regulated under severe stress, while a variety of small and large HSP families were up-regulated. The decrease in ribosomal proteins indicated that severe drought stress inhibited protein biosynthesis, while increased accumulation of HSPs possibly protected damage proteins under severe drought conditions (Li *et al.*, 2021).

Meanwhile, Zenda *et al*, (2018) performed a comparative leaf proteomic analysis of two maize lines, a drought-tolerant YE8112 and drought-sensitive MO17, under seven days of drought stress. The researchers used the isobaric tags for relative and absolute quantitation (iTRAQ) method to study the differentially expressed proteins, and validated stress-responsive genes using quantitative real-time PCR (qRT-PCR). The study identified more drought-responsive proteins in the drought-sensitive maize line than in the drought-tolerant one. The researchers concluded that drought stress was more severe in MO17, resulting in more differentially expressed proteins than in the tolerant line YE8112 (Zenda *et al.*, 2018). Furthermore, the drought-susceptible maize line exhibited an up-regulation of HSPs and ribosomal proteins. As a result, the researchers' findings indicate that the two maize lines have distinct stress response mechanisms at the seedling stage (Zenda *et al.*, 2018).

The objective of this chapter was to identify the root proteome changes of two maize varieties, CN07/8-224 and CN07/8-292 subjected to mild drought stress using iTRAQ, and further characterize the drought-responsive proteins using bioinformatics analysis.

4.2. Results

4.2.1. One dimensional gel electrophoresis of CN07/8-224 and CN07/8-292 root tissues

Seeds of two maize varieties, CN07/8224 and CN07/8-292, were germinated and grown on potting soil for seven days. Afterwards, the 7-day-old seedlings were randomly separated into watered-control and drought-stress treatment groups. Mild drought stress was imposed by withholding water for 14 days, and the controls continued to be watered for the entire duration of the experiment. All growth and drought stress treatment processes were conducted in the growth chamber. On day 14 of the stress treatment, plants were harvested for root protein extraction (Section 2.2.8). The extracted total soluble root protein (TSP) was quantified using the Bradford assay and 5 µg of the extracts were electrophoresed on a one-dimensional sodium dodecyl sulfate-polyacrylamide gel electrophoresis (1D SDS-PAGE). The maize root protein extracts were of a moderately good standard, according to the 1D gels. (Figure 4.1) for use in iTRAQ analysis.

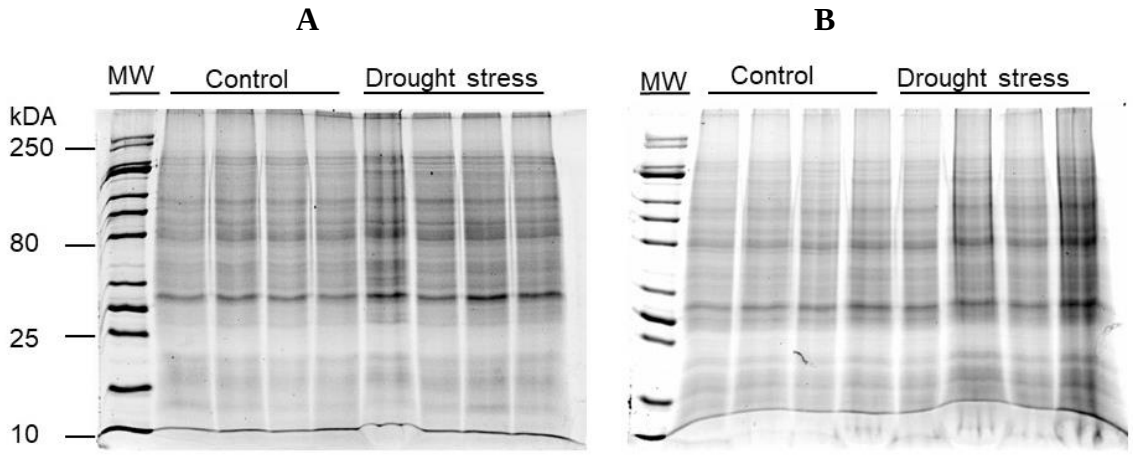

Figure 4.1: SYPRO Ruby-stained 1D gels of maize root protein shows (A) CN07/8-224 maize variety, while (B) shows the CN07/8-292 variety, each with four biological replicates for the treatment groups**.** Lane MW is the molecular weight marker measured in kDa.

4.2.2. iTRAQ analysis of the CN07/8-224 and CN07/8-292 root proteins

After cleaning up the raw iTRAQ dataset, a total of 1 230 and 1 558 proteins were positively identified in CN07/8-224 and CN07/8-292 maize varieties, respectively. Lists of drought-responsive proteins were also generated for each maize variety using a Student's *t* - test at $p \leq 0.05$. A total of 116 and 146 proteins were listed as differentially expressed under the imposed mild drought stress conditions for CN07/8-224 and CN07/8-292 maize varieties, respectively. In CN07/8-224, 52 up-regulated and 64 down-regulated drought-responsive proteins were identified. For CN07/8-292, 75 proteins were up-regulated, and 71 were down-regulated following the drought treatment. This data is summarised in Table 4.1 below.

Table 4.1: Summary of the iTRAQ datasets of the two maize varieties.

Maize variety	Identified proteins[a]	DEPs[b]	Up-regulated proteins[c]	Down-regulated proteins[d]
CN07/8-224	1 230	116	52	64
CN07/8-292	1 558	146	75	71

[a] Total number of identified proteins obtained from iTRAQ datasets after cleaning up the raw data.
[b] Total number of differentially expressed proteins (DEP) obtained using the Student's *t* - test at $p \leq 0.05$

[c]Total number of up-regulated proteins.

[d]Total number of down-regulated proteins.

4.2.3 Bioinformatics analyses

The lists of differentially expressed proteins and their bioinformatics analyses including functional groupings are shown in Tables 4.2 and 4.3 for CN07/8-224 and CN07/8-292 maize varieties, respectively.

Table 4.2: List of mild drought stress-responsive root proteins identified in CN07/8-224 using iTRAQ and tandem mass spectrometry.

Prot No[a]	Accession[b]	Protein Name[c]	Scor[d]	(95%) Cov[e]	Seq pep[f]	Ratio[g]	STD[h]	p-value[i]	GO analysis[j]			Protein family name
									B	F	C	
Primary/secondary metabolism												
27	A0A317YED6	Uncharacterized protein OS=*Zea mays* GN=Zm00014a	34.94	36.04	22	1.34	0.17	0.00774	Carbohydrate metabolic process	Hydrolase activity, hydrolysing O-glycosyl compounds	None	None predicted
40	A0A3L6EDF1	Fructokinase-2 OS=*Zea mays* GN=FRK2	31.81	54.93	17	0.79	0.06	0.02642	Fructose metabolic process	Fructokinase activity	Cytosol	None predicted
48	A0A317YDG1	DIMBOA UDP-glucosyltransferase BX9 OS=*Zea mays* GN=BX9	31.06	46.55	16	0.87	0.05	0.01243	None	UDP-glucosyltransferase activity	None	UDP-glucuronosyl/UDP-glucosyltransferase
85	A0A3L6E900	Putative alpha-glucosidase OS=*Zea mays* GN=Os06g0675700	23.92	21.08	12	1.09	0.06	0.03736	Cellular carbohydrate catabolic process	hydrolase activity, hydrolyzing O-glycosyl compounds	None	Glycoside hydrolase family 31
114	A0A3L6G9N3	Uncharacterized protein OS=*Zea mays* GN=Zm00014a	21.01	24.38	12	0.78	0.11	0.01830	Carbohydrate metabolic process	Beta glycosidase activity	None	Glycoside hydrolase family 1
137	A0A3L6EDY7	Stem glycoprotein OS=*Zea mays* GN=VSPA	18.96	42.52	11	1.36	0.21	0.02616	None	Acid phosphatase activity	None	Acid phosphatase, class B-like
146	A0A3L6FUZ6	Aldose 1-epimerase OS=*Zea mays* GN=Galm	18	42.74	9	1.21	0.11	0.01640	Hexose metabolic process	Carbohydrate binding	None	Aldose 1-/Glucose-6-phosphate 1-epimerase
205	A0A3L6EFD5	Beta-fructofuranosidase, cell wall isozyme OS=*Zea mays* GN=INVA	14.23	18.91	8	1.19	0.12	0.03168	Carbohydrate metabolic process	Hydrolase activity, hydrolysing O-glycosyl compounds	None	Glycoside hydrolase, family 32
268	A0A3L6FKW8	Chitinase OS=*Zea mays* GN=CHIA_3	12	45.42	27	1.37	0.20	0.01201	Carbohydrate metabolic process	Hydrolase activity, hydrolysing O-glycosyl compounds	None	None predicted
308	A0A317Y6D5	Beta-galactosidase OS=*Zea mays* GN=Os04g0620700	10.99	5.67	6	0.79	0.02	0.00002	Carbohydrate metabolic process	Beta-galactosidase activity	Integral component of membrane	Oligopeptide transporter, OPT superfamily
318	A0A317Y5Z0	PALP domain-containing protein OS=*Zea mays* GN=Zm00014a_037411	10.78	39.78	6	0.78	0.10	0.01710	Cysteine biosynthetic process from serine	Cysteine synthase activity	None	Cysteine synthase
342	A0A3L6D8U6	Glutamine synthetase OS=*Zea mays* GN=GS1-5	10.06	24.26	11	0.58	0.03	0.00054	Glutamine biosynthetic process	Glutamate-ammonia ligase activity	None	None predicted
363	A0A3L6E377	Alpha-galactosidase OS=*Zea mays* GN=AGAL3_0	9.65	12.65	5	1.13	0.04	0.00263	Cellular carbohydrate catabolic process	Raffinose alpha-galactosidase activity	None	Glycoside hydrolase, family 27

382	A0A3L6G5Q5	Laccase OS=*Zea mays* GN=LAC25_0	9.2	10.12	8	1.67	0.35	0.01272	Lignin catabolic process	Copper ion binding	Apoplast	Multicopper oxidase
398	A0A3L6E5T4	Assimilatory sulfite reductase (ferredoxin) OS=*Zea mays* GN=SIR	8.88	8.03	7	1.27	0.15	0.02206	None	Metal ion binding	Chloroplast nucleoid	Nitrite and sulphite reductase 4Fe-4S domain containing protein
430	A0A3L6FYD1	3-isopropylmalate dehydrogenase OS=*Zea mays* GN=IMDH2	8.19	15.72	4	0.77	0.14	0.03324	Leucine biosynthetic process	Magnesium ion binding	None	Isopropylmalate dehydrogenase
526	A0A317YJ97	Omega-amidase, chloroplastic OS=*Zea mays* GN=Zm00014a_010363	6.79	13.76	4	0.84	0.09	0.04148	Nitrogen compound metabolic process	Hydrolase activity, acting on carbon-nitrogen(but not peptide)bonds, in linear amides	None	None predicted
709	A0A317YIK2	Sucrose synthase OS=*Zea mays* OX=4577 GN=SUS4_1	4.89	6.88	6	1.42	0.18	0.00775	Sucrose metabolic process	Sucrose synthase activity	None	Sucrose synthase, plant/cyanobacteria
869	A0A3L6F9I0	Nicotianamine aminotransferase A OS=*Zea mays* GN=naat-A_1	4	7.25	2	0.79	0.07	0.01166	Biosynthetic process	Pyridoxal phosphate binding	None	Tyrosine/nicotianamine aminotransferase
920	A0A3L6ESA4	UTP--glucose-1-phosphate uridylyltransferase OS=*Zea mays* GN=UGPA_3	3.63	17.82	9	0.69	0.11	0.02252	UDP-glucose metabolic process	UTP: glucose-1-phosphate uridylyltransferase activity	None	UDPGP family
951	C4JAI3	Cyclase family protein OS=*Zea mays* GN=100502334	3.4	7.64	2	0.81	0.03	0.01468	Tryptophan catabolic process to kynurenine	Alrylformamidase activity	None	Kynurenine formamidase/cyclase-like
1008	A0A8J8YBP6	5'-methylthioadenosine/S-adenosylhomocysteine nucleosidase 1 OS=*Zea mays* GN=Zm00014a_031618	2.94	10.49	2	0.57	0.27	0.04797	Nucleoside metabolic process	Catalytic activity	None	5'-Methylthioadenosine/S-adenosylhomocysteine nucleosidase
1013	A0A3L6FH89	Acyl carrier protein OS=*Zea mays* GN=ACL1.1_1	2.91	14.12	2	1.74	0.35	0.01288	Fatty acid biosynthetic process	Acyl carrier activity	Chloroplast	Acyl carrier protein (ACP)
1746	A0A3L6F107	Glutamine synthetase OS=*Zea mays* GN=Zm00014a_014220	0.32	34.55	15	0.83	0.10	0.03224	Glutamine biosynthetic process	ATP binding	Integral component of membrane	None predicted
1975	A0A3L6G1W0	Phenylalanine ammonia-lyase OS=*Zea mays* GN=PAL_1	0.08	12.66	8	0.76	0.14	0.03582	Cinnamic acid biosynthetic process	Phenylalanine ammonia-lyase activity	Cytoplasm	Aromatic amino acid lyase
Disease/defence												
16	A0A3L6G1K4	Monodehydroascorbate reductase OS=*Zea mays* GN=AFRR	39.06	61.38	22	1.14	0.04	0.01340	Cellular oxidant detoxification	Flavin adenine dinucleotide binding	Peroxisomal matrix	None predicted
26	A0A3L6FW34	Peroxidase OS=*Zea mays* GN=Sb03g046810_3	35.2	62.79	23	1.46	0.33	0.03281	Response to oxidative stress	Peroxidase activity	Extracellular region	Plant peroxidase
31	A0A3L6F1R3	Catalase OS=*Zea mays* GN=CAT3	33.67	41.5	19	1.39	0.11	0.00181	Response to oxidative stress	Catalase activity	None	Catalase, mono-functional, haem-containing

45	A0A317YG24	Ricin B-like lectin R40C1 OS=*Zea mays* GN=R40C1	31.25	50.51	18	1.22	0.10	0.02343	None	Carbohydrate binding	None	Ricin B-like lectin EULS3-like
47	A0A3L6EK62	Peroxidase OS=*Zea mays* GN=PER3	31.1	62.2	22	1.29	0.16	0.01976	Response to oxidative stress	Peroxidase activity	Extracellular region	Plant peroxidase
62	A0A3L6FK29	Germin-like protein OS=*Zea mays* GN=Zm00014a	27.6	69.27	29	1.49	0.18	0.00334	None	Manganese ion binding	Apoplast	Germin
75	A0A3L6DPW9	Peroxidase OS=*Zea mays* GN=PER72	24.83	51.03	18	1.30	0.23	0.04571	Response to oxidative stress	Peroxidase activity	Extracellular region	Plant peroxidase
105	A0A8J8YL00	Peroxidase OS=*Zea mays* GN=Sb03g046810	21.82	56.97	12	1.13	0.04	0.03167	Response to oxidative stress	Peroxidase activity	Extracellular region	Plant peroxidase
122	A0A3L6G519	Peroxidase OS=*Zea mays* GN=PER66	20.16	50.77	22	1.39	0.10	0.00963	Response to oxidative stress	Peroxidase activity	Extracellular region	Plant peroxidase
160	A0A8J8XTI7	Peroxidase OS=*Zea mays* GN=PER2_3	16.94	26.97	9	1.13	0.07	0.01017	Response to oxidative stress	Peroxidase activity	None	Plant peroxidase
178	A0A8J8YK31	Heat shock protein 81-3 OS=*Zea mays* GN=HSP81-3	15.45	42.26	30	0.81	0.06	0.02798	Protein folding	ATP binding	None	Heat shock protein Hsp90 family
190	A0A3L6E1H1	Nitrile-specifier protein 5 OS=*Zea mays* GN=NSP5	15	39.40	10	0.70	0.04	0.00098	Response to zinc ion	Protein binding	None	None predicted
225	A0A8J8Y446	Glutathione transferase OS=*Zea mays* GN=GST1	13.09	38.79	9	0.87	0.05	0.00397	None	Transferase activity	None	Glutathione transferase family
376	A0A3L6EUP4	Dirigent protein OS=*Zea mays* GN=DIR2	9.28	39.18	7	1.16	0.08	0.04271	Phenylpropanoid biosynthesis process	None	Apoplast	Dirigent protein
381	A0A8J8XI05	Dirigent protein OS=*Zea mays* GN=DIR21_0	9.21	34.66	6	1.33	0.18	0.03891	None	None	None	Dirigent protein
419	A0A8J8XSM5	Germin-like protein OS=*Zea mays* GN=Os12g0155000_9	8.33	28.07	7	1.54	0.28	0.04385	None	manganese ion binding	None	Germin
475	A0A8J8XWI0	Germin-like protein OS=*Zea mays* GN=GER4_1	7.64	61.21	30	1.65	0.25	0.00406	None	Manganese ion binding	None	Germin
474	A0A8J8XIG9	Activator heat shock protein ATPase OS=*Zea mays* GN=ahsa_0	7.65	13.79	4	0.86	0.08	0.04131	None	Hsp90 protein binding	None	Activator of Hsp90 ATPase homologue 1-like
485	A0A8J8YSY3	Germin-like protein OS=*Zea mays* GN=Os04g0617900	7.56	41.06	8	1.26	0.05	0.04892	None	Manganese ion binding	None	Germin
544	A0A8J8Y9I9	Polygalacturonase inhibitor 1 OS=*Zea mays* GN=PGIP1	6.58	18.57	5	0.77	0.09	0.01183	None	Protein binding	None	None predicted
695	A0A3L6EJ76	Heat shock protein 17 OS=*Zea mays* GN=HSP70-17_0	5.1	4.01	3	1.23	0.17	0.04914	None	ATP binding	None	Heat shock protein 70 family
719	A0A3L6F4V7	PEROXIDASE_4 domain-containing protein OS=*Zea mays* GN=Zm00014a_039223	4.73	15.58	3	1.20	0.03	0.00392	Response to oxidative stress	Peroxidase activity	None	Plant peroxidase
798	A0A8J8YPB6	Peroxidase OS=*Zea mays* GN=PER59_1	4.08	8.23	2	1.47	0.16	0.00323	Response to oxidative stress	Peroxidase activity	None	Plant peroxidase
1003	A0A3L6E8R1	Inactive protein RESTRICTED TEV MOVEMENT 2 OS=*Zea mays* GN=RTM2_1	2.95	9.09	2	1.68	0.30	0.02619	None	Integral component of membrane	None	Small heat shock protein RTM2-like

1288	A0A3L6F138	CS domain-containing protein OS=*Zea mays* GN=OsI_027940_0	2	17.05	3	0.72	0.13	0.02500	None	Hsp90 protein binding	None	Co-chaperone protein p23-like
1290	A0A3L6G025	Prohibitin-2, mitochondrial OS=*Zea mays* GN=PHB2	2	10.24	2	0.45	0.26	0.04097	None	None	Mitochondrial inner membrane	Prohibitin
Energy												
13	A0A3L6F6D7	Glyceraldehyde-3-phosphate dehydrogenase OS=*Zea mays* GN=GAPC3	41.68	72.4	31	0.81	0.07	0.03070	Glucose metabolic process	NADP binding	None	Glyceraldehyde/Erythrose phosphate dehydrogenase family
17	A0A3L6E933	Vacuolar proton pump subunit B OS=*Zea mays* GN=VATB1	38.62	56.6	23	1.13	0.08	0.02771	ATP metabolic process	ATP binding	Proton-transporting V-type ATPase, V1 domain	V-type ATP synthase regulatory subunit B/beta
64	A0A3L6DHP8	Phosphoenolpyruvate carboxykinase (ATP) OS=*Zea mays* GN=PCKA	27	28.34	15	1.16	0.06	0.02171	Phosphorylation	Kinase activity	None	Phosphoenolpyruvate carboxykinase, ATP-utilising
267	A0A317YIW7	Phosphopyruvate hydratase OS=*Zea mays* GN=Zm00014a_030392	12	33.52	13	0.93	0.06	0.04822	Glycolytic process	Phosphopyvurate hydratase activity	Phosphopyvurate hydratase complex	Enolase family
349	A0A3L6EM29	NADH dehydrogenase [ubiquinone] iron-sulfur protein 1, mitochondrial OS=*Zea mays* GN=NDUS1_0	10	10.09	5	1.21	0.11	0.01303	ATP synthesis coupled electron transport	NADH dehydrogenase (ubiquinone) activity	Membrane	NADH:ubiquinone oxidoreductase, subunit G
438	A0A3L6E0V3	Putative V-type proton ATPase subunit H OS=*Zea mays* GN=Zm00014a_021074	8.1	8.09	4	1.43	0.13	0.00176	Proton transmembrane transport	Proton-transporting ATPase activity, rotational mechanism	Vacuolar proton-transporting V-type ATPase,V1 domain	ATPase, V1 complex, subunit H
733	A0A3L6EEY7	Uncharacterized protein OS=*Zea mays* GN=Zm00014a_001338	4.6	8.07	3	1.43	0.24	0.03068	Glycolytic process	ATP binding	None	Fructose-bisphosphate aldolase, class-II
823	A0A317YCH5	Chemocyanin OS=*Zea mays* GN=BABL_2	4.03	21.54	3	1.52	0.23	0.00946	None	Electron transfer activity	None	Phytocyanin
1175	A0A3L6EKQ0	V-type proton ATPase catalytic subunit A OS=*Zea mays* GN=VATA_1	2.05	49.28	25	1.43	0.22	0.01130	ATP metabolic process	ATP binding	Proton-transporting V-type ATPase,V1 domain	V-type ATP synthase catalytic alpha chain
Transporters												
243	A0A3L6DZ69	Mitochondrial outer membrane protein porin 1 OS=*Zea mays* GN=VDAC1_1	12.43	33.70	7	0.86	0.07	0.02950	Anion transmembrane transport	Voltage-gated anion channel activity	Mitochondrial outer membrane	Eukaryotic porin/Tom40
434	A0A3L6DGQ0	Dynamin-2A OS=*Zea mays* GN=DRP2A_0	8.16	6.40	4	1.12	0.07	0.04531	None	GTPase activity	Cytoplasm	Dynamin
680	A0A3L6E2G4	Importin-5 OS=*Zea mays* GN=Ipo5_0	5.23	3.02	3	0.77	0.03	0.00918	Protein import into nucleus	Protein binding	Cytoplasm	Importin beta family
906	A0A3L6DFP4	H(+)-exporting diphosphatase OS=*Zea mays* GN=Zm00014a_029196	3.77	3.94	3	1.39	0.02	0.04111	Proton transmembrane transport	Inorganic diphosphate phosphatase activity	Membrane	Pyrophosphate-energised proton pump
Proteolysis												
115	A0A3L6DXZ7	Carboxypeptidase OS=*Zea mays* GN=Zm00014a	20.89	28.00	11	1.18	0.10	0.02890	Proteolysis	Serine-type carboxypeptidase activity	None	Peptidase S10, serine carboxypeptidase

157	A0A3L6ER88	Aminopeptidase OS=*Zea mays* GN=Os02g0218200_1	17.26	11.69	8	1.17	0.07	0.02397	Proteolysis	Aminopeptidase activity	Endoplasmic reticulum	Peptidase M1
265	A0A317Y6Z6	Basic secretory protease OS=*Zea mays* GN=BSP_1	12.04	48.25	9	1.20	0.10	0.02090	Proteolysis	Peptidase activity	None	Uncharacterised protein family, basic secretory protein
341	A0A8J8YFT7	Oligopeptidase A OS=*Zea mays* GN=OOP	10.09	9.50	5	1.15	0.09	0.04469	Proteolysis	Metalloendopeptidase activity	None	Peptidase M3A/M3B
344	A0A3L6DE05	Aspartyl protease family protein OS=*Zea mays* GN=At5g10770_0	10.03	12.53	6	1.32	0.11	0.00336	Proteolysis	Aspartic-type endopeptidase activity	None	Aspartic peptidase A1 family
587	A0A3L6ETI0	Aspartyl protease family protein OS=*Zea mays* GN=At5g10770_2	6.06	15.27	4	1.13	0.09	0.04379	Proteolysis	Aspartic-type endopeptidase activity	None	Aspartic peptidase A1 family
675	A0A3L6G9T5	BTB/POZ and MATH domain-containing protein 4 OS=*Zea mays* GN=BPM4_3	5.3	36.81	4	0.84	0.11	0.02727	Protein ubiquitination	Protein binding	None	BTB/POZ and MATH domain-containing protein 1-6
984	A0A317YL57	Subtilisin-like protease SBT3.18 OS=*Zea mays* GN=SBT3.18	3.19	2.69	2	0.80	0.09	0.02973	Proteolysis	RNA binding	None	YTH domain containing protein
984	A0A317YL57	Subtilisin-like protease SBT3.18 OS=*Zea mays* GN=SBT3.18	3.19	2.69	2	0.80	0.09	0.02973	Proteolysis	RNA binding	None	YTH domain containing protein
1281	A0A3L6DD75	Proteasome subunit alpha type OS=*Zea mays* GN=Os06g0167600_1	2	20.40	4	0.64	0.17	0.02741	Ubiquitin-dependent protein catabolic process	None	Nucleus	Proteasome subunit alpha4
Protein synthesis												
124	A0A3L6E393	60S ribosomal protein L7a OS=*Zea mays* GN=RPL7A-2	20.09	32.56	10	0.76	0.11	0.02309	Ribosome biogenesis	RNA binding	Cytosolic large ribosomal subunit	Ribosomal protein L7Ae/L8/Nhp2 family
156	A0A8J8Y760	Eukaryotic translation initiation factor 5A OS=*Zea mays* GN=TIF5A	17.33	62.5	9	0.83	0.05	0.03042	Positive regulation of translational elongation	Translation initiation factor activity	None	Translation elongation factor IF5A-like
192	A0A3L6DV56	Elongation factor 1-delta 1 OS=*Zea mays* GN=Os07g0614500_1	14.95	34.28	10	0.71	0.14	0.01405	Translation elongation	Translation elongation factor activity	Eukaryotic translation elongation factor 1 complex	None predicted
231	A0A3L6EUP8	60S ribosomal protein L21-2 OS=*Zea mays* GN=RPL21E_1	12.85	48.78	8	0.71	0.07	0.00851	Translation	Structural constituent of ribosome	Ribosome	Ribosomal protein L21e
270	A0A8J8YPK3	40S ribosomal protein S24 OS=*Zea mays* GN=Zm00014a_026008	11.95	41.61	8	0.63	0.03	0.01100	Translation	Structural constituent of ribosome	Ribosome	Ribosomal protein S24e
309	B4FE90	40S ribosomal protein S8 OS=*Zea mays* GN=RPS8_0	10.99	32.58	6	0.81	0.08	0.02005	Translation	Structural constituent of ribosome	Ribosome	Ribosomal protein S8e/ribosomal biogenesis NSA2
340	A0A3L6G9I5	40S ribosomal protein S11 OS=*Zea mays* GN=RPS11_1	10.01	27.67	5	0.69	0.06	0.01028	Translation	Structural constituent of ribosome	Ribosome	Ribosomal protein S17/S11

395	A0A3L6FGZ0	60S ribosomal protein L26-1 OS=*Zea mays* GN=RPL26A_3	8.95	30.57	4	0.68	0.12	0.03869	Translation	RNA binding	Large ribosomal subunit	Ribosomal protein L26/L24, eukaryotic/archaeal
494	A0A8J8YNG3	60S ribosomal protein L23a OS=*Zea mays* GN=Zm00014a_002729	7.36	33.55	5	0.68	0.05	0.04711	Translation	Structural constituent of ribosome	Ribosome	Ribosomal protein L25/L23
522	B6SHZ1	40S ribosomal protein S5 OS=*Zea mays* GN=ZEAMMB73_Zm00001d008387	6.91	22.61	4	0.76	0.10	0.00644	Translation	Structural constituent of ribosome	Ribosome	Ribosomal protein S5/S7
633	A0A3L6EUK1	Serine/arginine-rich splicing factor RSZ23 OS=*Zea mays* GN=RSZ23_0	5.89	27.66	4	0.75	0.09	0.01013	None	RNA binding	None	None predicted
751	A0A8J8Y472	40S ribosomal protein S15 OS=*Zea mays* GN=RPS15_2	4.45	37.91	7	0.64	0.18	0.03286	Translation	RNA binding	Ribosome	Ribosomal protein S19/S15
770	B6SGI4	Ribosomal protein L37 OS=*Zea mays* GN=100284994	4.3	15.96	2	0.54	0.11	0.00538	Translation	Structural constituent of ribosome	Ribosome	Ribosomal protein L37e
812	A0A8J8XH92	40S ribosomal protein S24 OS=*Zea mays* GN=RPS24B_8	4.05	30.66	5	0.73	0.09	0.02472	Translation	Structural constituent of ribosome	Ribosome	Ribosomal protein S24e
917	A0A8J8XUB1	60S ribosomal protein L23 OS=*Zea mays* GN=RPL23A_1	3.66	40.00	2	0.73	0.07	0.04365	Translation	Structural constituent of ribosome	Ribosome	Ribosomal protein L14P
918	A0A3L6FZ45	60S ribosomal protein L27a-3 OS=*Zea mays* GN=RPL27AC_1	3.64	14.48	2	0.80	0.07	0.03576	Translation	Structural constituent of ribosome	Ribosome	Ribosomal protein L15
962	A0A3L6DFL2	40S ribosomal protein S20 OS=*Zea mays* GN=RPS20_2	3.33	34.11	4	0.66	0.17	0.00844	Translation	Structural constituent of ribosome	Ribosome	Ribosomal protein S10
1000	A0A8J8YHK9	Eukaryotic translation initiation factor 4C OS=*Zea mays* GN=IF1A_2	2.99	18.06	2	0.79	0.04	0.01794	Translational initiation	Translation initiation factor activity	None	Translation initiation factor 1A (eIF-1A)
1011	A0A3L6DJ71	Serine/arginine-rich splicing factor SR45 OS=*Zea mays* GN=SR45_1	2.92	6.30	2	0.77	0.07	0.04015	None	RNA binding	Nucleus	None predicted
1469	A0A3L6DYZ3	Elongation factor 1-alpha OS=*Zea mays* GN=REFA1_5	1.73	29.75	14	1.74	0.27	0.01234	Translational elongation	Translation elongation factor activity	None	Translation elongation factor EF1A, eukaryotic/archaeal
1566	A0A8J8XDR8	60S ribosomal protein L21-2 OS=*Zea mays* GN=Zm00014a_041611	1.17	48.78	8	0.69	0.15	0.02982	Translation	Structural constituent of ribosome	Ribosome	Ribosomal protein L21e
1594	A0A3L6DW13	Protein-synthesizing GTPase OS=*Zea mays* GN=eIF-2gamma_1	0.99	2.65	2	0.74	0.11	0.01923	None	Translation initiation factor activity	None	None predicted
Transcription												
293	A0A8J8XBD0	HMG-Y-related protein A OS=*Zea mays* GN=HMGIY2_0	11.4	20.73	6	0.72	0.03	0.00735	Regulation of DNA- templated transcription	DNA binding	Nucleus	High mobility group protein HMGA, plant
379	A0A8J8XM28	Nascent polypeptide-associated complex subunit beta OS=*Zea mays* GN=At1g73230	9.23	34.55	4	0.75	0.08	0.00937	None	None	None	Transcription factor BTF3
399	A0A8J8YR41	DNA-binding protein MNB1B OS=*Zea mays* GN=MNB1B	8.88	26.11	5	0.71	0.10	0.04970	None	DNA binding	None	High mobility group protein HMGB, plant
659	A0A317Y116	MBD domain-containing protein OS=*Zea mays* GN=At5g39865_5	5.48	4.91	3	0.76	0.06	0.00191	None	DNA binding	Nucleus	Methyl-CpG-binding domain-containing protein 10/11
686	A0A8J8YIM6	Multiple organellar RNA editing factor 8, chloroplastic/mitochondrial	5.18	13.10	4	0.79	0.09	0.01963	Cytidine to uridine editing	None	None	MORF/ORRM1/DAG-like

		OS=*Zea mays* GN=Zm00014a_013852										
1165	A0A3L6ELM0	Methyl-CpG-binding domain-containing protein 11 OS=*Zea mays* GN=MBD11	2.06	5.14	2	0.81	0.10	0.03286	None	DNA binding	Nucleus	Methyl-CpG-binding domain-containing protein 10/11
1177	A0A3L6FHG6	Histone H2A OS=*Zea mays* GN=H2A_1	2.05	25.16	5	0.44	0.03	0.02429	None	DNA binding	Nucleus	Histone H2A
1656	A0A3L6EAY7	DNA-directed RNA polymerase OS=*Zea mays* OX=4577 GN=USP_2	0.63	7.34	7	0.56	0.25	0.02784	Transcription, DNA templated	DNA –directed 5'-3' RNA polymerase activity	DNA –directed RNA polymerase activity	UDPGF family
1794	A0A3L6F2H5	HMG1/2-like protein OS=*Zea mays* GN=Zm00014a_009604	0.22	17.27	3	0.64	0.11	0.02772	None	None	None	High mobility group protein HMGB, plant
Unclassified												
116	A0A8J8YKA6	Alcohol dehydrogenase 1 OS=*Zea mays* GN=ADH1	20.84	39.69	13	0.66	0.11	0.00833	None	None	None	None predicted
187	A0A3L6E552	Protein TolB OS=*Zea mays* GN=tolB_2	15.11	14.35	7	1.23	0.12	0.02163	None	None	None	None predicted
276	A0A3L6FML3	Uncharacterized protein OS=*Zea mays* GN=Zm00014a_030226	11.82	31.62	10	1.30	0.11	0.02697	None	None	Integral component of membrane	None predicted
390	A0A3L6F769	Uncharacterized protein OS=*Zea mays* GN=Zm00014a_042645	9.08	13.57	4	1.15	0.09	0.02117	None	RNA binding	None	None predicted
401	A0A8J8YEP2	Proline-rich protein DC2.15 OS=*Zea mays* GN=14KD_5	8.76	37.40	5	1.74	0.52	0.04326	None	None	None	None predicted
644	A0A3L6DQ09	C2H2-type domain-containing protein OS=*Zea mays* GN=Zm00014a_011088	5.75	16.44	5	0.84	0.10	0.01852	None	None	None	None predicted
682	A0A3L6DUG0	Histone deacetylase HDT1 OS=*Zea mays* GN=HDT1_3	5.21	6.90	3	0.77	0.08	0.02156	None	None	None	None predicted
819	A0A8J8Y4L0	Proline-rich protein DC2.15 OS=*Zea mays* GN=14KD_4	4.03	26.32	2	1.70	0.43	0.03530	None	None	None	None predicted
877	A0A317YHJ8	Uncharacterized protein OS=*Zea mays* GN=Zm00014a_041931	4	15.42	2	0.77	0.13	0.01931	None	None	Integral component of membrane	None
1110	A0A8J8YIP3	Heterogeneous nuclear ribonucleoprotein 1 OS=*Zea mays* GN=Zm00014a_025134	2.2	15.12	5	0.69	0.13	0.04325	None	RNA binding	None	None predicted
1166	A0A3L6DX37	Uncharacterized protein OS=*Zea mays* GN=At5g01610_3	2.06	12.07	2	1.50	0.29	0.02698	None	None	None	Protein of unknown function DUF538
1176	A0A3L6F9B8	Alcohol dehydrogenase 2 OS=*Zea mays* GN=ADH2	2.05	17.15	5	0.69	0.03	0.00990	None	Zinc ion binding	None	None predicted

[a]Protein accession number obtained from the uniprot database (https//www.uniprot.org).

[b]Protein score generated by ProteinPilot software relating to the confidence of protein identification. A protein identification threshold of 1.3 was applied to the data, which only retains proteins identified with a 95% confidence.

[c] Percentage coverage is determined by the number of amino acids of sequenced peptides against the total length of the protein, with a threshold of at least 95% confidence.

[d] Sequenced peptide refers to the number of peptide that were sequenced and gave rise to protein identity. All proteins that were identified by means of a single peptide were filtered out of the dataset.

[e]robability value of the quantitative difference between the treatment and control protein abundance being due to chance alone.

[f] Ratio represents the average fold-change (n = 4) induced by treatment relative to control. Positive values indicate an up-regulation.

[g]Standard deviation of the ratios of drought stressed samples (n=4).

[h] Total number of differentially expressed proteins obtained using the Student's *t* - test at $p \leq 0.05$

[i] Gene ontology analysis as predicted on the IntePro database (https://www.ebi.ac.uk/interpro/) and UniProt database (http://www.uniprot.org). P denotes Biological Process, F denotes Functional Process, and C denotes Cellular Component.
conserved family name as predicted by InterPro database (http://www.ebi.ac.uk/interpro/).

Table 4.3: List of mild drought stress-responsive proteins identified in CN07/8-292 using iTRAQ and tandem mass spectrometry.

Prot No[a]	Accession [b]	Protein Name	Scor[c]	(95%) Cov[d]	Seq pep[e]	Ratio[f]	STD[g]	p-value[h]	GO analysis[i]			Protein family name[j]
									B	F	C	
Primary/secondary Metabolism												
4	A0A8J8YT78	Sucrose synthase OS=*Zea mays* GN=Zm00014a_011218	72.18	58.64	51	0.74	0.02	0.00501	Sucrose metabolic process	Sucrose synthase activity	None	Sucrose synthase, plant/cyanobacteria
8	A0A8J8XJQ9	Putative linoleate 9S-lipoxygenase 3 OS=*Zea mays* GN=Os03g0700400	57.51	49.02	47	0.84	0.08	0.04905	Lipid biosynthesis	Oxidoreductase activity	None	Lipoxygenase
12	A0A3L6DD69	Allene oxide synthase 2 OS=*Zea mays* GN=CYP74A2_0	52.87	65.77	29	0.78	0.12	0.02250	None	Monooxygenase activity	None	Cytochrome P450
49	A0A3L6GDS4	Chitinase OS=*Zea mays* GN=CHIB_1	35.8	76.60	54	0.59	0.15	0.02847	Chitin catabolic process	Chitinase activity	None	Glycoside hydrolase, family 19
55	A0A317YDG1	DIMBOA UDP-glucosyltransferase BX9 OS=*Zea mays* GN=BX9_3	34.43	51.72	21	1.18	0.06	0.03151	None	UDP-glucosyltransferase activity	None	UDP-glucuronosyl/UDP-glucosyltransferase
99	A0A3L6G4A8	Polyphenol oxidase, chloroplastic OS=*Zea mays* GN=PPO_4	26.14	29.48	12	1.23	0.13	0.04632	None	Catechol oxidase activity	None	None predicted
180	A0A3L6F814	Glycosyltransferase OS=*Zea mays* GN=Bx8_8	17.95	34.42	12	1.15	0.03	0.01478	None	UDP-glucosyltransferase activity	None	UDP-glucuronosyl/UDP-glucosyltransferase
276	A0A3L6EXI4	Chitinase 2 OS=*Zea mays* GN=CHIT2_0	13.95	40.91	9	0.76	0.07	0.01096	Carbohydrate metabolic process	Hydrolase activity, hydrolyzing O-glycosyl compounds	None	Chitinase-like
283	A0A8J8YSU2	GDSL esterase/lipase OS=*Zea mays* GN=At5g45910_9	13.64	27.99	12	1.38	0.06	0.02657	None	Hydrolase activity, acting on ester bonds	None	GDSL lipase/esterase
286	A0A8J8YNG8	Aldehyde dehydrogenase (NAD(+)) OS=*Zea mays* GN=AL7A1_0	13.57	23.48	7	0.83	0.04	0.04938	None	Oxidoreductase activity	None	Aldehyde dehydrogenase family 7 member A1-like
304	A0A3L6G306	Glucan endo-1,3-beta-glucosidase OS=*Zea mays* GN=GLC1_2	13.02	32.16	11	1.10	0.19	0.03507	Carbohydrate metabolic process	Glucan endo-1,3-beta-D-glucosidase activity	None	Glycoside hydrolase family 17
307	A0A3L6FDP2	Heparanase-like protein 1 OS=*Zea mays* GN=Zm00014a_008788	12.97	20.86	9	0.87	0.15	0.02013	None	Hydrolase activity, acting on glycosyl bonds	Membrane	Glycoside hydrolase, family 79
310	A0A8J8XDY6	Isocitrate dehydrogenase [NADP] OS=*Zea mays* GN=CICDH_0	12.93	39.32	18	0.83	0.14	0.04597	Isocitrate metabolic process	Isocitrate dehydrogenase (NADP+) activity	None	Isocitrate dehydrogenase NADP-dependent
356	A0A3L6DMT8	Ketol-acid reductoisomerase OS=*Zea mays* GN=Os05g0573700_4	11.67	21.44	9	0.78	0.10	0.01504	Branched chain amino acid	Isomerase activity	None	Ketol-acid reductoisomerase

									biosynthetic process				
360	A0A3L6DPG0	Glyoxysomal fatty acid beta-oxidation multifunctional protein MFP-a OS=*Zea mays* GN=MFPA_1	11.65	15.22	6	0.86	0.05	0.01719	Fatty acid beta-oxidation	3-hydroxyacyl-CoA dehydrogenase activity	Peroxisome	Enoyl-CoA hydratase/isomerase
368	B6THR9	3-isopropylmalate dehydrogenase OS=*Zea mays* GN=100283376	11.52	24.45	16	1.17	0.18	0.04054	Leucine biosynthetic process	Magnesium ion binding	None	Isopropylmalate dehydrogenase
374	A0A317Y448	Nucleoside diphosphate kinase OS=*Zea mays* GN=NDPK1	11.42	42.95	9	0.71	0.17	0.03702	Nucleoside diphosphate phosphorylation	ATP binding	None	Nucleoside diphosphate kinase
394	A0A317Y694	5-methyltetrahydropteroyltriglutamate--homocysteine S-methyltransferase OS=*Zea mays* GN=Os12g0623900	11.01	52.29	54	0.83	0.04	0.00233	Cellular amino acid biosynthetic process	Transferase	None	Cobalamin-independent methionine synthase
399	A0A3L6DNC1	Aspartate aminotransferase OS=*Zea mays* GN=aspC	10.9	18.53	6	0.69	0.13	0.01509	Biosynthetic process	Pyridoxal phosphate binding	None	None predicted
453	A0A317YGX3	Phosphopyruvate hydratase OS=*Zea mays* GN=Zm00014a_030392	10.07	59.26	14	0.85	0.11	0.02301	Glycolytic process	Phosphopyruvate hydratase activity	Phosphopyruvate hydratase complex	Enolase
455	A0A3L6F5Y7	Tricin synthase 1 OS=*Zea mays* GN=ROMT-15_0	10.05	37.71	4	0.75	0.07	0.00302	Methylation	O-methyltransferase activity	None	Class I-like SAM-dependent O-methyltransferase
480	A0A3L6FFU8	Cytokinin dehydrogenase OS=*Zea mays* GN=CKX1	9.68	17.04	5	1.56	0.09	0.01853	Cytokinin metabolic process	Cytokinin dehydrogenase activity	Extracellular space	None predicted
511	A0A3L6EIC9	Uncharacterized protein OS=*Zea mays* GN=Zm00014a_035353	9.26	12.31	15	1.19	0.15	0.03271	None	Oxidoreductase activity	None	Aldehyde oxidase/xanthine dehydrogenase
582	A0A317Y8E1	Purple acid phosphatase OS=*Zea mays* GN=Zm00014a_009198	8.19	18.97	5	0.83	0.06	0.00264	None	Acid phosphatase activity	Secreted	Purple acid phosphatase
589	A0A3L6FJJ7	D-amino-acid transaminase, chloroplastic OS=*Zea mays* GN=DAAT_1	8.12	18.00	4	1.33	0.15	0.03339	Folic acid biosynthetic process	Pyridoxal phosphate binding	None	Aminotransferase class IV
631	A0A8J8XV52	Nucleoside diphosphate kinase OS=*Zea mays* GN=NDK4_0	7.61	17.22	4	1.66	0.40	0.03333	Phosphorylation	Kinase activity	None	Nucleoside diphosphate kinase
652	A0A3L6F082	Adenosine kinase OS=*Zea mays* GN=ADK2_1	7.4	48.25	17	0.77	0.11	0.04930	Purine ribonucleoside salvage	Adenosine kinase activity	None	Adenosine kinase
665	A0A3L6E2M6	Metallophos domain-containing protein OS=*Zea mays* GN=100284811	7.16	21.41	4	0.81	0.12	0.04990	None	Hydrolase activity	None	Phosphoesterase At2g46880

729	A0A8J8Y191	NADH-cytochrome b5 reductase-like protein OS=*Zea mays* GN=CBR2	6.3	14.81	4	1.35	0.06	0.00130	None	Oxidoreductase activity	None	NADH:cytochrome b5 reductase-like
815	A0A8J8XJ53	NADH:ubiquinone reductase (non-electrogenic) OS=*Zea mays* GN=NDB2	5.76	7.97	3	0.86	0.05	0.01115	NADH oxidation	Oxidoreductase activity	Mitochondrion	Alternative NADH dehydrogenase
911	A0A3L6FKW8	Chitinase OS=*Zea mays* GN=CHIA_3	4.79	17.97	10	0.70	0.07	0.00185	carbohydrate metabolic process	hydrolase activity, hydrolyzing O-glycosyl compounds	None	None predicted
981	A0A3L6DDS7	Sinapine esterase OS=Zea mays GN=SCE3_1	4.23	11.74	3	1.40	0.17	0.02430	None	Hydrolase activity, acting on ester bonds	None	GDSL lipase/esterase
1016	A0A3L6DZ08	Nucleoside diphosphate kinase OS=*Zea mays* GN=NDKR	4.06	12.33	3	1.31	0.08	0.00662	Nucleoside diphosphate phosphorylation	Nucleoside diphosphate kinase activity	None	Nucleoside diphosphate kinase
1069	A0A3L6F2V9	Glycine cleavage system H protein OS=*Zea mays* GN=GDH2_8	4	14.37	3	1.38	0.07	0.00025	Glycine decarboxylation via glycine cleavage system	None	Mitochondrion	Glycine cleavage system H-protein/Simiate
1079	A0A8J8XHK8	Alpha-aminoadipic semialdehyde synthase OS=*Zea mays* GN=LKR	4	2.45	2	0.64	0.07	0.01274	L-lysine catabolic process to acetyl-CoA via saccharopine	Oxidoreductase activity	None	None predicted
1135	A0A3L6EYI9	GDSL esterase/lipase OS=*Zea mays* GN=At5g45910_12	3.63	9.95	2	0.67	0.21	0.02980	None	hydrolase activity, acting on ester bonds	None	GDSL lipase/esterase
1202	A0A3L6FU04	Putative pyridoxal 5'-phosphate synthase subunit PDX1.1 OS=*Zea mays* GN=PDX11_1	3.07	9.14	2	1.22	0.11	0.01394	Pyridoxal phosphate biosynthetic process	None	None	Pyridoxal 5'-phosphate synthase subunit PdxS/SNZ
1211	A0A3L6GFY8	3'(2'),5'-bisphosphate nucleotidase (Fragment) OS=*Zea mays* GN=Zm00014a_005636	3.03	5.13	2	1.31	0.13	0.01935	Sulfur compound metabolic process	3'(2'),5'-bisphosphate nucleotidase activity	None	Inositol monophosphatase-like
1225	A0A317YBS1	Beta-glucosidase BoGH3B OS=*Zea mays* GN=BACOVA_02659_5	2.91	15.92	8	0.70	0.13	0.02247	Carbohydrate metabolic process	Hydrolase activity, hydrolyzing O-glycosyl compounds	Extracellular region	None predicted
1351	C4JAI3	Cyclase family protein OS=*Zea mays* GN=100502334	2.26	14.18	3	0.60	0.24	0.00118	Tryptophan catabolic process to kynurenine	Arylformamidase activity	None	Kynurenine formamidase/cyclase-like
1432	A0A3L6E525	Type I inositol polyphosphate 5-phosphatase 1 OS=*Zea mays* GN=IP5P1	2.05	1.97	2	0.71	0.11	0.01570	Inositol phosphate dephosphorylation	Inositol-polyphosphate 5-phosphatase activity	None	Inositol polyphosphate 5-phosphatase, plant
1742	A0A3L6FV98	Aldose 1-epimerase OS=*Zea mays* GN=Galm_5	1.9	4.30	2	0.74	0.11	0.03242	Hexose metabolic process	Carbohydrate binding	None	Aldose 1-/Glucose-6-phosphate 1-epimerase

2298	A0A8J8YNI4	UDP-glucuronate decarboxylase OS=*Zea mays* GN=UXS6_1	0.14	28.24	9	1.71	0.41	0.02223	UDP-D-xylose biosynthetic process	UDP-glucuronate decarboxylase activity	None	UDP-glucuronic acid decarboxylase
Disease/defence												
37	A0A3L6ELZ4	Luminal-binding protein 2 OS=*Zea mays* GN=BIPE2_0	38.93	41.90	27	1.34	0.10	0.01974	None	ATP-dependent folding chaperone	None	Heat shock protein 70 family
74	A0A8J8XL66	Peroxidase OS=*Zea mays* GN=PER52_1	30.61	73.27	22	0.81	0.08	0.03207	Response to oxidative stress	Peroxidase activity	None	Plant peroxidase
153	A0A317Y444	Glutathione S-transferase F11 OS=*Zea mays* GN=GSTF11_1	20.19	53.44	11	1.46	0.21	0.01328	Glutathione metabolic process	Transferase activity	None	None predicted
236	A0A8J8Y5T1	Peroxidase 70 OS=*Zea mays* GN=PER70_2	15.17	53.33	12	1.32	0.06	0.03961	Response to oxidative stress	Peroxidase activity	None	Plant peroxidase
313	A0A3L6G2K7	Peroxidase OS=*Zea mays* GN=PER72_3	12.9	35.29	9	0.69	0.06	0.00917	Response to oxidative stress	Peroxidase activity	Extracellular region	Plant peroxidase
375	A0A3L6F3B8	T-complex protein 1 subunit delta OS=*Zea mays* GN=CCT4_1	11.39	16.82	6	1,.21	0.07	0.01718	Unfolded Protein folding	ATP binding	Cytoplasm	Chaperonin Cpn60/GroEL/TCP-1 family
416	A0A3L6FGJ5	Peroxidase 72 OS=*Zea mays* GN=Zm00014a_015662	10.58	30.22	8	1.31	0.07	0.00447	Response to oxidative stress	Peroxidase activity	None	Plant peroxidase
563	A0A8J8YQA4	Glutathione transferase OS=*Zea mays* GN=GSTF8_3	8.41	16.7	4	1.33	0.17	0.00375	None	Transferase activity	None	Glutathione transferase family
585	A0A8J8XI72	Glutathione peroxidase OS=*Zea mays* GN=GPX6_0	8.14	27.64	5	0.73	0.15	0.04273	Response to oxidative stress	Peroxidase activity	None	Glutathione peroxidase
586	A0A3L6DXC2	Peroxidase OS=*Zea mays* GN=PER17_1	8.13	14.70	4	0.76	0.03	0.01281	Response to oxidative stress	Peroxidase activity	Extracellular region	Plant peroxidase
632	A0A3L6EUP4	Dirigent protein OS=*Zea mays* GN=DIR2	7.61	39.18	6	0.83	0.05	0.04731	Phenylpropanoid biosynthetic process	None	Apoplast	Dirigent protein
644	A0A8J8XKM9	Peroxidase OS=*Zea mays* GN=Zm00014a_014490	7.52	16.08	6	0.76	0.07	0.01475	Response to oxidative stress	Peroxidase activity	None	Plant peroxidase
655	A0A3L6F3B3	Uncharacterized protein OS=*Zea mays* GN=Zm00014a_012373	7.36	19.62	4	1.21	0.05	0.00174	Protein folding	Hsp70 protein binding	None	Heat shock protein Sti1-like
925	A0A3L6FWW0	Putative plastid-lipid-associated protein 2, chloroplastic OS=*Zea mays* GN=PAP2_2	4.67	6.92	4	0.64	0.07	0.04440	None	None	None	Plastid-lipid-associated protein
1109	A0A3L6G0M8	Putative phospholipid hydroperoxide glutathione peroxidase 6, mitochondrial OS=*Zea mays* GN=Zm00014a_019400	3.88	21.25	3	1.38	0.15	0.00773	Response to oxidative stress	Glutathione peroxidase activity	None	Glutathione peroxidase
1196	A0A3L6EEE7	Putative acetyltransferase OS=*Zea mays* GN=At3g50280_1	3.11	7.57	2	0.72	0.14	0.02497	None	acyltransferase activity, transferring groups	None	None

										other than amino-acyl groups		
1738	A0A3L6EH99	Peroxidase OS=*Zea mays* GN=PER51_3	1.92	5.50	2	1.56	0.24	0.04297	Response to oxidative stress	Peroxidase activity	Extracellular region	Plant peroxidase
Energy												
73	A0A3L6EBR4	Isocitrate dehydrogenase [NADP] OS=*Zea mays* GN=CICDH_3 PE=3	30.91	45.30	20	0.86	0.08	0.04548	Isocitrate metabolic process	Isocitrate dehydrogenase (NADP+) activity	None	Isocitrate dehydrogenase NADP-dependent
78	A0A3L6F482	Pyruvate kinase OS=*Zea mays* GN=Os11g0148500_0	29.8	37.76	19	0.71	0.14	0.03404	Glycolytic process	Pyruvate kinase activity	None	Pyruvate kinase
272	A0A3L6EU51	Pyruvate dehydrogenase E1 component subunit alpha OS=*Zea mays* GN=Zm00014a_033742	14.08	31.66	10	1.15	0.04	0.00049	Glycolytic process	Pyruvate dehydrogenase (acetyl-transferring) activity	Intracellular membrane-bounded organelle	Pyruvate dehydrogenase (acetyl-transferring) E1 component, alpha subunit, subgroup y
386	A0A3L6EYU8	Citrate synthase OS=*Zea mays* GN=Zm00014a_041159	11.17	13.77	5	1.37	0.18	0.01936	Citrate(Si)-synthase activity	Acyltransferase activity, acyl groups converted into alkyl on transfer	None	Citrate synthase
691	A0A3L6FI63	V-type proton ATPase kksubunit E OS=*Zea mays* GN=Zm00014a_026117	6.75	9.20	3	1.38	0.24	0.04220	Proton transmembrane transport	Proton-transporting ATPase activity, rotational mechanism	Proton-transporting two-sector ATPase complex, catalytic domain	V-type ATPase subunit E
917	A0A3L6FLW7	Phosphoglycerate kinase OS=*Zea mays* GN=PGKH_0	4.75	7.267	10	1.36	0.23	0.00044	Glycolytic process	Phosphoglycerate kinase activity	None	Phosphoglycerate kinase
971	A0A3L6E3B2	NADH dehydrogenase [ubiquinone] iron-sulfur protein 4, mitochondrial OS=*Zea mays* GN=FRO1_0	4.27	25.35	2	1.36	0.22	0.00958	Electron transport chain	None	Mitochondrial respiratory chain complex I	NADH dehydrogenase ubiquinone Fe-S protein 4, mitochondrial
1044	A0A3L6E9R8	Phosphotransferase OS=*Zea mays* GN=HXK6_0	4.01	6.11	2	0.81	0.01	0.00250	Glycolytic process	Hexokinase activity	None	Hexokinase
1163	A0A3L6FB30	2-C-methyl-D-erythritol 4-phosphate cytidylyltransferase OS=*Zea mays* GN=Zm00014a_019285	3.42	7.77	2	0.76	0.01	0.02980	Isoprenoid biosynthetic process	Catalytic activity	None	Cytidylyltransferase IspD/TarI
Transporters												
771	A0A317YC64	Exportin-2 OS=*Zea mays* GN=CAS_2	6.02	7.08	3	0.53	0.21	0.01243	Intracellular protein transport	Small GTPase binding	None	None predicted
715	A0A3L6EEC4	Mitochondrial dicarboxylate/tricarboxylate transporter DTC OS=*Zea mays* GN=DTC_0	6.41	10.58	3	0.51	0.16	0.04308	Transmembrane transport	None	None	Mitochondrial carrier protein

1087	A0A8J8YBI3	SAM domain-containing protein OS=*Zea mays* GN=Zm00014a_040369	4	9.25	2	0.63	0.06	0.00348	Protein insertion into mitochondrial inner membrane	Protein binding	TIM22 mitochondrial import inner membrane insertion complex	Mitochondrial import inner membrane translocase subunit TIM22
Proteolysis												
120	A0A3L6FZA4	Basic 7S globulin OS=*Zea mays* GN=BG_0	24.17	60.99	48	0.65	0.14	0.01002	Proteolysis	Aspartic-type endopeptidase activity	None	Aspartic peptidase A1 family
463	A0A8J8XEV6	26S proteasome non-ATPase regulatory subunit 13 B OS=*Zea mays* GN=RPN9B_0	9.96	14.81	6	1.49	0.02	0.00563	None	None	Proteasome complex	26S Proteasome non-ATPase regulatory subunit 13
508	A0A3L6F3B5	26S proteasome non-ATPase regulatory subunit 3 homolog A OS=*Zea mays* GN=ZEAMMB73_Zm00001d053232	9.29	13.10	5	1.29	0.03	0.01168	Regulation of protein catabolic process	Enzyme regulator activity	Proteasome complex	None predicted
638	A0A3L6GCC1	26S proteasome non-ATPase regulatory subunit 8 A OS=*Zea mays* GN=RPN12A_1	7.57	23.97	5	0.73	0.04	0.01863	Proteolysis	None	Proteasome regulatory particle	26S proteasome non-ATPase regulatory subunit Rpn12
982	A0A3L6EXI6	Senescence-specific cysteine protease SAG39 OS=*Zea mays* GN=SAG39_3	4.22	11.30	3	0.52	0.12	0.03152	Proteolysis	Cysteine-type peptidase activity	None	None predicted
1122	A0A3L6ERU3	Dipeptidyl aminopeptidase 4 OS=*Zea mays* GN=dap4	3.77	3.02	2	0.69	0.14	0.00983	Proteolysis	Serine –type peptidase activity	None	None predicted
Protein synthesis												
2	A0A8J8Y1U0	Elongation factor 2 OS=*Zea mays* GN=LOS1_2	84.11	62.51	74	1.27	0.14	0.03536	Protein biosynthesis	Translation elongation factor activity	None	None predicted
43	A0A3L6E6H8	Elongation factor 1-gamma 2 OS=*Zea mays* GN=Os02g0220500_	37.75	52.99	23	1.18	0.07	0.02880	Translational elongation	Translation elongation factor activity	None	Elongation factor-gamma, plant
187	A0A8J8YN98	40S ribosomal protein S19 OS=*Zea mays* GN=RPS19A_1	17.69	53.79	11	1.72	0.29	0.01419	Translation	Structural constituent of ribosome	Ribosome	Ribosomal protein S19e
203	A0A3L6EEF2	Ubiquitin-40S ribosomal protein S27a OS=*Zea mays* GN=UBF9_1	17.03	49.03	11	1.15	0.07	0.01804	Translation	Structural constituent of ribosome	Ribosome	None predicted
269	A0A8J8XDY2	40S ribosomal protein S17-4 OS=*Zea mays* GN=RPS17D	14.22	55.63	14	1.55	0.07	0.03251	Translation	Structural constituent of ribosome	Ribosome	Ribosomal protein S17e
279	A0A3L6DV56	Elongation factor 1-delta 1 OS=*Zea mays* GN=Os07g0614500_1	13.88	29.68	10	0.82	0.06	0.00044	Translational elongation	Translation elongation factor activity	Eukaryotic translation elongation factor 1 complex	None predicted

325	A0A3L6EJJ2	Elongation factor Tu, mitochondrial OS=*Zea mays* GN=TUFA_0	12.62	18.97	8	1.16	0.17	0.03072	Protein biosynthesis	Translation elongation factor activity	None	None predicted
328	Q9FYS0	40S ribosomal protein S6 OS=*Zea mays* GN=rps6-2	12.51	30.68	7	1.28	0.08	0.02715	Translation	Structural constituent of ribosome	Ribosome	Ribosomal protein S6e
566	A0A3L6G8Z7	60S ribosomal protein L7-4 OS=*Zea mays* GN=RPL7D_0	8.39	22.54	6	1.66	0.24	0.01447	Maturation of LSU-rRNA from tricistronic rRNA transcript (SSU-rRNA, 5.8S rRNA, LSU-rRNA)	Structural constituent of ribosome	Cytosolic large ribosomal subunit	Ribosomal protein L7/L30
667	A0A3L6E697	Protein transport protein SEC13 B OS=*Zea mays* GN=SEC13B_2	7.14	12.76	4	0.78	0.13	0.03410	Protein transport	Structural molecule activity	None	Protein of unknown function DUF789
683	A0A8J8XT72	60S ribosomal protein L14-1 OS=*Zea mays* GN=RPL14A_1	6.91	33.33	7	1.31	0.19	0.03991	Translation	Structural constituent of ribosome	Ribosome	Ribosomal protein L14
887	A0A3L6G3C8	Protein-synthesizing GTPase OS=*Zea mays* GN=eIF-2gamma_0	4.93	9.05	3	1.21	0.07	0.00185	Protein biosynthesis	Translation initiation factor activity	None	None predicted
928	A0A317Y4T5	60S ribosomal protein L10a OS=*Zea mays* GN=Zm00014a_011473	4.66	19.70	2	1.35	0.22	0.00804	None	Ribosomal protein	Ribosome	Ribosomal protein L1/ribosomal biogenesis protein
1035	B6SH48	40S ribosomal protein S21 OS=*Zea mays* GN=RPS21_1	4.03	23.46	2	1.49	0.20	0.02761	Translation	Structural constituent of ribosome	Ribosome	Ribosomal protein S21e
1171	A0A8J8XYD4	Ribosomal protein L15 OS=*Zea mays* GN=Zm00014a_043538	3.34	10.78	2	1.18	0.10	0.02654	Translation	Structural constituent of ribosome	Ribosome	Ribosomal protein L15e
1362	A0A8J8XQ96	30S ribosomal protein S8, chloroplastic OS=*Zea mays* GN=RPS15AA_1	2.21	37.91	8	1.40	0.05	0.01402	Translation	Structural constituent of ribosome	Ribosome	Ribosomal protein S8
1047	A0A317Y6M7	Diaminopimelate epimerase OS=*Zea mays* GN=DAPF_2	4.01	7.73	2	1.41	0.09	0.00444	Lysine biosynthetic process via diaminopimelate	Diaminopimelate epimerase activity	Cytoplasm	Diaminopimelate epimerase, DapF
1553	A0A8J8XG00	40S ribosomal protein S12 OS=*Zea mays* GN=Zm00014a_038722	2	49.29	5	1.27	0.13	0.01733	Translation	Structural constituent of ribosome	Ribosome	Ribosomal protein S21e
1565	A0A3L6DUJ3	60S ribosomal protein L17 OS=*Zea mays* GN=RPL17_2	2	14.04	3	2.11	0.47	0.01123	Translation	Structural constituent of ribosome	large ribosomal subunit	Ribosomal protein L22/L17
1199	A0A8J8YRV9	60S ribosomal protein L9 OS=*Zea mays* GN=RPL9_3	3.07	44.74	8	0.76	0.09	0.02689	Translation	Structural constituent of ribosome	Ribosome	Ribosomal protein L6 InterPro entry

2016	A0A8J8XT75	Eukaryotic translation initiation factor 2 subunit alpha OS=*Zea mays* GN=At2g40290_0	0.67	8.24	2	0.52	0.25	0.04676	Protein biosynthesis	Translation initiation factor activity	None	Translation initiation factor 2, alpha subunit
Transcription												
216	A0A3L6FA53	Proline--tRNA ligase OS=*Zea mays* GN=At3g62120_0	15.95	25.39	9	0.93	0.04	0.03559	Prolyl-tRNA aminoacylation	Proline tRNA ligase activity	Cytoplasm	Proline-tRNA ligase, class IIa
240	A0A3L6E3A8	Formate--tetrahydrofolate ligase OS=*Zea mays* GN=THFS	15.02	14.44	8	0.86	0,07	0.02597	Tetrahydrofolate interconversion	Formate-tetrahydrofolate ligase activty	None	Formate-tetrahydrofolate ligase, FTHFS
261	A0A8J8XQR7	Putative LL-diaminopimelate aminotransferase, chloroplastic OS=*Zea mays* GN=AGD2_0	14.49	26.62	9	0.82	0.31	0.03474	Biosynthetic process	Transaminase activity	None	LL-diaminopimelate aminotransferase/aminotransferase ALD1
333	A0A3L6FIW2	RGG repeats nuclear RNA binding protein A OS=*Zea mays* GN=RggA_0	12.37	25.40	7	1.31	0.14	0.04238	None	RNA binding	None	RNA binding protein HABP4/SERBP1
1141	A0A3L6DMM3	Nucleosome assembly protein OS=*Zea mays* GN=NAP1:2_0	3.6	7.67	3	1.71	0.16	0.00035	Nucleosome assembly	None	Nucleus	Nucleosome assembly protein (NAP)
1226	A0A3L6EDE8	Histone H2A OS=*Zea mays* GN=Os05g0113900_0	2.91	40.76	16	1.31	0.03	0.03498	None	DNA binding	Nucleus	Histone H2A
1395	A0A3L6GCH2	Histone H2A OS=*Zea mays* GN=Os12g0530000	2.1	31.62	3	1.18	0.09	0.00530	None	DNA binding	Nucleus	Histone H2A
Signal transduction												
930	A0A8J8XH27	Annexin OS=*Zea mays* GN=ANN2	4.66	7.96	3	1.30	0.09	0.04876	None	Calcium ion binding	None	Annexin
1075	A0A3L6DD18	Mitogen-activated protein kinase OS=*Zea mays* GN=MPK6	4	9.11	2	0.69	0.10	0.03523	Protein phosphorylation	MAP kinase activity	None	None predicted
1084	A0A3L6EMG7	Mitochondrial Rho GTPase OS=*Zea mays* GN=Zm00014a_034294	4	5.40	2	0.45	0.28	0.03975	Small GTPase mediated signal transduction	GTPase activity	Integral component of mitochondrial outer membrane	Small GTPase
1233	A0A8J8XGC8	Ras-related protein RABF2b OS=*Zea mays* GN=RABF2B_0	2.89	12.09	2	0.67	0.12	0.04884	None	GTPase activity	None	Small GTPase
Translation												
128	A0A3L6E4Z8	Guanine nucleotide-binding protein subunit beta-like protein A OS=*Zea mays* GN=RACK1A_0	23.09	51.80	13	0.84	0.04	0.00450	None	Ribosome binding	Small ribosomal subunit	Small (40S) ribosomal subunit Asc1/RACK1
1245	A0A3L6FCY7	N-terminal acetyltransferase A complex auxiliary subunit NAA15 OS=*Zea mays* GN=NAA15_1	2.81	2.68	2	0.80	0.03	0.03176	None	Transferase activity	Plastid	N-terminal acetyltransferase A, auxiliary subunit
Cell structure												

1012	B4F989	Actin-7 OS=*Zea mays* GN=103629275	4.07	50.40	3	0.82	0.10	0.01801	None	ATP binding	Cytoskeleton	Actin family
1159	B4FQC4	Serine--tRNA ligase OS=*Zea mays* GN=100272738	3.45	9.17	3	1.21	0.05	0.00385	Seryl-tRNA aminoacylation	Serine tRNA ligase activity	Cytosol	Serine-tRNA ligase, type1
Unclassified												
23	A0A3L6FU97	Alpha-mannosidase OS=*Zea mays* GN=At3g26720	45.65	32.09	30	0.87	0.07	0.02758	Mannose metabolic process	Alpha-mannosidase	None	None predicted
80	A0A3L6EXC4	Monodehydroascorbate reductase OS=*Zea mays* GN=AFRR_0	29.56	53.58	18	0.90	0.06	0.02826	None	Oxidoreductase activity	None	None predicted
159	A0A317Y977	Putative aldo-keto reductase 2 OS=*Zea mays* GN=Zm00014a_008388	19.33	30.35	9	1.20	0.03	0.02946	None	None	None	None predicted
163	A0A8J8YF83	Peptidylprolyl isomerase OS=*Zea mays* GN=FKBP70_0	18.95	19.14	10	1.14	0.06	0.01548	None	Isomerase activity	None	None predicted
214	A0A8J8XES5	CBS domain-containing protein CBSX3, mitochondrial OS=*Zea mays* GN=CBSX3_0	16.32	49.76	12	1.27	0.18	0.03870	None	None	None	None predicted
305	A0A8J8YKV7	DLH domain-containing protein OS=*Zea mays* GN=Zm00014a_023841	12.99	40.42	6	1.29	0.04	0.01642	None	Hydrolase activity	None	None predicted
308	A0A8J8XG74	Putative cinnamyl alcohol dehydrogenase OS=*Zea mays* GN=CAD	12.95	37.87	6	1.33	0.05	0.03373	None	Oxidoreductase activity	None	None predicted
329	A0A3L6DKD9	NAD(P)H dehydrogenase (quinone) OS=*Zea mays* GN=Zm00014a_024219	12.5	50.25	9	1.23	0.04	0.00214	None	NAD(P)H dehydrogenase (quinone) activity	None	Flavoprotein WrbA-like
346	A0A3L6F9B8	Alcohol dehydrogenase 2 OS=*Zea mays* GN=ADH2	11.95	42.22	11	0.67	0.14	0.04403	None	Oxidoreductase activity	None	None predicted
347	A0A3L6EXR3	FAM10 family protein OS=*Zea mays* GN=At4g22670	11.95	13.75	6	1.32	0.17	0.01504	None	Protein dimerization activity	Plastid	None predicted
372	A0A8J8Y4R2	Jasmonate-induced protein OS=*Zea mays* GN=Zm00014a_030223	11.46	24.19	16	0.73	0.13	0.03131	None	None	None	None predicted
499	A0A3L6DLA6	Embryo-specific protein ATS3A OS=*Zea mays* GN=ATS3A	9.44	35.50	5	1.23	0.06	0.00229	None	Protein binding	None	Embryo-specific ATS3
646	A0A3L6FVU1	Remorin OS=*Zea mays* GN=REMO_0	7.5	35.12	5	1.47	0.30	0.04751	None	None	None	None predicted
658	A0A3L6D9I6	Protein DJ-1 B OS=*Zea mays* GN=DJ1B_2	7.26	22.95	4	0.61	0.12	0.01659	None	None	None	Protein/nucleic acid deglycase DJ-1

675	A0A8J8XVA2	Lipid transfer protein EARLI 1 OS=*Zea mays* GN=EARLI1_2	7.02	30.83	4	0.55	0.16	0.03399	None	None	None	None predicted
681	A0A8J8YEP2	Proline-rich protein DC2.15 OS=*Zea mays* GN=14KD_5	6.94	42.75	6	0.77	0.08	0.00331	None	None	None	None predicted
694	A0A317Y3U7	Osmotin-like protein OS=*Zea mays* GN=OLP1_1	6.69	27.85	6	1,21	0.12	0.04375	None	None	None	Thaumatin family
769	A0A8J8YNA3	Putative cinnamyl alcohol dehydrogenase 1 OS=*Zea mays* GN=CAD1_3	6.02	19.30	5	0.78	0.06	0.01869	None	Oxidoreductase activity	None	None predicted
853	A0A8J8YNA9	Glutathione transferase OS=*Zea mays* GN=GSTF8_2	5.25	24.89	3	1.38	0.20	0.01945	None	Transferase activity	None	None predicted
874	A0A3L6DC60	Protein EXORDIUM OS=*Zea mays* GN=EXO_3	5.07	15.55	4	1.62	0.19	0.00177	None	None	Extracellular space	Protein EXORDIUM-like
949	A0A8J8XK82	NADH-u_ox-rdase domain-containing protein OS=*Zea mays* GN=Zm00014a_015568	4.47	45.62	2	0.60	0.24	0.02652	None	None	None	None predicted
959	A0A3L6DPZ2	Omega-hydroxypalmitate O-feruloyl transferase OS=*Zea mays* GN=HHT1_7	4.4	8.61	3	1.17	0.06	0.04101	None	Acyltransferase activity, transferring groups other than amino-acyl groups	None	None predicted
990	A0A8J8YBL4	Uncharacterized protein OS=*Zea mays* GN=At4g28440_4	4.17	28.47	3	1.10	0.06	0.03908	None	None	None	None predicted
1015	A0A317YK58	3-oxo-Delta(4,5)-steroid 5-beta-reductase OS=*Zea mays* GN=5BPOR_0	4.07	15.15	20	0.75	0.12	0.00346	None	None	None	None predicted
1043	A0A8J8XTU6	Cortical cell-delineating protein OS=*Zea mays* GN=CCDP_6	4.01	31.75	4	0.49	0.20	0.00250	None	None	None	None predicted
1176	A0A3L6GF22	Uncharacterized protein OS=*Zea mays* GN=Zm00014a_010243	3.3	15.60	3	2.14	0.78	0.04804	None	None	None	ABA/WDS induced protein
1249	A0A3L6DPI9	Hydroxyphenylpyruvate reductase OS=*Zea mays* GN=HPPR_0	2.79	7.01	2	1.30	0.06	0.01413	None	NAD binding	None	None predicted
13001	A0A3L6FJK1	Universal stress protein PHOS32 OS=*Zea mays* GN=PHOS32_0	2.47	8.81	2	1.50	0.18	0.03324	None	None	None	Universal stress protein A family
1367	A0A3L6EAR6	Heterogeneous nuclear ribonucleoprotein 1 OS=*Zea mays* GN=RNP1_14 P	2.19	12.65	4	0.64	0.11	0.01911	None	mRNA binding	None	None predicted
1776	A0A3L6GF22	Uncharacterized protein OS=*Zea mays* GN=Zm00014a_010243	3.3	15.60	3	2.14	0.78	0.04804	None	None	None	ABA/WDS induced protein

1902	A0A8J8YDU2	Stromal cell-derived factor 2-like protein OS=*Zea mays* GN=Zm00014a_011359	1.11	14.36	2	1.45	0.10	0.00842	None	None	None	Not predicted
2300	A0A3L6FTA1	Uncharacterized protein OS=*Zea mays* GN=Zm00014a_027366	0.14	9.92	2	1.72	0.36	0.02223	None	None	None	ABA/WDS induced protein

[a]Protein accession number obtained from the uniprot database (https//www.uniprot.org).

[b]Protein score generated by Protein Pilot software relating to the confidence of protein identification. A protein identification threshold of 1.3 was applied to the data, which only retains proteins identified with a 95% confidence.

[c] Percentage coverage is determined by the number of amino acids of sequenced peptides against the total length of the protein, with a threshold of at least 95% confidence.

[d]Sequenced peptide refers to the number of peptide that were sequenced and gave rise to protein identity. All proteins that were identified by means of a single peptide were filtered out of the dataset.

[e]Probability value of the quantitative difference between the treatment and control protein abundance being due to chance alone.

[f]Standard deviation of the ratios of drought stressed samples (n=4).

[g] Ratio represents the average fold-change (n = 4) induced by treatment relative to control. Positive values indicate an up-regulation.

[h] Total number of differentially expressed proteins obtained using the Student's *t* - test at $p \leq 0.05$

[i] Gene ontology analysis as predicted on the IntePro database (https://www.ebi.ac.uk/interpro/) and UniProt database (http://www.uniprot.org). P denotes Biological Process, F denotes Functional Process, and C denotes Cellular Component.

[j] Conserved family name as predicted by InterPro database (http://www.ebi.ac.uk/interpro/).

4.2.4 The distribution of drought-responsive proteins in a Venn diagram

To study the differential impact of the mild water stress treatment on the root tissue, the distribution of drought-responsive proteins between the two maize varieties is presented in a Venn diagram (Figure 4.2). Only seven drought-responsive proteins were shared between the two varieties. Of these seven common proteins, three were up-regulated, while four were down-regulated in CN07/8-224, whereas one was up-regulated and six were down-regulated in CN07/8-292. These common drought-responsive proteins were distributed in the functional categories of primary/secondary metabolism (3), disease/defence (1), protein synthesis (1), and unclassified (2). The details of these common proteins are shown in Table 4.4.

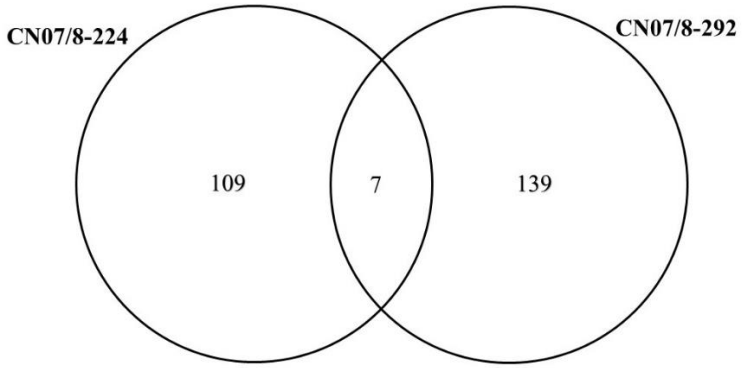

Figure 4.2: Venn diagram showing the common drought-responsive proteins of the two maize varieties under mild drought stress.

Table 4.4: List of common drought-responsive proteins between the two maize varieties.

Accession[a]	Protein Name	CN07/8-224			CN07/8-292			Protein family name[e]
		Ratio[b]	STD[c]	p- value[d]	Ratio	STD	p- value	
Primary/secondary metabolism								
A0A317YDG1	DIMBOA UDP-glucosyltransferase BX9 OS=*Zea mays* GN=BX9	0.87	0.05	0.01243	1.18	0.06	0.03151	UDP-glucuronosyl/UDP-glucosyltransferase
A0A3L6FKW8	Chitinase OS=*Zea mays* GN=CHIA_3	1.37	0.20	0.01201	0.70	0.07	0.00185	None predicted
C4JAI3	Cyclase family protein OS=*Zea mays* GN=100502334	0.81	0.03	0.01468	0.60	0.24	0.00118	Kynurenine formamidase/cyclase-like
Disease/defence								
A0A3L6EUP4	Dirigent protein OS=*Zea mays* GN=DIR2	1.16	0.08	0.04271	0.83	0.05	0.04731	Dirigent protein
Protein synthesis								
A0A3L6DV56	Elongation factor 1-delta 1 OS=*Zea mays* GN=Os07g0614500_1	0.71	0.14	0.01405	0.82	0.06	0.00044	None predicted
Unclassified								
A0A8J8YEP2	Proline-rich protein DC2.15 OS=*Zea mays* GN=14KD_5	1.74	0.52	0.04326	0.77	0.08	0.00331	None predicted
A0A3L6F9B8	Alcohol dehydrogenase 2 OS=*Zea mays* GN=ADH2	0.69	0.03	0.00990	0.67	0.14	0.04403	None predicted

[a]Protein accession number obtained from the Uniprot database (https//www.uniprot.org).
[b]Ratio represents the average fold-change (n = 4) induced by treatment relative to control.
[c]Standard deviation of the ratios of drought stressed samples (n=4).
[d] Total number of differentially expressed proteins obtained using the Student's *t* - test at $p \leq 0.05$
[e]Conserved family name as predicted by InterPro database (http://www.ebi.ac.uk/interpro/).

4.2.5 Bioinformatics analyses on the drought-responsive proteins

The GO annotations of the drought-responsive proteins of each maize variety (Tables 4.2 and 4.3) were arranged according to the three terms: biological processes, molecular functions, and cellular components. The results revealed that a large number of the proteins had no known biological processes (28.4% and 36.3%), and glycolytic process (1.7% and 3.4%), proteolysis (6.9% and 2.7%), response to oxidative stress (7.8% and 6.2%), and translation (12.1% and 7.5 %) were the most represented common biological processes for CN07/8-224 and CN07/8-292, respectively. ATP metabolic process (1.7%), ribosome biogenesis (0.9%) and cellular oxidant detoxification (0.9%) were some of the biological processes unique to CN07/8-224. On the other hand, protein biosynthesis (2.8%), isocitrate metabolic process (1.4%), glutathione metabolic process (0.68%) were identified only in CN07/8-292 (Figure 4.3).

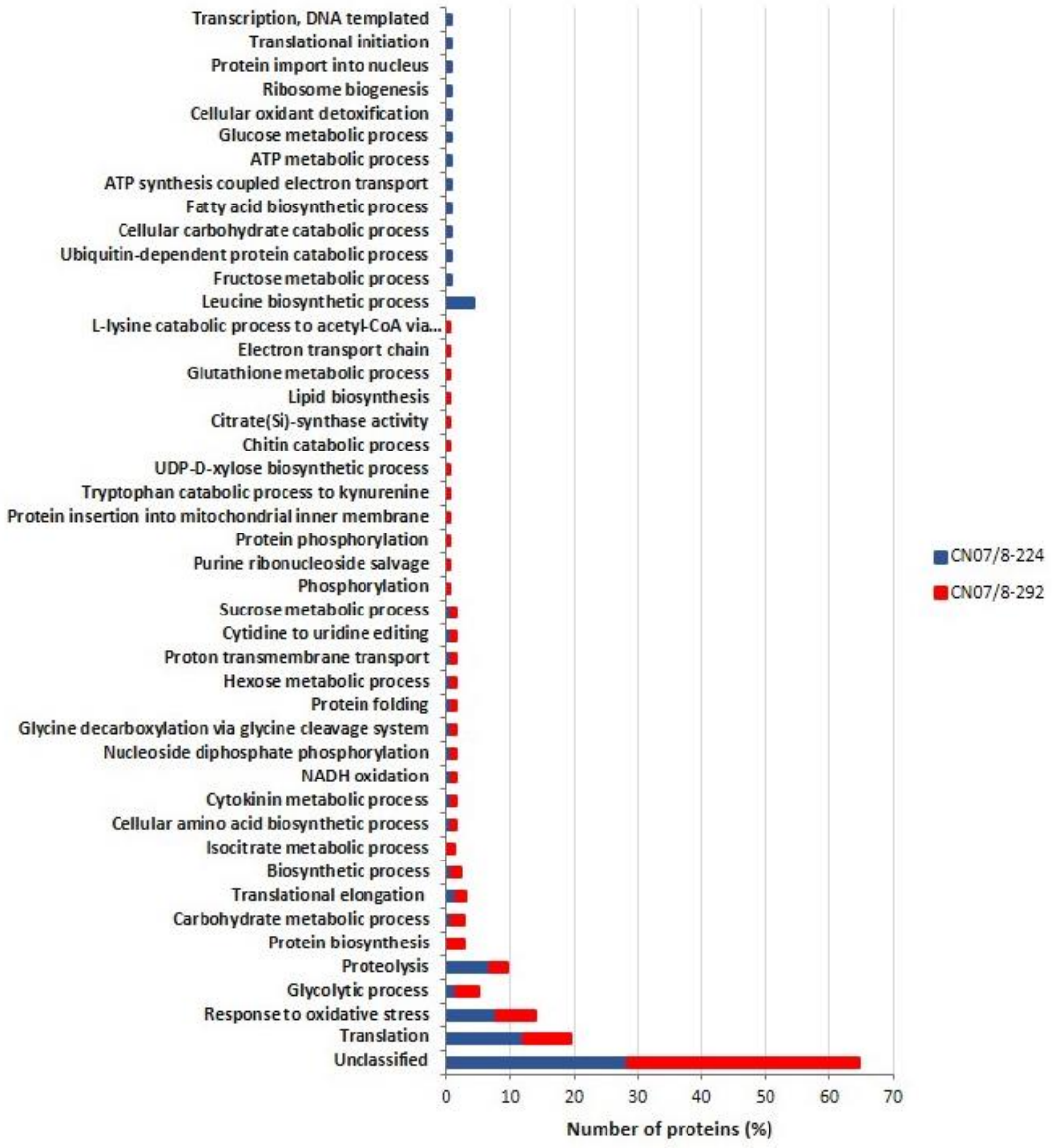

Figure 4.3: Biological processes of the identified maize root drought responsive proteins based on GO annotations.

4.2.6 GO annotations on the molecular activities of the proteins associated with maize root drought response.

The highly represented molecular functions were ATP binding (4.3% and 2.1%), RNA binding (6.9% and 0.68%), peroxidase activity (6.9% and 5.5%), structural constituent of ribosome (10.3% and 8.3%), for CN07/8-224 and CN07/8-292 varieties, respectively. However, proteins of unknown molecular functions were also abundant in both maize varieties (Figure 4.4). Some of the unique molecular functions were catalytic activity (0.9%), NADP binding (0.9%), and peptidase activity (0.9%) in CN07/8-224. In CN07/8-292, ATP-dependent folding chaperone (0.9%), enzyme regulator activity (0.9%), and ribosomal protein (0.9%) were uniquely identified.

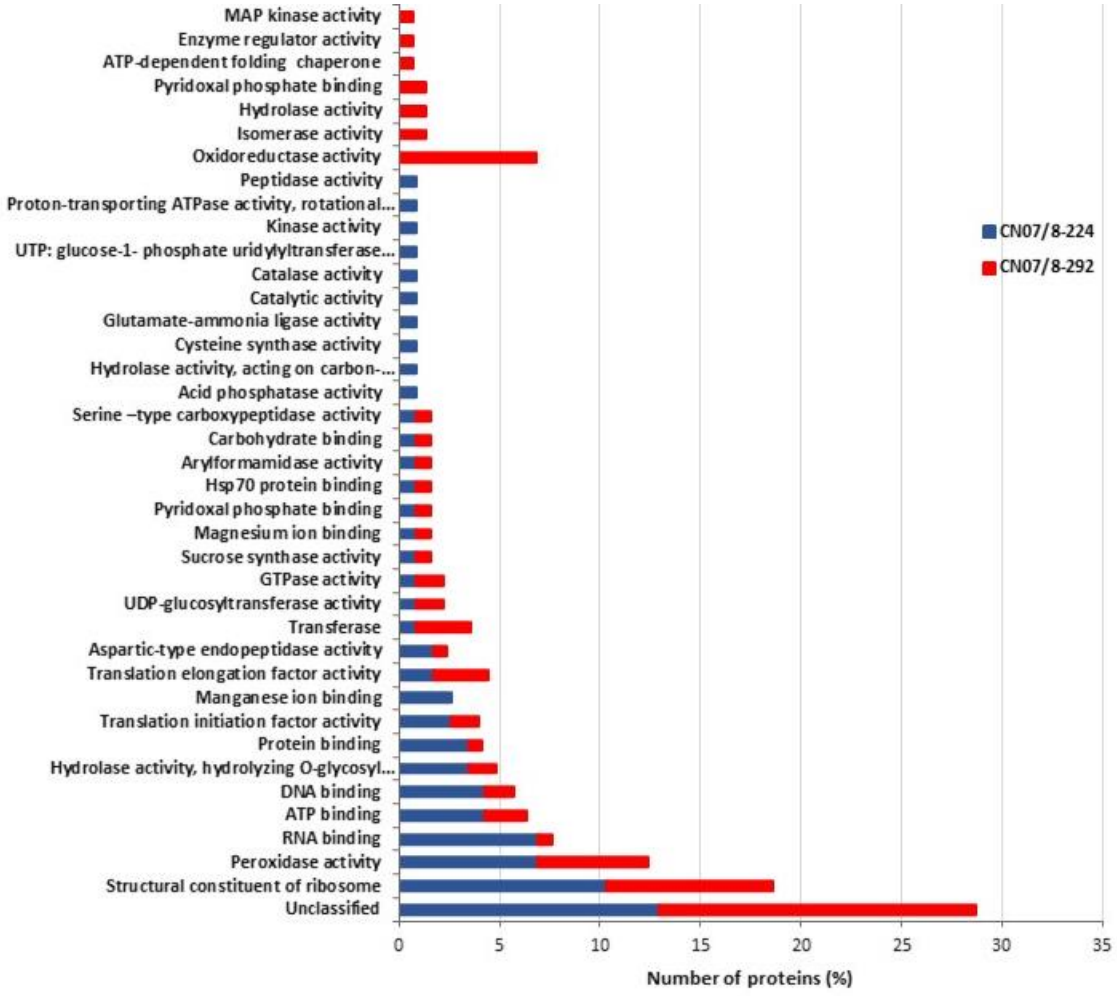

Figure 4.4: Molecular functions of the identified maize root drought responsive proteins based on GO annotations.

4.2.7 GO annotations on the cellular activities of the proteins associated with maize root drought response.

The cellular component analysis showed that proteins were mostly located in the cytoplasm (2.6% and 2.1%), nucleus (5% and 2%), ribosome (11% and 7%), and extracellular region (11.1% and 7.6%), and unknown locations (39.3% and 62.5%) for CN7/8-224 and CN07/8-292, respectively (Figure 4.5). The apoplast (2.6%), chloroplast (0.9%), and endoplasmic reticulum (0.9%) were some of the uniquely identified protein locations in CN07/8-224, while in the CN07/8-292, some of identified proteins were uniquely located in the proteasome complex (1.4%), mitochondrion (1.4%), and cytoskeleton (1.4%) (Figure 4.5).

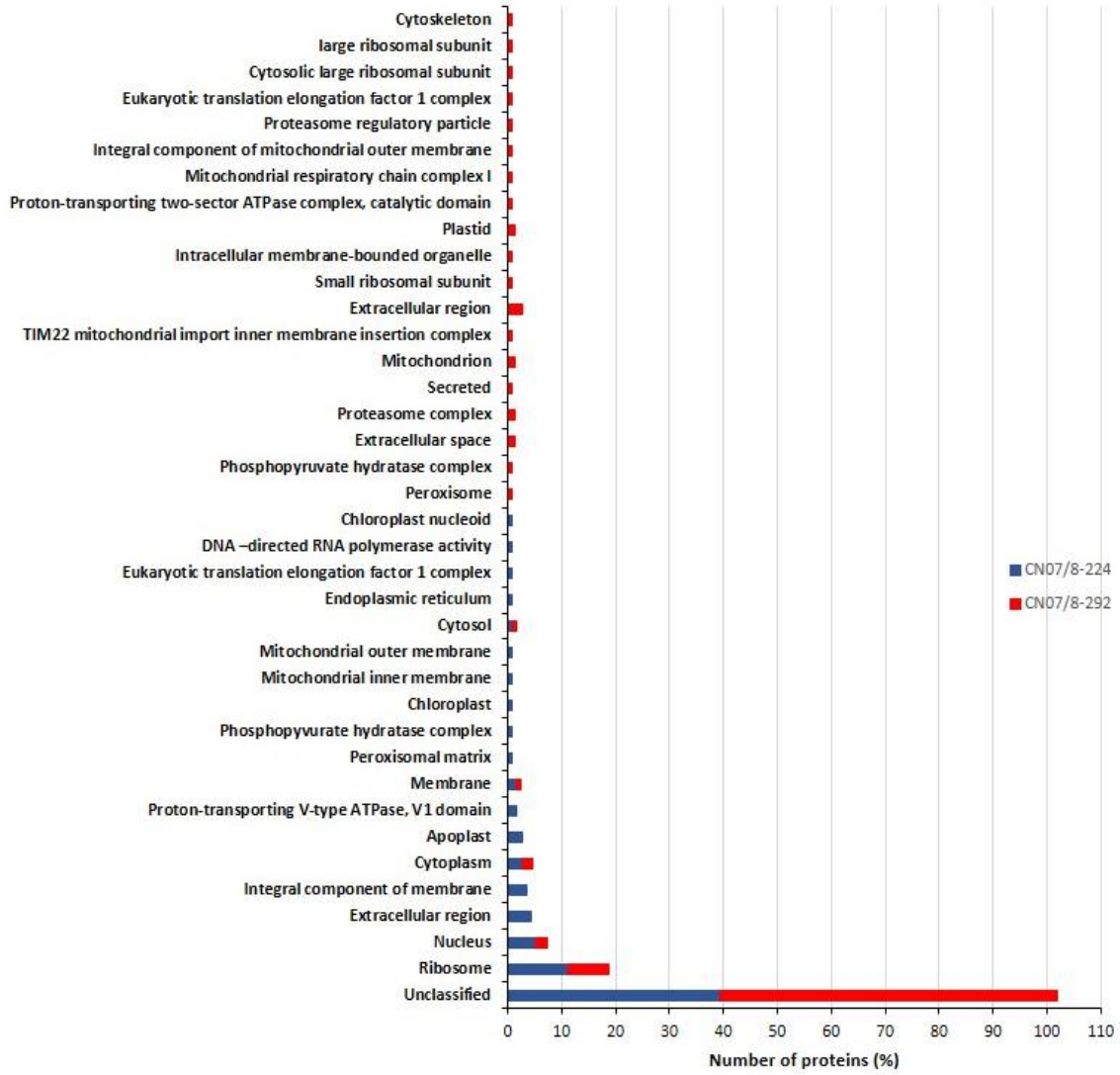

Figure 4.5: Cellular component of the identified maize root drought responsive proteins based on GO annotations.

4.2.8. Functional categories of differentially expressed proteins in maize root tissue

The drought-responsive proteins of CN07/8-224 and CN07/8-292 maize varieties were classified into functional categories according to Bevan *et al*, (1998) and listed in Tables 4.2 and 4.3, respectively. This data is further depicted in Figures 4.6 below. A large proportion of these proteins were involved in primary/secondary metabolism (22% and 32%), disease/defence (21% and 10%), and protein synthesis (19% and 13%), energy (6% and 8%), while 9% and 18% were not classified into any functional groups in CN07/8-224 and CN07/8-292, respectively. Translation (1%), and cell structure (1%), and signal transduction (3%) were only identified in CN07/8-292.

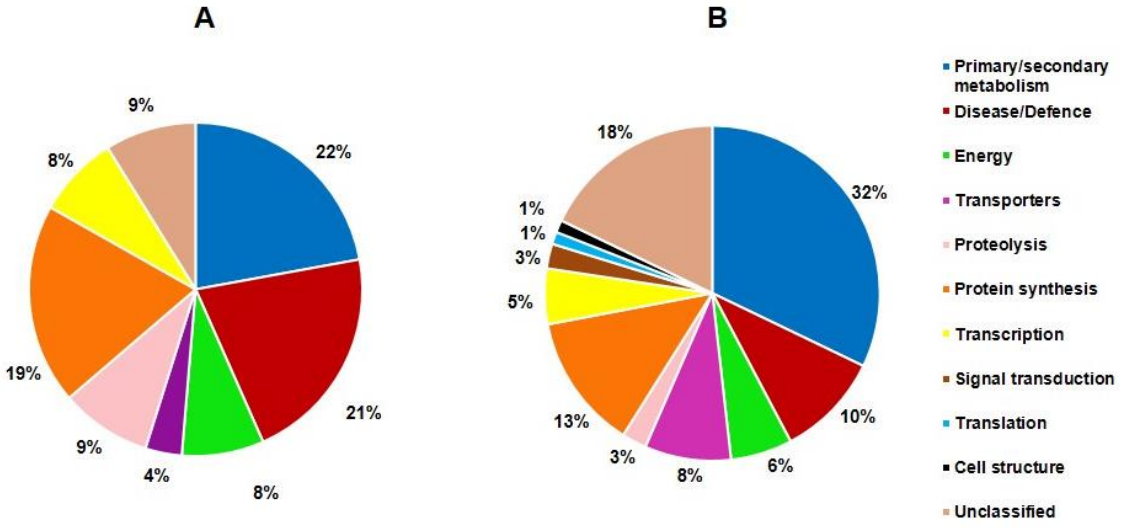

Figure 4.6: The distribution of drought-responsive maize root proteins according to functional groups. (A) drought-responsive proteins of CN07/8-224 and (B) drought-responsive proteins of CN07/8-292 maize varieties.

The proportion of up- and down-regulated proteins in each functional group are shown in Figure 4.7. In CN07/8-292, there were more up-regulated proteins in the protein synthesis functional category than in CN07/8-224. On the other hand, more proteins were down-regulated in the protein synthesis functional group in CN07/8-224 than in CN07/8-292. Furthermore, they were more up-regulated proteins in disease/defence, energy, and proteolysis functional categories in CN07/8-224, but more down-regulated proteins in signal transduction, translation, and proteolysis categories in CN07/8-292 than CN07/8-224 (Figure 4.7).

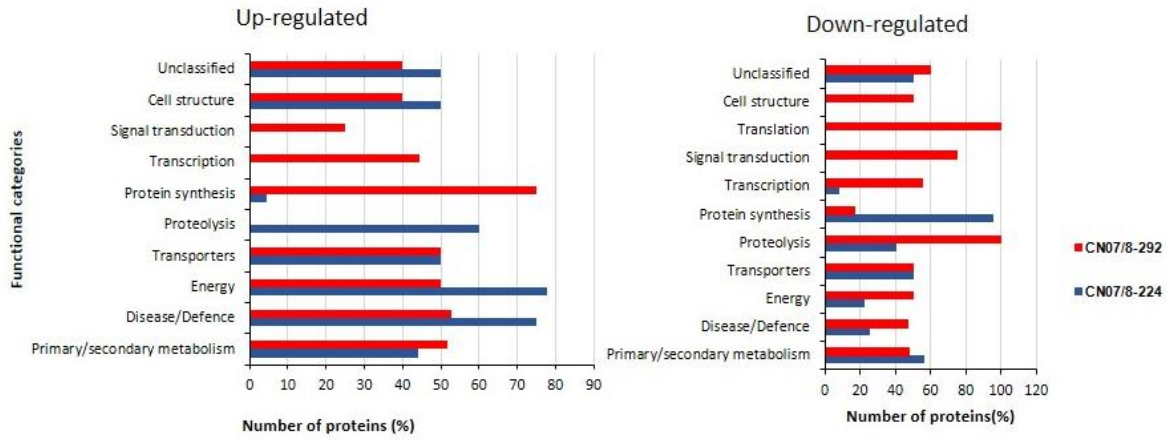

Figure 4.7: Differences in the protein accumulation within each functional group between CN07/8-224 and CN07/8-292 under mild drought stress.

4.3. Discussion

In order to understand how plants, adapt to mild drought stress, this study identified root proteome changes of two maize varieties CN07/8-224 and CN07/8-292 using iTRAQ, and bioinformatically analysed the differentially expressed proteins (Table 4.2 and Table 4.3). According to the results obtained, the two maize varieties performed differently under the imposed mild drought-stressed conditions with CN07/8-292 having a higher number of drought responsive proteins than CN07/8-224 (Table 4.1). This could possibly mean that the two varieties experienced drought stress differently.

Changes in the expression of genes associated with drought response may prevent the synthesis of functional proteins usually produced under optimum growth conditions and instead lead to the production of stress-specific proteins (Li *et al.*, 2020). Drought stress proteins include dirigent proteins, dehydrins, heat shock proteins (HSPs), and late embryonic abundant (LEA) proteins (Li *et al.*, 2020). These proteins are essential in stabilising membrane proteins and in osmotic adjustment (Benešová *et al.*, 2012). Furthermore, drought-responsive proteins that regulate metabolic pathways and activities either enhance or hinder a plant's tolerance to drought stress (Yang *et al.*, 2014). In some cases, different varieties within a plant species may exhibit common and unique drought stress-responsive proteins when exposed to similar levels of water deprivation. This has been reported in drought studies of sorghum roots (Goche *et al.*, 2020), maize leaves (Benešová *et al.*, 2012), and wheat leaves (Cheng *et al.*, 2016).

In the current study, a dirigent protein is amongst the seven common proteins identified in both CN07/8-224 and CN07/8-292 maize varieties after exposure to the mild drought treatment (Figure 4.2; Table 4.4). However, its expression patterns differed in the two maize varieties,

with an up-regulation in CN07/8-224 and a down-regulation in CN07/8-292. Dirigent proteins are known to play a role in lignin biosynthesis and other stress stress-adaptive in plants (Paniagua *et al.*, 2017). According to earlier studies, sugarcane was significantly enriched with digirent proteins that responded to drought stress (Li *et al.*, 2022). Another study found that transgenic tobacco lines which abundantly expressed dirigent protein genes of the *Saccharum* spp (ScDIRs) subfamily, DIR b/d (ScDIR5 and ScDIR11) and DIRc (ScDIR7 and ScDIR40), were more likely to survive drought (Li *et al.*, 2022). Therefore, the increased accumulation of a dirigent protein in CN07/8-224 and its down-regulation in CN07/8-292 could possibly mean that CN07/8-224 had the ability to strengthen the cell wall to avoid the dehydration-induced damage.

As summarised in Figure 4.6, the two maize varieties also showed differences in the proportion of proteins within each functional group. The largest represented group for either of the maize varieties was that of primary and secondary metabolism. This group included proteins involved in the metabolism of amino acids, carbohydrates, lipids, lignin, nucleosides, sulfur and cytokinins (Tables 4.2 and 4.3). All these primary and secondary metabolites are necessary for normal cell function with or without external stress factors (Yao *et al.*, 2020). For example, amino acids are the primary agents of nitrogen distribution throughout the plant body (Yao *et al.*, 2020). The carbohydrates are crucial energy sources, carbon skeletons for organic molecules, and storage materials (Trouvelot *et al.*, 2014). As already stated above lignin is linked to not just plant growth and development but also to the plant's ability to improve mechanical strength of the stem tissues (Ma *et al.*, 2009). Although there were more up-regulated primary/secondary metabolism proteins in CN07/8-292 than in CN07/8-224 (Table 4.2; Figure 4.7), it is significant to highlight that the two varieties of maize expressed quite a diverse range of metabolites. For instance, CN07/8-224 possessed a significant number of

pathways for the metabolism of carbohydrates and amino acids that responded to the moderate water deprivation stress (Figures 4.6; and 4.7). However, CN07/8-292 had a much more diverse group of metabolites that respond to the stress (Figures 4.6; and 4.7). For example, this maize variety has metabolic pathways of carbohydrates, amino acids, fatty acids, nucleosides and other secondary metabolites being affected by drought. Therefore, it is very difficult to postulate on the probable significance of these findings until further functional validation studies are conducted.

Plants have evolved antioxidant defence systems to protect cells from oxidative damage caused by ROS under various stresses, including water limitation (Kosová *et al.*, 2011). In the current study, many proteins related to the antioxidant defence systems were identified as responsive to water stress. These proteins were classified into the disease/defence functional category (Tables 4.2 and 4.3). Examples of the identified antioxidant enzymes include peroxidase, catalase, glutathione S-transferase and glutathione peroxidase for the CN07/8-292 maize variety (Table 4.3). For CN07/8-224, examples of identified antioxidant enzymes are monodehydroascorbate reductase, peroxidase and catalase (Table 4.2). For example, peroxidases remove hydrogen peroxide (H_2O_2) radicals in plants caused by oxidative stress and occur in different plant tissues, including roots and leaves (Farooq *et al.*, 2019). The oxidative stress disrupts the functioning and wellbeing of plants.

In the current study, 18 of the 24 peroxidases in CN07/8-224 roots were up-regulated (Figure 4.7). In contrast, only 9 of the 17 peroxidases in CN07/8-292 had increased accumulation (Figure 4.7). The high accumulation of peroxidases may have helped CN07/8-224 to quench ROS and reduce the level of oxidative damage more effectively than in CN07/8-292. In addition, the results observed in the present study correlated with those reported by Zenda *et*

al, (2018), where more antioxidant enzymes effectively eliminated ROS accumulated in Chang 7-2, a drought-tolerant maize line, when compared to the sensitive line TS141.

Germin and germin-like proteins (GLPs) are water-soluble glycoproteins of the cupin subfamily exclusive to plants (Bernier and Berna, 2001; Wang *et al.*, 2013). They function in plant growth and development processes, as well as in defence responses (Barman *et al.*, 2015; Liu *et al.*, 2016). Through its oxalate oxidase or superoxide dismutase (SOD) activity, the GLP protein acts as a cofactor during the cross-linking of plant cell wall proteins at the site of pathogenic infection to strengthen the cell wall (Yuan *et al.*, 2021). In the current study, the germin proteins identified were up-regulated in CN07/8-224 and listed under the defence/disease category, which could mean that these proteins assist in maintaining the CN07/8-224 plant cells to cope with drought stress.

Energy metabolism is essential for plant development and stress response and is one of the most critical pathways in plants that regulate sugar biosynthesis, conversion, and carbon distribution (Farooq *et al.*, 2009). According to the functional catalogue of plant genes described by Bevan *et al*, (1998), the energy functional group consists of genes and proteins involved in photosynthesis, glycolysis, and electron transport, amongst others. Some of these pathways respond to biotic and abiotic stresses primarily by affecting the supply of ATP to plants (Li *et al.*, 2020) and have been identified as drought-responsive in sorghum (Goche *et al.*, 2020; Li *et al*., 2020), and maize (Li *et al*., 2021).

In this study, energy-related glycolysis, glucose metabolic, and ATP metabolic processes were significantly altered in response to drought stress (Tables 4.2 and 4.3; Figure 4.3). For example, a total of 7 out of 9 (77.7%), and 5 out of 10 (50%) energy-related proteins were up-regulated

in CN07/8-224 and CN07/8-292 under the imposed mild drought stress conditions, respectively (Figure 4.7). The up-regulated proteins belong to protein families of enolase, fructose-bisphosphate aldolase, class-II phytocyanin, and V-type ATP synthase regulatory subunit B/beta, and NADH dehydrogenase ubiquinone Fe-S protein 4, mitochondrial. In addition, the proteins are involved in biological processes of glycolytic process, electron transport chain and ATP metabolic process (Tables 4.2 and 4.3; Figure 4.4). Similarly, Zeng *et al*, (2019) observed an increase in the glycolysis/gluconeogenesis pathway in the two maize varieties (Chang 7-2 and TS141), which resulted in significant production of ATP and NADPH in response to drought. This energy could be utilised in metabolic activities directly related to the protection of plant cells against dehydration, and other physiological processes involved in the maintenance of plant growth and development. (Farooq *et al*., 2009). Therefore, the observed up-regulation of the above-mentioned energy-related proteins possibly imply that the ATP production processes were activated for the provision of energy for a wide range of functions under water stress conditions.

Another highly represented drought-responsive functional group was that of protein synthesis (Tables 4.2 and 4.3). These proteins were involved in the biological processes of protein biosynthesis, ribosome biogenesis, translational elongation, and translation (Figure 4.3). Overall, protein synthesis-related proteins were more up-regulated in CN07/8-292 than in CNO7/8-224 (Table 4.2 and 4.3; Figure 4.7), and most of the drought responsive proteins are involved in translation. On the contrary, translation, translation elongation, and ribosome biogenesis proteins were down-regulated in CN07/8-224. The down-regulation of the identified proteins in CN07/8-224 possibly implies that the synthesis of proteins was inhibited in this maize variety under drought stress. The same trend was observed in a study where

ribosomal proteins were down-regulated under severe drought stress in maize (Shaanke 9) seedlings (Li *et al*., 2021).

Furthermore, transcription and translation are co-related processes for the synthesis of proteins and metabolites (Zheng *et al.*, 2010). Under conditions of drought stress, changes in transcriptional processes assist plants in modulating the expression of genes in response to the stress (Libault *et al*., 2009). This will later result in changes in the protein and metabolite profiles on plants in response to the prevailing stress conditions (Libault *et al.*, 2009). In this study, four of the nine transcription-related proteins were up-regulated in CN07/8-292, which tallies well with the protein synthesis results discussed above. In CN07/8-224, however, all nine drought-responsive proteins involved in transcription were down-regulated. Both these trends in the accumulation of transcription related proteins align well with the protein synthesis results discussed above, as a high transcription output, resulted in increased protein synthesis and vice versa.

Drought-responsive proteins may also be involved in proteolysis (Zheng *et al*., 2010). Proteolysis is the cleavage of peptide bonds between two amino acid residues and the process occurs in all living organisms (Beaubier e*t al*., 2019). Six out of 10 drought responsive proteins were up-regulated in CN07/8-224, while for CN07/8-292 all proteolysis-related proteins were down-regulated under drought stress conditions.

Apart from the well-characterised proteins that could easily be grouped into specific functional classes (Figures 4.3; 4.4; and 4.5), a large number of the mild-stress responsive proteins identified in the current study were unclassified. Similar to this, many proteomic studies on sorghum carried out by our research team revealed complex protein networks that may enable

sorghum responses to water limitation (Goche *et al*., 2020). While the probable functions of these unclassified proteins are not yet known, they could be presenting proteins with important functions in drought response. Therefore, more work needs to be done to validate these proteins.

Chapter 5

General conclusions and recommendations

Maize (*Zea mays*) is a cereal crop that plays a crucial role in maintaining global food supply. However, like most plant species, it is vulnerable to drought, which can significantly influence crop productivity. With climate change causing increased drought stress, there is a need to improve the drought resistance of maize plants. To do so, it is necessary to understand the physiological and molecular mechanisms of drought response in the entire plant. Previous research has found that the ability to withstand drought is closely linked to the growth and development of maize roots. Therefore, the current study aimed to evaluate the morpho-physiological and biochemical changes of two maize varieties in response to water limitation and identify root proteome changes in the varieties using proteomic tools. The two maize types, CN07/8-224 and CN07/8-292, used in this study lack published data on their levels of drought tolerance, and their drought phenotypic traits are unknown. However, these two lines form part of a maize breeding program at the Agricultural Research Council, Potchefstroom, South Africa.

In conclusion, the combined physiological and biochemical results obtained in this study have demonstrated the important adaptive responses of maize leaves and roots under water limiting conditions. Conclusively, an elongated root length system of the CN07/8-224 variety ensured a higher shoot length growth. Compared to the CN07/8-224 control plants, the CN07/8-224 drought treated plants had a lower level of chlorophyll pigments, including carotenoids, and supported by a lighter shade of the green leaves (Figure 3.2). The results are consistent with the idea that chloroplasts produce a lot of reactive oxygen species under drought stress, which

could further lower the chlorophyll content resulting in lower rate of photosynthesis. Questions about the CN07/8-224 variety's defence mechanisms to drought stress conditions are further raised by the lack of a significant increase in the amount of malondialdehyde (MDA) and that of hydrogen peroxide in the drought-treated plants compared to their respective control. By a non-significant increase in MDA and hydrogen peroxide levels and a high accumulation of antioxidant enzymes, the CN07/8-292 variety experienced more drought stress. The antioxidant enzymes are responsible for protecting the plants against oxidative damage caused by drought stress. Therefore, this could possibly mean that higher activity of antioxidant enzymes acted as a defence mechanism to cope with the stress. However, additional validation experiments are necessary to determine the relative degrees of drought resilience of these two maize varieties as there are no major differences in the physiological and biochemical data obtained between the two maize varieties.

At the proteomic level, this study found that there were differences in the number and regulation patterns of drought-responsive proteins between the CN07/8-224 and CN07/8-292 maize varieties under mild water stress conditions. CN07/8-224 had 52 up-regulated and 64 down-regulated proteins, while CN07/8-292 had 75 up-regulated and 71 down-regulated proteins. Only seven proteins were common between the two varieties, with different regulation patterns in each. Future validation studies are also required to ascertain the proteomics results.

Indeed, the current study provided a foundation for future studies aimed at understanding the drought tolerance in these two maize varieties. Therefore, recommendations for future work are as follows:

i. To expose the maize plants to severe water limitation stress and sample plant tissues at different time points for example 7, 14, 21, and 28 days for analyses. Such drought experiments could provide more insight into the physiological, biochemical, and molecular processes recruited by each maize variety under both mild and severe drought stress.

ii. To conduct a metabolite profiling study under mild and severe drought-stress conditions to establish possible molecular markers for drought tolerance.

iii. To validate target genes identified in the proteomic analysis of this study using quantitative real-time polymerase chain reaction (qRT-PCR).

iv. To compare the differentially expressed proteins of the current study to those identified in other cereals such as sorghum (Goche *et al.*, 2020). Plant breeding programs can use these selected drought marker genes to develop genetic resources for developing maize genotypes with improved drought resistance.

References

Agurla, S., Gahir, S., Munemasa, S., Murata, Y., Raghavendra, A.S. 2018. Mechanism of stomatal closure in plants exposed to drought and cold stress. *Advanced Experimental Medicinal Biology*. 1081, 215 - 232.

Ahmad, N., Malagoli, M., Wirtz, M. and Hell, R. 2016. Drought stress in maize causes differential acclimation responses of glutathione and sulfur metabolism in leaves and roots. *BMC Plant Biology*. 161, 247 - 253

Ali, Q., Anwar, F., Ashraf, M., Saari, N. and Perveen, R. 2013. Ameliorating effects of exogenously applied proline on seed composition, seed oil quality and oil antioxidant activity of maize (*Zea mays L*.) under drought stress. *International Journal of Molecular Sciences*. 14, 818 - 835.

Andrés, Z., Pérez-Hormaeche, J., Leidi, E.O., Schlücking, K., Steinhorst, L., McLachlan, D.H., Schumacher, K., Hetherington, A.M., Kudla, J., Cubero, B., Pardo, J.M. 2014. Control of vacuolar dynamics and regulation of stomatal aperture by tonoplast potassium uptake. *Proceedings of National Academy of Sciences*. 111, 1806 - 1814.

Anjum, S.A., Xie, X.Y., Wang, L.C., Saleem, M.F., Man, C. and Lei, W. 2011. Morphological, physiological and biochemical responses of plants to drought stress. *African Journal of Agricultural Research.* 6 , 2026 - 2032.

Anjum, S.A., Ashraf, U., Tanveer, M., Khan, I., Hussain, S., Shahzad, B., Zohaib, A., Abbas, F., Saleem, M.F., Ali, I. and Wang, L.C. 2017. Drought induced changes in growth, osmolyte accumulation and antioxidant metabolism of three maize hybrids. *Frontiers in Plant Science*. *8*, 69.

Araújo, W.L., Nunes-Nesi, A., Nikoloski, Z., Sweetlove, L.J., Fernie, A.R. 2012. Metabolic control and regulation of the tricarboxylic acid cycle in photosynthetic and heterotrophic plant tissues. *Plant Cell & Environment*. 35, 1 - 21.

Asgharipour, M.R. 2011. Effect of potassium supply on drought resistance in sorghum: Plant growth and macronutrient content Energy analysis of surface and subsurface drip-tape irrigation View Project Extended exergy analysis (EAA) of two canola-farming systems in Khorramabad, Iran. *Pakistan Journal of Agricultural Science.* 48, 197 - 204.

Ashraf, M.F.M.R. and Foolad, M.R. 2007. Roles of glycine betaine and proline in improving plant

abiotic stress resistance. *Environmental and Experimental Botany*. 59, 206 - 216.

Aslam, M., Zamir, M.S.I., Afzal, I., Yaseen, M., Mubeen, M. and Shoaib, A. 2013. Drought stress, its effect on maize production and development of drought tolerance through potassium application. *Cercetări Agronomice în Moldova*. 46, 99 - 114.

Asseng, S., Ritchie, J.T., Smucker, A.J.M., Robertson, M.J. 1998. Root growth and water uptake during water deficit and recovering in wheat. *Plant Soil*. 201, 265 - 273.

Badr, A., El-Shazly, H.H., Tarawneh, R.A., Börner, A. 2020. Screening for drought tolerance in maize (*Zea mays L.*) germplasm using germination and seedling traits under simulated drought conditions. *Plants*. 9, 565.

Bagheri, V., Shamshiri, M.H., Shirani, H., Roosta, H.R. 2018. Nutrient Uptake and Distribution in Mycorrhizal Pistachio Seedlings under Drought Stress.

Bayoumi, T.Y., Eid, M.H. and Metwali, E.M. 2008. Application of physiological and biochemical indices as a screening technique for drought tolerance in wheat genotypes. *African Journal of Biotechnology*. 7, 1 - 12

Barman, A.R. and Banerjee, J. 2015. Versatility of germin-like proteins in their sequences, expressions, and functions. *Functional and Integrative Genomics*. 15, 533 - 548.

Barrios-Masias, F.H., Knipfer, T., McElrone, A.J. 2015. Differential responses of grapevine rootstocks to water stress are associated with adjustments in fine root hydraulic physiology and suberization. *Journal of Experimental Botany*. 66, 6069 - 6078.

Barrs, H.D. and Weatherley, P.E. 1962. A re-examination of the relative turgidity technique for estimating water deficits in leaves. *Australian Journal of Biological Sciences*. 15, 413-428.

Beaubier, S., Framboisier, X., Ioannou, I., Galet, O. and Kapel, R. 2019. Simultaneous quantification of the degree of hydrolysis, protein conversion rate and mean molar weight of peptides released in the course of enzymatic proteolysis. *Journal of Chromatography B*. 1105, 1 - 9.

Benešová, M., Hola, D., Fischer, L., Jedelský, P.L., Hnilička, F., Wilhelmová, N., Rothova, O., Kočová, M., Prochazkova, D., Honnerova, J. and Fridrichova, L. 2012. The physiology and proteomics of drought tolerance in maize: early stomatal closure as a cause of lower tolerance to short-term dehydration. *Plos*, 38017.

Bernier, F. and Berna, A. 2001. Germins and germin-like proteins: plant do-all proteins. But what do they do exactly. *Plant Physiology and Biochemistry*. 39, 545 - 554.

Bevan M, Bancroft I, Bent E, Love K, Goodman H, Dean C, Bergkamp R, Dirkse W, Van Staveren M, Stiekema W (1998) Analysis of 1.9 Mb of contiguous sequence from chromosome 4 of Arabidopsis thaliana. Nature. 391,485 – 488

Bizana, G., Ricardo. Gird, P.B., François, C, and Juan, M.R.L. 2014. New Insights into the Regulation of Aquaporins by the Arbuscular Mycorrhizal Symbiosis in Maize Plants under Drought Stress and Possible Implications for Plant Performance. *Molecular Plant-Microbe Interactions*. 27, 349 - 363.

Blum,A. 2005. Drought resistance,water-use effiency,and yield potential-are-they compatible, dissonant, or mutually exclusive?. *Australlian Journal of Agricultural Research*. 56, 1159 - 1168.

Blum, A. 2017. Osmotic adjustment is a prime drought stress adaptive engine in support of plant production. *Plant, cell & environment*. 40, 4 - 10.

Bradford, M.M. 1976. A rapid and sensitive method for the quantitation of microgram quantities of protein utilizing the principle of protein-dye binding. *Analytical Biochemistry*. 72, 24 - 254.

Brandt, B., Brodsky, D.E., Xue, S., Negi, J., Iba, K., Kangasjärvi, J., Ghassemian, M., Stephan, A.B., Hu, H. and Schroeder, J.I. 2012. Reconstitution of abscisic acid activation of SLAC1 anion channel by CPK6 and OST1 kinases and branched ABI1 PP2C phosphatase action. Proceedings of the National Academy of Sciences. 109, 10593 - 10598.

Cai, Y., Cao, F., Cheng, W., Zhang, G. and Wu, F. 2011. Modulation of exogenous glutathione in phytochelatins and photosynthetic performance against Cd stress in the two rice genotypes differing in Cd tolerance. *Biological Trace Element Research*. 143, 1159 - 1173.

Carminati, A., Javaux, M. 2020. Soil Rather Than Xylem Vulnerability Controls Stomatal Response to Drought. *Trends Plant Science*. 25, 868 - 880.

Cattivelli, L., Rizza, F., Badeck, F.W., Mazzucotelli, E., Mastrangelo,A.M. 2008. Drought tolerance improvement in crop plants: an intergrated view from breeding to genomics. *Field Crops Research*. 1, 1 - 14.

Cheng, L., Wang, Y., He, Q., Li, H., Zhang, X. and Zhang, F. 2016. Comparative proteomics illustrates the complexity of drought resistance mechanisms in two wheat (*Triticum aestivum* L.) cultivars under dehydration and rehydration. *BMC Plant Biology*. 16, 1 - 23.

Chimenti, C.A, Marcantonio, M., Hall A.J. 2006. Divergent selection for osmotic adjustment results in improved drought tolerance in maize (*Zea mays L.*) in both early growth and flowering phases. *Field Crops Research*. 95, 305 - 315.

Choi, H.G., Moon, B.Y. and Kang, N.J. 2015. Effects of LED light on the production of strawberry during cultivation in a plastic greenhouse and in a growth chamber. *Scientia Horticulturae*. 189, 22 - 31.

Cruz de Carvalho, Maria.H. 2008. Drought stress and reactive oxygen species: production, scavenging and signalling. *Plant Signalling & Behaviour*. 3, 156 - 165.

Dev, R., Dayal, D., Yadav, O.P. 2018. Thornless cactus: an unconventional, valuable fodder resource in arid region of India. *Indian Farming*. 68, 101 - 103.

Dong, A., Yang, Y., Liu, S., Zenda, T., Liu, X., Wang, Y., Li, J. and Duan, H. 2020. Comparative proteomics analysis of two maize hybrids revealed drought-stress tolerance mechanisms. *Biotechnology & Biotechnological Equipment*. 34, 763 - 780.

Fàbregas, N., Fernie, A.R. 2019. The metabolic response to drought. *Journal Experimental of Botany*. 70, 1077 - 1085.

Fang, Y. and Xiong, L. 2015. General mechanisms of drought response and their application in drought resistance improvement in plants. *Cellular and Molecular Life Sciences*. 72, 673 - 689.

Farooq, M., Wahid, A., Kobayashi, N., Fujita, D.B.S.M.A. and Basra, S.M.A. 2009. Plant drought stress: effects, mechanisms and management. Springer, Dordrecht. *In Sustainable Agriculture*. 153 - 188.

Farooq, M.A., Niazi, A.K., Akhtar, J., Farooq, M., Souri, Z., Karimi, N. and Rengel, Z. 2019. Acquiring control: The evolution of ROS-Induced oxidative stress and redox signaling pathways in plant stress responses. *Plant Physiology and Biochemistry*. 141, 353 - 369.

Gholamin, R. and Khayatnezhad, M. 2020. Study of bread wheat genotype physiological and biochemical responses to drought stress. Helix-The Scientific Explorer| Peer Reviewed *Bimonthly International Journal*. 10, 87 - 92.

Goche, T., Shargie, N.G., Cummins, I., Brown, A.P., Chivasa, S. and Ngara, R. 2020. Comparative physiological and root proteome analyses of two sorghum varieties responding to water limitation. *Scientific Reports*. 10, 1 - 18.

Gokul, A., Fahiem Carelse, M., Niekerk, L.A., Klein, A., Ludidi, N., Mendoza-Cozatl, D. and Keyster, M. 2021. Exogenous 3, 3′-Diindolylmethane Improves Vanadium Stress Tolerance in Brassica napus Seedling Shoots by Modulating Antioxidant Enzyme Activities. *Biomolecules*. 11, 436**.**

Hameed, A., Sheikh, M.A., Jamil, A. and Basra, S.M.A. 2013. Seed priming with sodium silicate enhances seed germination and seedling growth in wheat (*Triticum aestivum L.*) under water deficit stress induced by polyethylene glycol. *Pakistan Journal Life and Social Science*. 11, 19 - 24.

Hasanuzzaman, Mirza & Hossain, Mohammad Anwar & Teixeira da Silva, Jaime & Fujita, Masayuki. 2019. Plant Response and Tolerance to Abiotic Oxidative Stress: *Antioxidant Defense Is a Key Factor*. 10, 1-8.

Hayano-Kanashiro, C., Calderón-Vázquez, C., Ibarra-Laclette, E., Herrera-Estrella, L. and Simpson, J. 2009. Analysis of gene expression and physiological responses in three Mexican maize landraces under drought stress and recovery irrigation. *Plos. 4*, 1-14.

Hossain, M., Li, J., Sikdar, A., Hasanuzzaman, M., Uzizerimana, F., Muhammad, I., Yuan, Y., Zhang, C., Wang, C. and Feng, B. 2020. Exogenous melatonin modulates the physiological and biochemical mechanisms of drought tolerance in tartary buckwheat (*Fagopyrum tataricum (L.) Gaertn*). *Molecules*. 25, 2828.

Hu, Y., Burucs, Z. and Schmidhalter, U. 2008. Effect of foliar fertilization application on the growth and mineral nutrient content of maize seedlings under drought and salinity. *Soil Science and Plant Nutrition*. *54*, 133-141.

Islam, M.R., Hu, Y., Mao, S., Jia, P., Eneji, A.E. and Xue, X. 2011. Effects of water-saving superabsorbent polymer on antioxidant enzyme activities and lipid peroxidation in corn (*Zea mays L.*) under drought stress. *Journal of the Science of Food and Agriculture*. 91, 813-819.

Islam, W., Idrees, A., Waheed, A. and Zeng, F. 2022. Plant responses to drought stress: microRNAs in action. *Environmental Research*. 215, 114282.

Jakubczyk, K., Dec, K., Kałduńska, J.U.S.T.Y.N.A., Kawczuga, D.O.R.O.T.A., Kochman, J. and Janda, K.A.T.A.R.Z.Y.N.A. 2020. Reactive oxygen species-sources, functions, oxidative damage. *Polski merkuriusz lekarski: organ Polskiego Towarzystwa Lekarskiego*. 48, 124 - 127.

Kaur, G. and Asthir, B. 2017. Molecular responses to drought stress in plants. *Biologia Plantarum*. 61, 201 - 209.

Khan, N., Bano, A., Rahman, M.A., Guo, J., Kang, Z. and Babar, M. 2019. Comparative physiological and metabolic analysis reveals a complex mechanism involved in drought tolerance in chickpea (*Cicer arietinum L.*) induced by PGPR and PGRs. *Scientific Reports*. 9. 1 - 19.

Kohli, S.K., Khanna, K., Bhardwaj, R., Abd_Allah, E.F., Ahmad, P. and Corpas, F.J. 2019. Assessment of subcellular ROS and NO metabolism in higher plants: multifunctional signaling molecules. *Antioxidants*. 8, 641.

Kosová, K., Vítámvás, P., Prášil, I. T. and Renaut, J. 2011. Plant proteome changes under abiotic stress—contribution of proteomics studies to understanding plant stress response. *Journal of Proteomics*. 74, 1301 - 1322.

Laemmli, U.K.1970. Cleavage of structural proteins during the assembly of the head of bacteriophage T4. *Nature*.227, 680-685.

Laxa, M., Liebthal, M., Telman, W., Chibani, K. and Dietz, K.J. 2019. The role of the plant antioxidant system in drought tolerance. *Antioxidants*. 8, 94.

Li, H., Li, Y., Ke, Q., Kwak, S.S., Zhang, S. and Deng, X. 2020. Physiological and differential proteomic analyses of imitation drought stress response in *Sorghum bicolor* root at the seedling stage. *International Journal of Molecular Sciences*. 21, 9174.

Li, H.J., Wang, Y.F., Zhao, C.F., Yang, M., Wang, G.X. and Zhang, R.H. 2021. The quantitative proteomic analysis provides insight into the effects of drought stress in maize. *Photosynthetica*. 59, 1- 11.

Li, L., Zhang, H., Tang, M. and Chen, H. 2021. Nutrient uptake and distribution in mycorrhizal cuttings of Populus× canadensis 'Neva'under drought stress. *Journal of Soil Science and Plant Nutrition*. 21, 2310 - 2324.

Li, P., Lin, P., Zhao, Z., Li, Z., Liu, Y., Huang, C., Huang, G., Xu, L., Deng, Z., Zhang, Y. and Zhao, X. 2022. Gene Co-Expression Analysis Reveals Transcriptome Divergence between Wild and Cultivated Sugarcane under Drought Stress. *International Journal of Molecular Sciences*. 23, 569.

Libault, M., Joshi, T., Benedito, V.A., Xu, D., Udvardi, M.K. and Stacey, G. 2009. Legume transcription factor genes: what makes legumes so special. *Plant Physiology*. 151, 991 - 1001.

Liu Q, Yang J, Yan S, Zhang S, Zhao J, Wang W, Yang T, Wang X, Mao X, Dong J, Zhu X, Liu B. 2016.The germin-like protein OsGLP2-1 enhances resistance to fungal blast and bacterial blight in rice. *Plant Molecular Biology*. 92, 411-423.

Liu S, Zenda T, Li J, Wang Y, Liu X, and Duan H. 2020. Comparative transcriptomic analysis of contrasting hybrid cultivars reveal key drought responsive genes and metabolic pathways regulating drought stress tolerance in maize at various stages. *PLos* .15, 1- 27.

Ma, Q.H. 2009. The expression of caffeic acid 3-O-methyltransferase in two wheat genotypes differing in lodging resistance. *Journal of Experimental Botany*. 60, 2763 - 2771.

Marcińska, I., Czyczyło-Mysza, I., Skrzypek, E., Filek, M., Grzesiak, S., Grzesiak, M.T., Janowiak, F., Hura, T., Dziurka, M., Dziurka, K. and Nowakowska, A. 2013. Impact of osmotic stress on physiological and biochemical characteristics in drought-susceptible and drought-resistant wheat genotypes. *Acta Physiologiae Plantarum*. 35, 451 - 461.

Mittler, R. 2006. Abiotic stress, the field environment and stress combination. *Trends in Plant Science*. 11, 15 - 19.

Mohammadi Alagoz, S., Zahra, N., Hajiaghaei Kamrani, M., Asgari Lajayer, B., Nobaharan, K., Astatkie, T., Siddique, K.H.M., Farooq, M. 2022. Role of Root Hydraulics in Plant Drought Tolerance. *Journal of Plant Growth Regulion*. 1 - 15.

Moharramnejad, S.A.J.J.A.D., Sofalian, O., Valizadeh, M., Asghari, A., Shiri, M. and Ashraf, M.U.H.A.M.M.A.D. 2019. Response of maize to field drought stress: oxidative defence system,osmolytes accumulation and photosynthetic pigments. *Pakistan Journal of Botany*. 3, 799 - 807.

Nadarajah, K.K. 2020. ROS homeostasis in abiotic stress tolerance in plants. International *Journal of Molecular Sciences*. 21, 5208.

Naorem, A., Patel, S., Hassan, S., Louhaichi, M., Sarker, A. 2022. Response of cactus pear (Opuntia ficus-indica Mill.) to boron and farmyard manure application under arid soils conditions in Kutch, Gujarat. *Acta Horticulture*. 187 - 196.

Ngara, R. 2009. A proteomic analysis of drought and salt stress responsive proteins of different sorghum varieties. PhD thesis. University of the Western Cape, South Africa.

Osakabe, Y., Osakabe, K., Shinozaki, K. and Tran, L.S.P. 2014. Response of plants to water stress. *Frontiers in Plant Science*. 5, 86.

Paniagua, C., Bilkova, A., Jackson, P., Dabravolski, S., Riber, W., Didi, V., Houser, J., Gigli-Bisceglia, N., Wimmerova, M., Budínská, E. and Hamann, T. 2017. Dirigent proteins in plants: modulating cell wall metabolism during abiotic and biotic stress exposure. *Journal of Experimental Botany*. 68, 3287 - 3301.

Parveen, A., Liu, W., Hussain, S., Asghar, J., Perveen, S. and Xiong, Y. 2019. Silicon priming regulates morpho-physiological growth and oxidative metabolism in maize under drought stress. *Plants.* 8, 431.

Praba, M.L., Cairns, J.E., Babu, R.C. and Lafitte, H.R. 2009. Identification of physiological traits underlying cultivar differences in drought tolerance in rice and wheat. *Journal of Agronomy and Crop Science. 195*, 30 - 46.

Qi J, Song CP, Wang B, Zhou J, Kangasjärvi J, Zhu JK, Gong Z. 2018. Reactive oxygen species signalling and stomatal movement in plant responses to drought stress and pathogen attack. *Journal of Integral Plant Biology*. 60, 805 – 826.

Reddy, A. R., Chaitanya, K. V. and Vivekanandan, M. 2004. Drought-induced responses of photosynthesis and antioxidant metabolism in higher plants. *Journal of Plant Physiology*. 161, 1189 - 1202.

Rhodes,David and Nadolska-Orczyk,Anna. 2001. .*Plant Stress Physiology*. 10, 1038.

Riboni, M., Test, A.R., Galbiati, M., Tonelli, C., Conti, L. 2016. ABA-dependent control of GIGANTEA signalling enables drought escape via up-regulation of FLOWERING LOCUS T in Arabidopsis thaliana. *Journal Experimental of Botany*. 67, 6309 – 6322.

Ramadan, H.A., Al-Niemi, S.N. and Hamdan, T.T. 1986. Water stress, soil type and phosphorus effects on corn and soybean. II. Effects on nutrients in plant tissues. *Iraqi Journal of Agricultural Sciences Zanco*. 4, 79 – 88.

Saad-Allah, K.M., Nessem, A.A., Ebrahim, M.K. and Gad, D. 2021. Evaluation of drought tolerance of five maize genotypes by virtue of physiological and molecular responses. *Agronomy*. 12, 59.

Sandhya,V., Ali Sk, Z.,Grover,M.,Reddy,G.,Venkateswarlu,B. 2010. Effect of plant growth promoting Pseudomonas spp. on compatible solutes, antioxidant status and plant growth of maize under drought stress. *Plant Growth Regulations*. 10,79 - 80.

Sassine, Y.N., Bejjani, R., Tabet, E., Abdel-mawgoud, A.M.R., Yordanova, M.H., Alturki, S.M. 2021. Effect of drought and mono-potassium phosphate (MKP) on some physiological attributes and macronutrient translocation in potato crop. 1327, 181 – 188.

Shafiq, S., Akram, N.A., Ashraf, M., García-Caparrós, P., Ali, O.M. and Latef, A.A.H.A. 2021. Influence of glycine betaine (natural and synthetic) on growth, metabolism and yield production of drought-stressed maize (*Zea mays L.*) plants. *Plants*. 10, 2540.

Shahzad, M.A., Jan, S.U., Afzal, F., Khalid, M., Gul, A., Sharma, I., Sofo, A., Ahmad, P. 2016. Drought stress and morphophysiological responses in plants. Water Stress and Crop Plants: *A Sustainable*. 2, 452 – 467.

Shao,H.B.,Chu.L.Y.,Jallel,C.A.,Manivannan,P.,Panneerselvam,R.,Shao,M.A. 2009.Understanding water deficit stress-induced changes in the basic metabolism of higher plants biotechnologically and sustainably improving agriculture and the ecoenvironment in arid regions of the globe. *Critical Reviews in Biotechnology*. 2, 131 - 151.

Shavrukov,Y.,Kurishbayev,A.,Jataye,S.,Shvidchenko,V.,Zotova,L.,Koekemoer,F.,de Groot,S.,Soole,K.and Langeridge,P. 2017 Early flowering as a drought escape mechanism in plants:How can it aid wheat production?, *Fronteirs in Plant Science*. 8, 1950.

Smirnoff, N., Arnaud, D. 2019. Hydrogen peroxide metabolism and functions in plants. *New Phytology*. 221, 1197 - 1214.

Smith, S.J., Kroon, J.T., Simon, W.J., Slabas, A.R., Chivasa, S. 2015. A novel function for Arabidopsis CYCLASE1 in programmed cell death revealed by isobaric tags for relative and absolute quantitation (iTRAQ) analysis of extracellular matrix proteins. *Molecular & Cellular Proteomics*. 14, 1556 - 1568.

Song, L., Jin, J. and He, J. 2019. Effects of severe water stress on maize growth processes in the field. *Sustainability*. *11*, 1 - 15.

Su, X., Fan, X., Shao, R., Guo, J., Wang, Y., Yang, J., Yang, Q. and Guo, L. 2019. Physiological and iTRAQ-based proteomic analyses reveal that melatonin alleviates oxidative damage in maize leaves exposed to drought stress. *Plant Physiology and Biochemistry*. 142, 263 - 274.

Szabados L, and Savoure A. 2010. Proline:a multifunctional amino acid.*Trends in Plant Science.* 15, 89- 97.

Talaat, N.B., Shawky, B.T. and Ibrahim, A.S. 2015. Alleviation of drought-induced oxidative stress in maize (*Zea mays L.)* plants by dual application of 24-epibrassinolide and spermine. *Environmental and Experimental Botany*. 113, 47 - 58.

Trouvelot, S., Héloir, M.C., Poinssot, B., Gauthier, A., Paris, F., Guillier, C., Combier, M., Trdá, L., Daire, X. and Adrian, M. 2014. Carbohydrates in plant immunity and plant protection: roles and potential application as foliar sprays. *Frontiers in Plant Science*. 592.

Tumova L, Tarkowska D, R ehorova K, Markova H, Kocova M, Rothova O. 2018. Drought-tolerant and drought-sensitive genotypes of maize (*Zea mays L*.) differ in contents of endogenous brassinosteroids and their drought induced changes. *PLos.* 3, 1 - 22.

Vineeth, T., Kumar, P., Krishna, G. 2016. Bioregulators protected photosynthetic machinery

by inducing expression of photorespiratory genes under water stress in chickpea.

Photosynthetica. 54, 234 - 242.

Wang, T., Chen, X., Zhu, F., Li, H., Li, L., Yang, Q., Chi, X., Yu, S. and Liang, X. 2013. Characterization of peanut germin-like proteins, AhGLPs in plant development and defense. *PLos*. 8, 61722.

Wang, X., Zenda, T., Liu, S., Liu, G., Jin, H., Dai, L., Dong, A., Yang, Y. and Duan, H. 2019. Comparative proteomics and physiological analyses reveal important maize filling-kernel drought-responsive genes and metabolic pathways. *International Journal of Molecular Sciences*. 20, 37 - 43.

Wei, L., Zhang, D., Xiang, F. and Zhang, Z. 2009. Differentially expressed miRNAs potentially involved in the regulation of defense mechanism to drought stress in maize seedlings. *International Journal of Plant Sciences*. *170*, 979 - 989.

Wellburn, A.R. 1994. The spectral determination of chlorophylls a and b, as well as total carotenoids, using various solvents with spectrophotometers of different resolution. *Journal of Plant Physiology*. 144. 307-313.

Xiong,L.,Wang, R.G., Mao,G and Koczan, J.M. 2006. Identification of Drought Tolerance Determinants by Genetic Analysis of Root Response to Drought Stress and Abscisic Acid. *Plant Physiology*. 142, 106 5 – 1074.

Yang, L., Jiang, T., Fountain, J.C., Scully, B.T., Lee, R.D., Kemerait, R.C., Chen, S. and Guo, B. 2014. Protein profiles reveal diverse responsive signalling pathways in kernels of two maize inbred lines with contrasting drought sensitivity. *International Journal of Molecular Sciences*. 15, 18892- 18918.

Yang, L., Fountain, J.C., Wang, H., Ni, X., Ji, P., Lee, R.D., Kemerait, R.C., Scully, B.T. and Guo, B. 2015. Stress sensitivity is associated with differential accumulation of reactive oxygen and nitrogen species in maize genotypes with contrasting levels of drought tolerance. *International Journal of Molecular Sciences*. 16, 24791 - 24819.

Yang, S.H.U.S.H.E.N. and Deng, X.I.P.I.N.G. 2015. Effects of drought stress on antioxidant enzymes in seedlings of different wheat genotypes. *Pakistan*. *Journal of. Botany*. 4, 49 - 56.

Yuan, B., Yang, Y., Fan, P., Liu, J., Xing, H., Liu, Y. and Feng, D. 2021. Genome-wide identification and characterization of Germin and Germin-Like Proteins (GLPs) and their response under Powdery Mildew Stress in Wheat (*Triticum aestivum L.*). *Plant Molecular Biology Reporter*. 39, 821 - 832.

Zenda, T., Liu, S., Wang, X., Jin, H., Liu, G. and Duan, H. 2018. Comparative proteomic and physiological analyses of two divergent maize inbred lines provide more insights into drought-stress tolerance mechanisms. *International Journal of Molecular Sciences*. *19*, 3225.

Zheng, J., Fu, J., Gou, M., Huai, J., Liu, Y., Jian, M., Huang, Q., Guo, X., Dong, Z., Wang, H. and Wang, G. 2010. Genome-wide transcriptome analysis of two maize inbred lines under drought stress. *Plant Molecular Biology*. 72, 407 - 421.

Zeng, W., Peng, Y., Zhao, X., Wu, B., Chen, F., Ren, B., Zhuang, Z., Gao, Q, and Ding, Y. 2019. Comparative proteomics analysis of the seedling root response of drought-sensitive and drought-tolerant maize varieties to drought stress. *International Journal of Molecular Sciences*. 20, 27 - 93.

Zhang, X., Lei. L, Lai, J., Zhao, H. Song, W. 2018. Effects of drought stress and water recovery on physiological responses and gene expression in maize seedlings. *BMC Plant Biology*. 18, 1 - 16.